



January 2012

# High Grade Carbon From Crop Oil Tars

Nathan Bosquez

Follow this and additional works at: <https://commons.und.edu/theses>

---

## Recommended Citation

Bosquez, Nathan, "High Grade Carbon From Crop Oil Tars" (2012). *Theses and Dissertations*. 1334.  
<https://commons.und.edu/theses/1334>

This Thesis is brought to you for free and open access by the Theses, Dissertations, and Senior Projects at UND Scholarly Commons. It has been accepted for inclusion in Theses and Dissertations by an authorized administrator of UND Scholarly Commons. For more information, please contact [zeinebyousif@library.und.edu](mailto:zeinebyousif@library.und.edu).

HIGH GRADE CARBON FROM CROP OIL TARS

by

Nathan Michael Bosquez  
Bachelor of Science, University of Minnesota Duluth, 2009

A Thesis

Submitted to the Graduate Faculty

of the

University of North Dakota

in partial fulfillment of the requirements

for the degree of

Master of Science

Grand Forks, North Dakota

December

2012

Copyright 2012 Nathan Bosquez

This thesis, submitted by Nathan Michael Bosquez in partial fulfillment of the requirements for the Degree of Master of Science from the University of North Dakota, has been read by the Faculty Advisory Committee under whom the work has been done and is hereby approved.

---

Dr. Wayne Seames

---

Dr. Steven Benson

---

Dr. Robert Wills

This thesis meets the standards for appearance, conforms to the style and format requirements of the Graduate School of the University of North Dakota, and is hereby approved.

---

Dr. Wayne Swisher  
Dean of the Graduate School

---

Date

## PERMISSION

Title            High Grade Carbon from Crop Oil Tars

Department    Chemical Engineering

Degree           Master of Science

In presenting this thesis in partial fulfillment of the requirements for a graduate degree from the University of North Dakota, I agree that the library of this University shall make it freely available for inspection. I further agree that permission for extensive copying for scholarly purposes may be granted by the professor who supervised my thesis work or, in his absence, by the chairperson of the department or the dean of the Graduate School. It is understood that any copying or publication or other use of this thesis or part thereof for financial gain shall not be allowed without my written permission. It is also understood that due recognition shall be given to me and to the University of North Dakota in any scholarly use which may be made of any material in my thesis.

Nathan Michael Bosquez  
November 21, 2012

## TABLE OF CONTENTS

LIST OF FIGURES .....	vii
LIST OF TABLES.....	ix
ACKNOWLEDGEMENTS.....	x
ABSTRACT.....	xi
CHAPTER	
I. BACKGROUND	
1.1 High Grade Carbon Materials .....	1
1.1.1 Biomass Char from Pyrolysis .....	2
1.1.2 Coking.....	3
1.1.1.1 Coking Reactions .....	5
1.1.1.2 Petroleum Coking Processes .....	6
1.1.3 Types of Coke .....	14
1.2 Motivation for Renewable Carbon Products.....	18
1.3 Renewable Fuel Process at UND .....	18
1.4 Hypothesis of Research.....	20
II. EXPERIMENTAL METHODS	
2.1 Obtaining Representative Tars.....	22
2.2 Initial TGA Testing.....	23
2.3 Lab Scale Coker .....	25
2.4 Analysis of Solid Products .....	29
2.4.1 Carbon Content .....	29
2.4.2 Moisture Content/Volatile Matter/Fixed Carbon/Ash Content.....	29
2.5 Analysis of Liquid Products.....	31
2.5.1 Liquid Analysis.....	31

2.5.2 Acid Analysis.....	33
2.6 Analysis of Gas Products .....	34
III. RESULTS & DISCUSSION	
3.1 Initial TGA Testing.....	36
3.2 Lab Scale Coking Experiments .....	39
3.3 Analysis of Solid Products .....	43
3.3.1 Carbon Content .....	43
3.3.2 Moisture Content/Volatile Matter/Fixed Carbon/Ash Content.....	45
3.4 Analysis of Liquid Products.....	50
3.4.1 Liquid Analysis .....	50
3.4.2 Acid Analysis.....	53
3.5 Analysis of Gas Products .....	56
IV. CONCLUSION	
4.1 Research of Lab Scale Coking.....	62
4.2 Future Work.....	63
APPENDICES .....	64
APPENDIX A: Lab Scale Coker Operation .....	65
APPENDIX B: Mass Balances from Preliminary Coking Testing.....	71
APPENDIX C: Carbon Content Calibrations .....	72
APPENDIX D: Moisture Content/Volatile Matter/Fixed Carbon/Ash Content Graphs ..	76
APPENDIX E: GC SimDist Liquid Analysis.....	86
APPENDIX F: Acid Analysis Calibrations .....	98
APPENDIX G: Gas Chromatography Calibrations & Additional Analysis.....	100
REFERENCES .....	104

## LIST OF FIGURES

Figure	Page
1. Simplified Process Flow Diagram of a Petroleum Refinery.....	4
2. Simplified Fluid Coking Process .....	7
3. Simplified Flexi Coking Process .....	8
4. Simplified Delayed Coking Process .....	9
5. Detailed Process Flow Diagram for the Delayed Coking Process.....	10
6. Diagram of the Coke Drum Drilling Cycle.....	11
7. Photograph of the blades inside of a Continuous Coking Furnace.....	12
8. Process Flow Diagram of Continuous Coking.....	13
9. Simplified Process Flow Diagram of the Renewable Fuel Process at UND .....	19
10. Photograph of the TA Instruments SDT Q600 TGA .....	24
11. Photograph of the Lab Scale Coking Reactor.....	25
12. Process Flow Diagram of Coking Reactor Using Atmospheric Pressure.....	26
13. Process Flow Diagram of Coking Reactor Using Vacuum Pressure .....	28
14. Photograph of the Shimadzu TOC-VCSN Carbon Analyzer and SSM 5000A.....	29
15. Photograph of the TA Instruments SDT Q600 TGA .....	30
16. Photograph of the Perkin Elmer Clarus 480 Gas Chromatograph SimDist.....	32
17. Photograph of the Thermo Scientific Nicolet IR 200 FT-IR .....	33
18. Photograph of the SRI 8610C Gas Chromatograph.....	34



19.	Initial TGA Testing on D-300 Bottoms .....	37
20.	Coke Formation for Varied Nitrogen Flow Rates Based on Time .....	38
21.	Coke Formation for Varied Nitrogen Flow Rates Based on Temperature .....	38
22.	Coking Reactor Temperature Versus Time for Atmospheric Pressure Coking of D-300 Bottoms .....	40
23.	Coking Reactor Temperature Versus Time for Vacuum Pressure Coking of D-300 Bottoms.....	41
24.	Coke Formation Versus Temperature from Batch Atmospheric Pressure Coking Reactions of Crop Oil Cracking Derived Tars.....	43
25.	Moisture Content/Volatile Matter/Fixed Carbon/Ash Content Evolution for a 464 °C_1 (test 1) Coke Sample.....	45
26.	The Volatile Matter Content in Coke Samples .....	50
27.	Hydrocarbon Cut Concentrations in Liquid Samples Collected After Coking.....	53
28.	Acid Concentration of Liquid Samples Collected After Coking.....	55

## LIST OF TABLES

Table	Page
1. Mass Balance for Coking Reactor Batch Experiments in Weight %.....	41
2. Carbon Content in Coke Samples.....	44
3. Moisture Content/Volatile Matter/Fixed Carbon/Ash Content of Coke Samples ....	47
4. Coke Yield Normalized to Fixed Carbon Fraction (wt %).....	49
5. Coke Properties for Aluminum Anode-Grade Carbon Products .....	49
6. The Concentration of Fuel Cuts in Liquid Samples Collected After Coking (wt % C) .....	52
7. Peak Heights and Total Acid Concentrations of Liquid Samples Collected After Coking .....	54
8. Gas Components from 497 °C Atmospheric Pressure Coking (mol %).....	57
9. Gas Components from 484 °C Atmospheric Pressure Coking (mol %).....	58
10. Gas Components from 474 °C Atmospheric Pressure Coking (mol %).....	58
11. Gas Components from 464 °C_1 Atmospheric Pressure Coking (mol %).....	58
12. Gas Components from 465 °C_2 Atmospheric Pressure Coking (mol %).....	58
13. Gas Components from 462 °C_3 Atmospheric Pressure Coking (mol %).....	59
14. Gas Components from 453 °C Atmospheric Pressure Coking (mol %).....	59
15. Gas Components of Measurable Gas for 464 °C_1, 465 °C_2, and 462 °C_3 Coking (mol %).....	60

## ACKNOWLEDGEMENTS

I am greatly indebted to the UND Department of Chemical Engineering for providing this opportunity to work on a research project. I would like to thank Dr. Wayne Seames who supervised me with enormous support and encouragement through this research work. I am extremely grateful for his supervision in moving me forward to finish my project. I would also like to thank Dr. Steven Benson for his support as my other co-advisor and Dr. Robert Wills for his assistance and guidance through this research work. I would like to acknowledge all of the other graduate students and staff engineers involved with the crop oil project for their contributions.

I am grateful to Hanying Xu of the UND Department of Engineering & Mines for allowing me to use the Shimadzu TOC-V<sub>CSN</sub> Carbon Analyzer and SSM 5000A.

I would like to thank Mr. David Hirschmann and Mr. Harry Feilen for their help in building my lab scale coking equipment and assistance around the lab. Without all of these people mentioned this project would not be possible.

## ABSTRACT

Current research at the University of North Dakota studies the conversion of crop oils into fuels such as diesel and jet fuel. A by-product of this conversion process is a high molecular weight tar, which can be further processed into carbon products such as carbon black, coke, activated carbon, and carbon fibers. This research focuses on converting the tar into high purity carbon. Currently coal and petroleum tars are used to make carbon products and are important nonrenewable sources to replace by the use of crop oil tars.

Lab-scale experiments have shown that the tars produced during crop oil cracking can be converted into a pure, granulated carbon product. This conversion, known as carbonization, occurs at reasonable conditions and is accomplished by refining the residual tars into high purity carbon through pyrolysis of the tar in an inert atmosphere. Residual tars are converted into carbon, while simultaneously removing and recovering distillates to be recycled back through the system where they can be processed into other fuel and chemical products.

The carbonization of tar was performed through the use of a lab scale coking reactor. The independent variables were coking temperature and either vacuum or atmospheric pressure. Process conditions were sought to optimize the production of solid coke, while simultaneously minimizing the formation of gas products. An overall mass

balance for carbonization was calculated. Characterization of the solid coke was performed by carbon content analysis and moisture content/volatile matter/fixed carbon/ash content evolution analysis. Characterization of the liquid phase was performed by liquid analysis for fuel cuts and acid concentration analysis. The gas phase was characterized by gas chromatography.

Carbon products were successfully produced in this research. The coking of heavy, residual tars using a temperature above 460 °C and at atmospheric pressure resulted in the maximum formation of bio-derived coke, while also minimizing the formation of low value gas products. These process conditions produced a little more than 10 wt % coke. The coke contains 92 wt % carbon, with the balance primarily volatile matter. Therefore, calcining the coke may be needed, depending on the applications sought for this coke. The liquid phase contained 91 wt % heavy fuel oil and diesel fuel cuts, and had an acid concentration of between 4.0-6.7 wt % acid. Analysis of the non-condensable gas phase presented a mixture of light hydrocarbons, carbon monoxide, carbon dioxide, and hydrogen. Both the liquid phase and gas phase streams can be recycled back through the process.

# CHAPTER I

## BACKGROUND

### 1.1 High Grade Carbon Materials

A high value carbonaceous material is any product that is predominantly made up of elemental carbon and typically consists of either granular carbon products, such as carbon black, coke and activated carbon, or carbon fibers. Currently coal and petroleum derived tars are used to produce these materials. The formation of carbon materials typically occurs during pyrolysis processes when coal, petroleum oils or vegetable oils are converted into useable energy [1]. Pyrolysis is the thermo-chemical decomposition of organic materials at elevated temperatures without the presence of oxygen. It is most commonly used to produce gaseous and liquid fuel products while leaving behind a solid char [2].

Based on physical and chemical characterization properties the char can be used in numerous applications. Properties such as surface area, ash content, carbon content, physical strength, electrical conductivity, coefficient of thermal expansion, etc., all determine the appropriate applications for various carbon products. Chars of lower surface area (carbon black) that are not ideal for activated carbon are used in tires, plastics, and toner and printer inks [3]. Higher surface area chars can be activated and used to adsorb colored or odorous substances from gas or liquid streams, in applications such as water treatment plants. Carbon fibers are produced by further processing tar into

pitch, a very heavy residual oil that is often solid at room temperatures. The pitch is then melt spun and thermally treated to form carbon fibers. Granular carbon products are formed from the incomplete combustion or thermal decomposition of hydrocarbons. There are many more applications for coke products, which are made from further processing the chars. The production and applications of coke will be further discussed in section 1.1.2 and section 1.1.3.

### *1.1.1 Biomass Char from Pyrolysis*

Pyrolysis of solid biomass produces a gas and an organic liquid product, as well as leaving behind a solid char [2]. There are many examples of research done with different agricultural by-products to produce this char, which typically is further processed by activating the char through physical or chemical methods to produce activated carbon. Carbon products, including activated carbon, can theoretically be produced from any material rich in elemental carbon [4]; hence the idea of using biomass to produce carbon arose. The study of producing activated carbon from biomass waste and agricultural by-products is becoming increasingly popular because in addition to dealing with the disposal of waste these by-products are available at relatively low costs and are a renewable source of carbon products that have the potential to replace existing coal and petroleum carbon products [5].

Ahmedna [5] *et al* produced granular activated carbons from rice straw, rice hulls, sugarcane bagasse, and pecan shells through pyrolysis in a nitrogen atmosphere. It was found that the properties of the char varied depending on the precursor and process conditions. Some characteristics that are considered when finding a suitable precursor include low volatile content, high carbon yield, and narrow molecular weight distribution.

higher yields in carbonization can be obtained if precursors have high aromatic and low aliphatic carbon content [6]. Fan [7] *et al* used fast pyrolysis, which is just a more rapid thermal decomposition, to produce char from oat hulls and corn stover. Lafi [8] produced activated carbon from acorns and olive seeds as a means of using a waste product and making a useful product to reduce costs in a wastewater treatment plant. Martinez [9] *et al* also made use of a by-product to increase economic return and reduce pollution by producing activated carbon from olive stones and walnut shells. Lastly, Savova [10] *et al* converted almond shells, nut shells, apricot stones, cherry stones, and grape seeds to carbon adsorbents and Srinivasakannan and Bakar [11] used rubber tree wood sawdust.

There are countless sources that have the potential for the production of carbon products. Although there has not been much done to study the use of pyrolyzed crop oil residues in the production of carbon products, crop oil cracking is a specialized form of biomass pyrolysis. Thus, the studies discussed above can be beneficial as starting points in the current research which is the subject of this thesis.

### *1.1.2 Coking*

Before the use of biomass, high value carbonaceous materials were typically produced from coal and petroleum using heavy residual feedstocks accumulated during processing. However, a petroleum refinery coke is more similar to the tars derived from crop oil cracking and is the process that was more closely imitated in this research. In petroleum refineries, high value fuel products like gasoline, jet fuel, diesel fuel, and motor oils are upgraded and separated from crude petroleum oil, leaving a heavy tar residue.



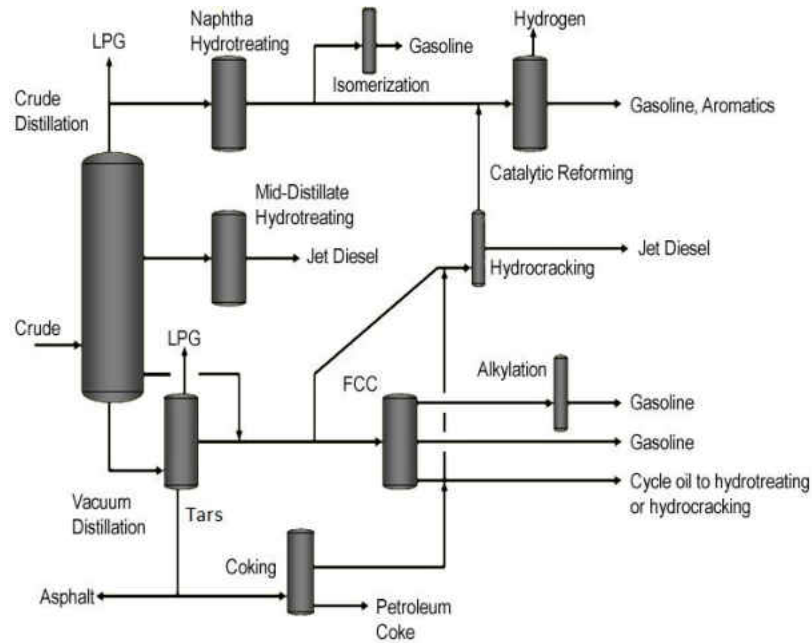


Figure 1: Simplified Process Flow Diagram of a Petroleum Refinery [12]

Figure 1 shows a process of how crude petroleum oil is refined into fuels with resulting tars from the bottoms of the vacuum distillation column. Additional middle distillate fuels can be produced from the tars by processing it at high temperatures (460 °C to 510 °C) to crack large hydrocarbons into smaller hydrocarbons. This process, called coking, generates a hard, coal-like porous substance called petroleum coke [13]. Petroleum coke (petcoke) is a solid, high purity carbonaceous material with a high carbon-to-hydrogen ratio but also contains small amounts of residual hydrocarbons (volatile matter) as well as sulfur and trace amounts of metals [14].

The most common materials used to feed the coking process are atmospheric distillation residue, vacuum distillation residue, thermal tar, and decant oil (catalytically cracked clarified oil) [14].

At most petroleum refineries, it is more profitable to limit coke generation due to the relatively low market value of petcoke, compared with middle distillate fuel products

[15]. This is mainly due to the sulfur, vanadium, nickel, iron, and silicon contents in addition to other impurities that exist in petroleum coke. These high molecular weight impurities concentrate in the petcoke. The chemical composition depends upon the composition of the original feedstocks that are processed [16]. In recent years, the impurity levels in petroleum cokes have been progressively increased, since refineries have had to accommodate a higher proportion of heavy, sour crudes. As these impurities become concentrated in the coke, undesirable coke properties can be produced, leading refiners to try to maximize lighter, high value liquid products and minimize coke formation [17]. Since crude petroleum feedstocks contain more impurities than the renewable tars generated during crop oil cracking, it may be advantageous to maximize coke production from this process.

#### *1.1.1.1 Coking Reactions*

The formation of petroleum coke comes from one of two basic reactions: de-alkylation and de-hydrogenation. De-alkylation occurs when high molecular weight hydrocarbons, such as asphaltenes and resins, are subjected to high temperatures in the coking process. A highly disordered and cross-linked carbon residue structure results from the reaction, which is evident from a substantial difference in the hydrogen atom concentration measured in the resin-asphaltene feed and formed coke. The coke generated from resin-asphaltene compounds is unsuitable for special applications because of the amorphous character, in conjunction with the high concentrations of impurities [14].

The de-hydrogenation reaction mechanism depends upon the cleavage of hydrogen from heavy oils with succeeding condensation of the free radicals to form high

molecular weight compounds containing high carbon-to-hydrogen ratios. The coke subsequently formed has a more crystalline appearance than the resin-asphaltene based coke because of fewer cross-linkages within the structure. The coke formed from the dehydrogenation reaction mechanism is a premium grade product suitable for calcining and graphitization because it is generated from feedstock such as thermal cracker tars, catalytic cracker slurry, and decant oil, which are high in aromatics and low in resin-asphaltenes [14].

#### *1.1.1.2 Petroleum Coking Processes*

Petroleum coke is currently produced by one of three processes: fluidized bed coking (fluid coking), flexi-coking, or delayed coking [14]. The initial product of the coking process is green coke, which can be further processed at higher temperatures, exceeding 1000 °C, to produce calcined coke.

*Fluid Coking.* Fluid coking (Figure 2) is a continuous fluidized bed process, where warm coke particles are fed at temperatures above 500 °C and stay in contact with re-circulated slurry, allowing the coking process to occur [16]. Fluid coke regularly contains less residual hydrocarbons than coke from delayed coking but more than calcined coke, and transpires as spherical grains less than 1 cm in diameter [14]. Due to its availability in sub-millimetric sizes and high contents of sulfur and metals, fluid coke accounts for no more than 10 % of the coke used in the aluminum industry since it hinders milling and connections for anodes [16], a primary application for high grade carbon.

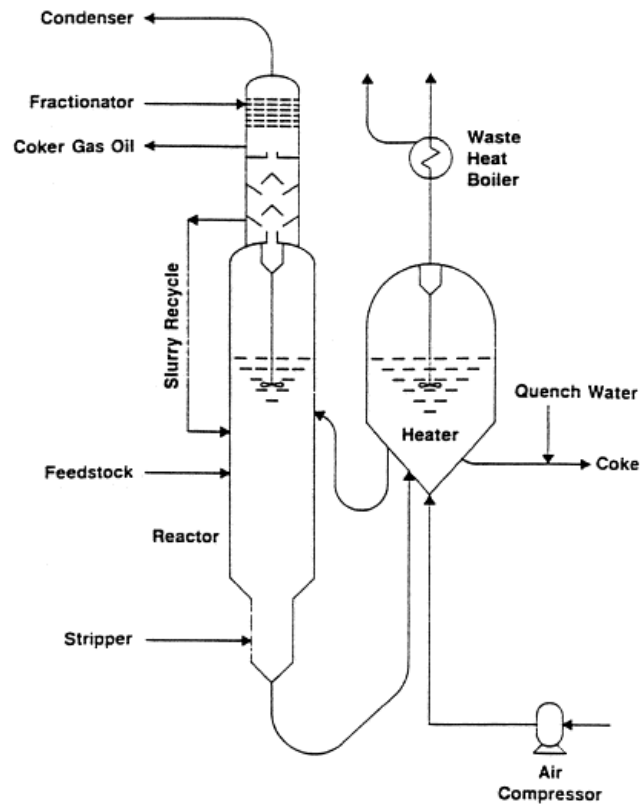


Figure 2: Simplified Fluid Coking Process [18]

*Flexi Coking.* Flexi coke (Figure 3) is produced from a modified fluidized bed process in which most of the coke (up to 97 %) is converted to a low Btu fuel gas (20 to 40 Btu/scf) for use in the refinery wherein it was produced. Solid flexi coke has a smaller particle size and lower volatile matter content than fluid coke and is therefore dustier than its counterpart [14].

*Delayed Coking.* The delayed coking process (Figures 4 and 5) is a thermal cracking, semi-batch continuous process in which thermal cracking and condensation

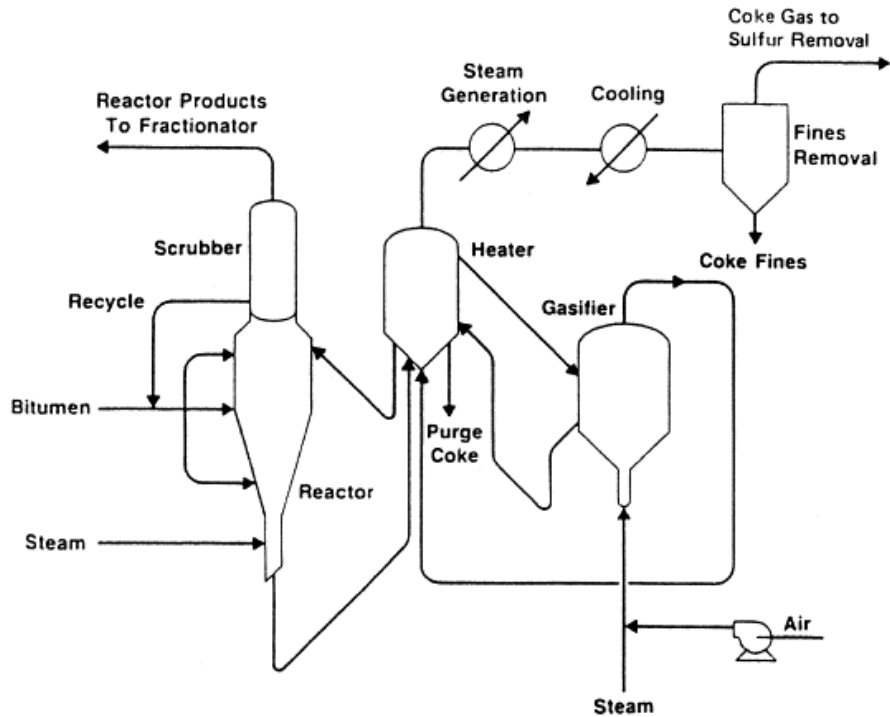


Figure 3: Simplified Flexi Coking Process [18]

occur as well as de-hydrogenation and polymerization to form green coke. Delayed coking is the primary technology used for upgrading petroleum residuum into liquid and gas products along with solid coke and accounts for more than 92 % of the total coke production in the United States [14]. The coke produced from this process also represents 90 % of the coke used in the aluminum industry [16]. Bottoms from the atmospheric and vacuum distillation columns typically form the feed to the delayed coking unit fractionator. The feed in most cases arrives cold to the fractionator although in some units the feed is preheated to around 400 °C before entering the column.

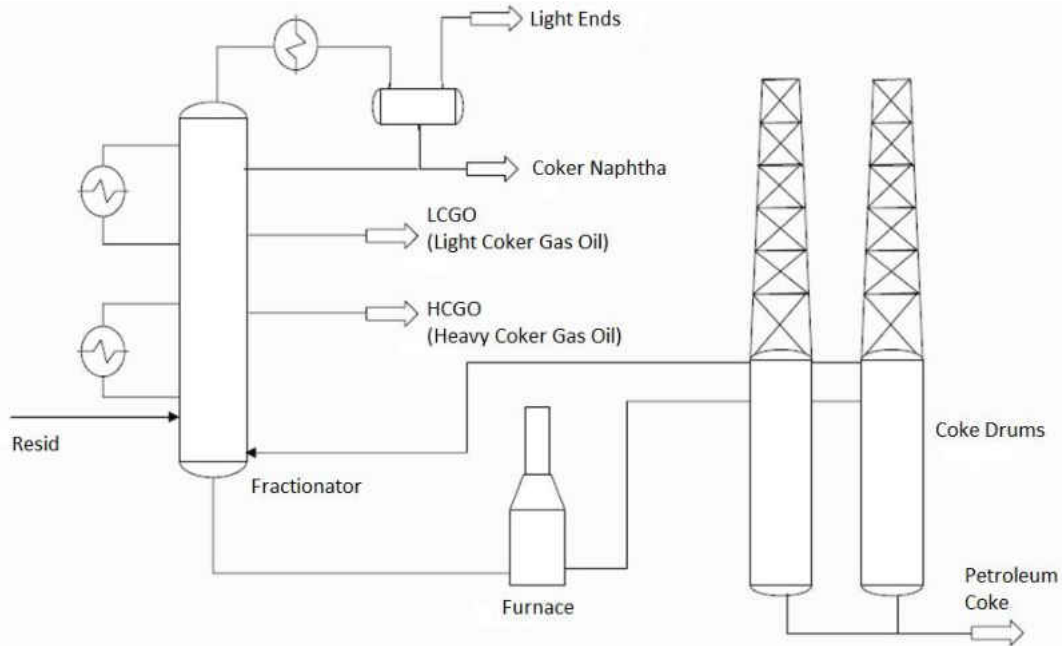


Figure 4: Simplified Delayed Coking Process [12]

The residual feedstock (Resid, Fig 4) is mixed with condensed recycle in the bottom part of the fractionator. The feed is then pumped to the heater (furnace) where it is quickly heated to reach a thermal cracking temperature of about 480-510 °C. To prevent coke formation in the heater coils and to maintain minimum velocity, steam is injected in the heater coils. A favorable heater design configuration allows for one half of the heater to be offline while the other half remains online. The offline half can then be de-coked, which allows for continuous furnace operation. The feed partially vaporizes and the heated coke drum feed is then ‘delayed’, with a short residence time in the heaters. The coker feed is converted to lighter hydrocarbons and solid coke in the coke drums. The vapors leave from the top of the coke drums. The drums have to be operated in pairs, thus a minimum of two coker drums are required. While one drum receives the heater discharge the other one can be de-coked.

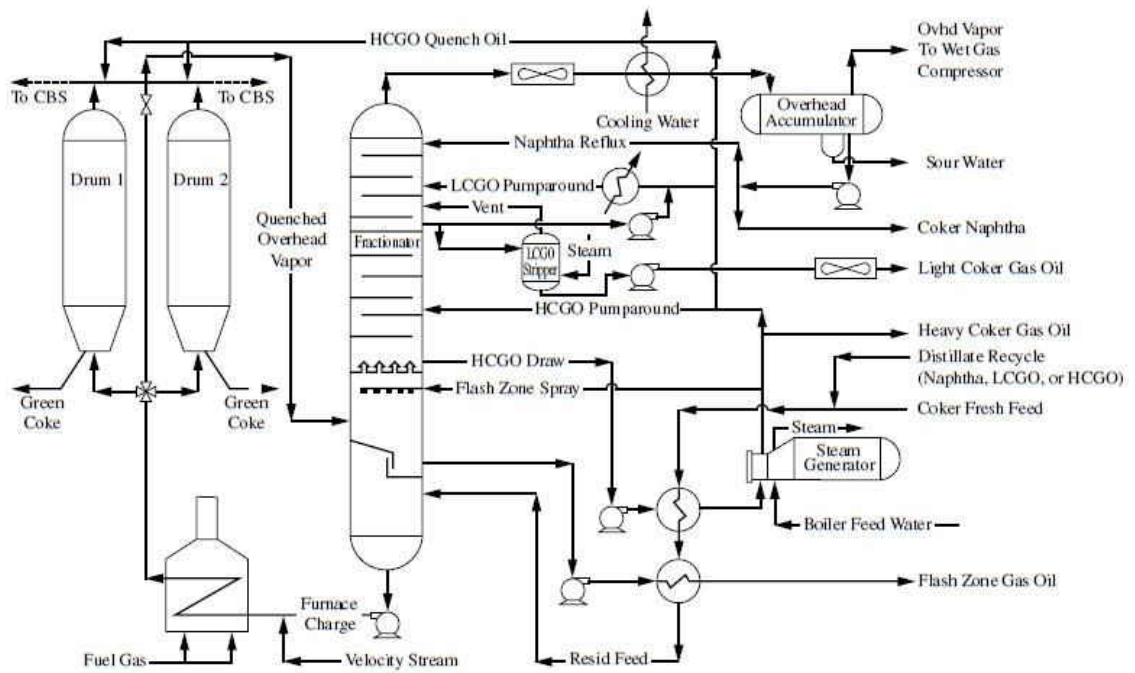


Figure 5: Detailed Process Flow Diagram for the Delayed Coking Process [15]

The vapor from the drum flows to the fractionator where it is quenched with the fresh incoming feed. It is then washed with hot pump-around oil in the wash trays. Doing this cools the vapor and condenses the recycled stream. Fresh feed combines with this recycle stream and is pumped from the fractionator to the heater. Partial condensation of the overhead vapor takes place in the fractionator column, after which the vapor stream flows to the fractionator overhead drum. The fractionator stream is refluxed with condensed liquids collected in the overhead drum. Vapor and liquid separation is carried out in the drum, and the vapor flows under pressure control to the gas compressor. A heavy coker gas oil (HCGO) pump-around stream, which is circulated through the fractionator tower, primarily functioning as a coolant for the vapors and for condensing the heavy gas oil, is withdrawn from the fractionator as a product. The hot pump-around stream is used for steam generation. The light coker gas

oil (LCGO) is steam stripped and cooled before being stored. Steam stripping is done to remove light ends and clean the product stream.

The coke drums are important to provide reaction time to allow the coking reactions to reach completion and collect the solid coke formed. Coke is accumulated in the drum continually until it reaches a predetermined level, at which the furnace effluent is directed through a switch valve from the full drum into the other pre-warmed, de-coked drum [15]. Once the full coking drum is taken offline it undergoes cooling before the decoking process occurs (Figure 6).

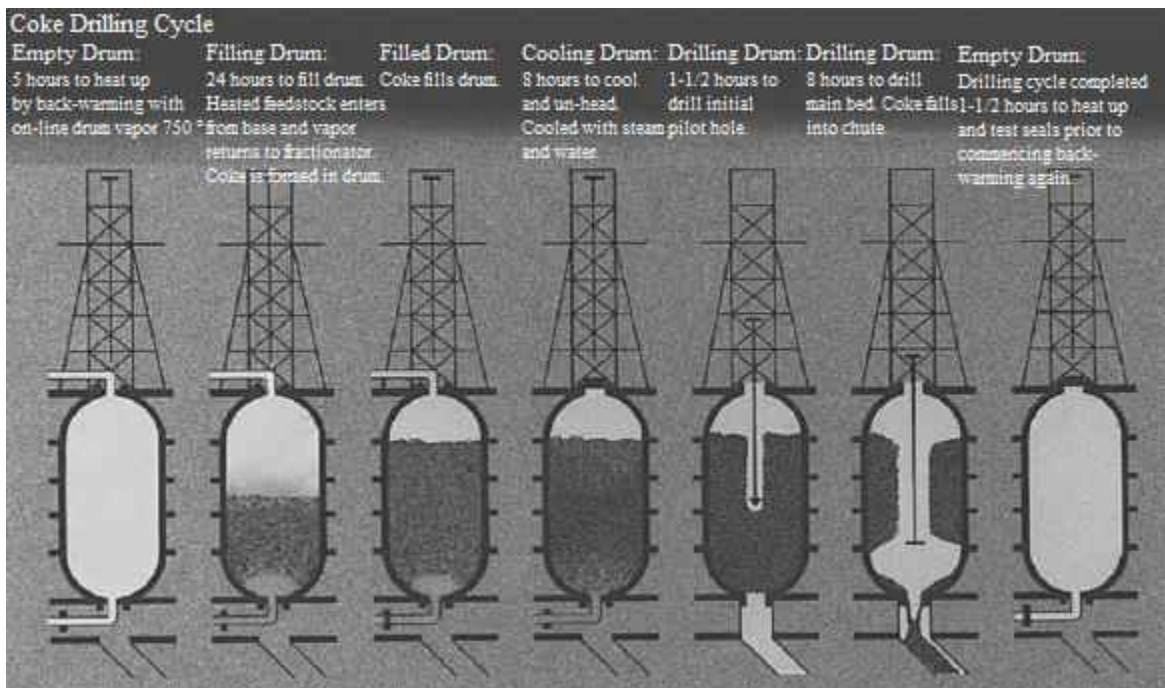


Figure 6: Diagram of the Coke Drum Drilling Cycle [15]

Coke is removed hydraulically using a jet water pump from the drum. A water stream of high-pressure (2500 to 4500 psig) and high-volumetric-flow (900 to 1300 GPM) cuts away the coke and the coke is collected at the bottom [15].

*Continuous Coking.* Most refineries at present day employ fluidized bed coking or delayed coking, with approximately 90 % of them using the delayed coking process as



of 2011 [19]. Both of these coking processes have received many upgrades over the years to continually optimize the process. However, there is a new design that has emerged within recent years that could change the technology of coking. This continuous coking process uses a matrix of closely passing blades that continually mix and scrape heavy, residual feedstock while also acting as a screw to move the material horizontally through a furnace. Heavy residual feedstocks from a conventional residuum heater in a coking plant are fed into this coking process, where volatiles and solid, dry petroleum coke particles are continuously discharged [19] (Figure 8).



Figure 7: Photograph of the blades inside of a Continuous Coking Furnace [20]

Figure 7 shows a possible configuration for the blades that would continuously scrape and move residuals through the coking process. Continuous coking uses a kneading and mixing action to continuously expose new residuum surface to the vapor space, producing a faster and more complete removal of volatile matter from the produced petroleum coke [19].

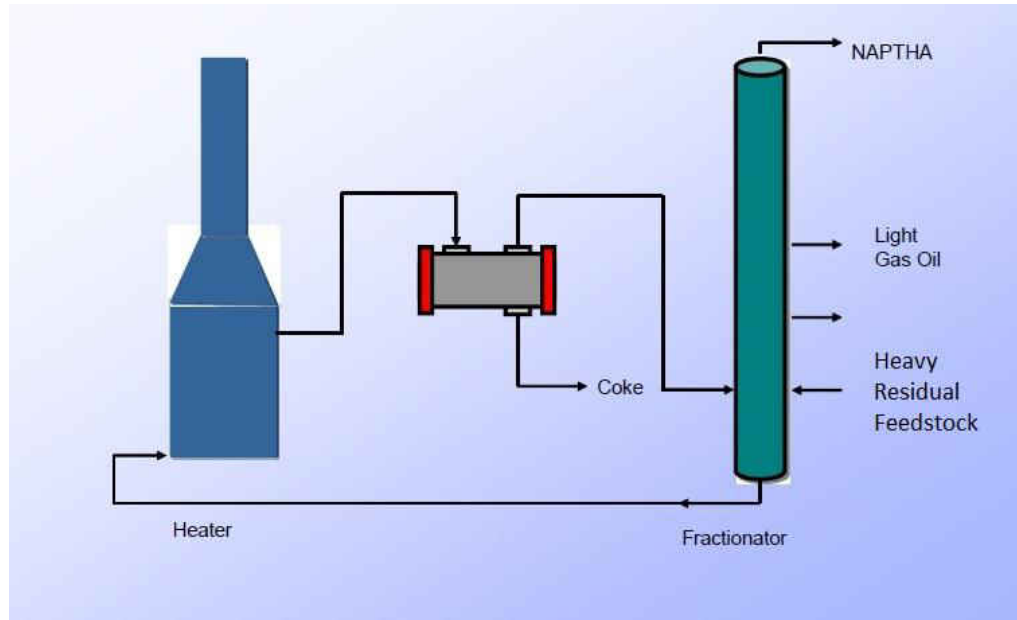


Figure 8: Process Flow Diagram of Continuous Coking [19]

Heavy residual oil is fed from a fired heater at a temperature of 460-540 °C and flows directly into one end of the horizontal reactor. This mixing action causes new surfaces of the residual oil to be exposed to the gas phase several times per second, causing rapid mass transfer of volatiles into the gas phase. This rapid reduction of volatiles in the residuum mass causes the carbonization reaction rates to accelerate, enabling continuous, rapid production of solid petroleum coke particles thereby producing a coke of uniform composition and size [19].

In theory, continuous coking seems to be the best coking process to refine heavy residual tars. However, it is a very new process and has not been put into operation at many refineries. There are some problems and difficulties that need to be resolved. Equipment is very expensive since it is a new process and the configuration of the scraping blades is incredibly mechanically complicated. This makes the construction of the equipment selective to a handful of companies.

In summary, coking is useful to recover even more liquid and gas products in addition to producing coke. The coking process has been an important aspect of processing vacuum residuals and other heavy feedstocks in oil refining for over 70 years because it significantly improves refinery yields and profit margins [19].

### *1.1.3 Types of Coke*

Petroleum coke is the main component used in the production of anodes for aluminum industries [16]. This application, as well as others, will be further discussed in the applications section. Petroleum coke is made up of elemental carbon organized primarily as a porous polycrystalline carbon matrix having a high carbon-to-hydrogen ratio [14]. It is a black solid material resulting from the high temperature treatment of heavy petroleum process streams and residues [17]. “Petroleum coke” is often used in place of the term “green coke”. Green coke is the initial product in the coking process and can be used as fuel in gasification and metallurgical processes or as feedstock to be further processed at higher temperatures to make calcined coke [14].

*Green Coke.* The composition of green coke consists of 88-95 % carbon, 3-4 % hydrogen, 1-2 % nitrogen, 0.58-6 % sulfur and 1-7 % oxygen. It is chemically stable and inert under normal conditions [16]. Hardened residual hydrocarbons, or volatile matter, occupy the pores of the green coke matrix but can be distilled off during the calcining process. Volatile matter in green coke is usually between 4 % and 15 %, but can be up to 21 % [14]. The amount of volatile matter in green coke is dependent upon the temperature of the coking drum as well as the cycle time and drum pressure. Green coke contains higher levels of volatile matter than calcined coke because of the lower temperatures used in its production [14]. In most cases, green coke is calcined to

improve the physical properties that are needed for specific applications, although if it is not suitable for calcining the green coke is burned as fuel [15]. The coke is then referred to as fuel grade coke.

The market for fuel grade coke is 50 million tons per year worldwide and competes with other fuels, mainly coal. Advantages that exist for fuel grade coke are that it has a higher heating value than coal since the heating value of coke is 14,000 Btu/lb while coal fluctuates between 8,000 and 12,000 Btu/lb [15]. Also coke has low moisture content and less dust formation during hauling.

The ash content of fuel grade petroleum coke is normally 0.5 to 1.0 weight %, which is lower than that of coal, which is typically 2 to 20 weight % ash depending on the source [15]. The disadvantages of fuel grade petroleum coke are that petcoke has a higher sulfur content, lower volatile matter content, and sometimes increased hardness than coal coke. The concentration of sulfur in petroleum coke is 4 to 7 wt % while coal is typically lower. Depending on the design of the burner, a solid fuel with a higher-volatile matter to maintain a stable flame may be required, eliminating the use of coke. Finally, crushing equipment may limit the hardness of the solid fuel that can be pulverized for use in power plants [15].

*Calcined Coke.* Other than for fuel or gasification, most applications require green coke to be calcined to improve its physical and chemical properties [14]. In calcining, green coke is subjected to high temperatures (usually above 1000 °C) in a reducing, inert atmosphere to liberate methyl groups and hydrogen that are attached to aromatic rings [15]. The resulting hard, dense calcined coke is nearly pure carbon with very low hydrogen content and trace amounts of sulfur and metals [21]. The calcining

process removes practically all of the residual oil and moisture content of the coke and improves its physical characteristics.

Calcined coke is characterized by wt % ash, wt % sulfur, wt % volatile matter, ppm nickel, and ppm vanadium. These properties of calcined coke are all dependent upon the green coke used, which goes back to the properties of the heavy residuals that are coked, and overall resulting from the feedstock originally used [21].

Calcined coke is usually a dustier material than green coke because of the lower oil content [21]. Physical properties are improved in calcined coke such as: increased physical strength, higher electrical conductivity [15], and lower coefficient of thermal expansion [14]. The calcination process of petroleum coke utilizes extremely high temperatures to remove metals and impurities, which in turn lowers the ash content. An advantage with crop oil coke is the low metal content, which wouldn't require the severe conditions needed for calcination [22]. All of these properties create a calcined petcoke material that is highly desirable for the use in the aluminum and steel industries [15].

Contingent upon its physical and chemical characteristics and the feedstock it was derived from, calcined coke is classified as shot, sponge, or needle coke [17]. Shot coke is a solid fuel occurring as small, hard spheres [17]. Shot coke is created from low API gravity, high asphaltene and resin petroleum precursors through the de-alkylation reaction mechanism [14].

Sponge coke is mostly used for anode-grade coke. This type of coke is dull black with a porous, amorphous structure [17]. It can be derived from asphaltic residuals, paraffinic-naphthenic residuals or virgin petroleum feedstocks, which contain large numbers of cross-linkages [16]. Another source for generation of sponge coke may be

gas bubble percolation inside the coke drum [14]. Sponge coke has an isotropic texture, which means properties are the same in all directions [16]. The properties of sponge coke vary depending upon the formation mechanism and coke structures although sponge coke is commonly used as a mixture with shot coke and needle coke [16].

Needle coke appears as silver-gray crystalline needles and has an anisotropic structure [17]. Needle coke is derived from condensation and polymerization through cross-linking of condensed aromatic hydrocarbons during coking reactions [16]. The dehydrogenation reaction mechanism occurs with high aromatic hydrocarbon feedstocks when needle coke is formed [14]. The properties of needle coke are: a small coefficient of thermal expansion, small volumetric density, relatively soft, and easy to become graphitic [16].

*Applications.* The most important application for calcined coke is as anode grade coke for use in the aluminum smelting process with 12 million tons per year produced worldwide [15]. Pitch is combined with calcined coke and formed into anodes for the electrolytic dissociation of aluminum from alumina ( $\text{Al}_2\text{O}_3$ ). Liberated oxygen is combined with carbon, which is consumed in the smelting process, forming carbon dioxide. Trace elements are detrimental to the operation of the aluminum cells and reduce the purity of the final aluminum product [15].

Calcined petroleum coke is also used in the reduction of titanium sands in the chloride process for producing  $\text{TiO}_2$ , which is the white pigment used in a variety of applications, such as paint production and the whitewalls in tire manufacturing. Production of titanium dioxide grade coke is between 700,000 and 800,000 tons per year [15].

Other applications include the manufacturing of graphite electrode production for arc furnaces [21], increasing the carbon content for steel and cast iron, or as a feedstock for petrochemical-grade carbon monoxide production. Calcined coke can also be used as a reducing agent for a variety of metal purification processes [15], used in polycarbonate plastics, or in carbon refractory bricks for blast furnaces. Finally coke is used as a packing media for anode baking furnaces and in cathodic protection systems of pipelines [14].

## 1.2 Motivation for Renewable Carbon Products

There are numerous advantages motivating the use of renewables. Fossil fuels are a finite resource and the continuing increases in the price of petroleum have driven research to explore renewable fuel sources [23]. Bio-fuels are made from renewable resources and are easily available since they can be produced domestically and contribute to sustainability [24]. Less carbon monoxide, particulates, and sulphur emissions are produced from the use of bio-fuels and therefore biofuels have the potential to reduce the environmental impact from applications [24]. The carbon dioxide emissions generated represent a carbon dioxide cycle in combustion [25].

The commercial challenges involved with bio-fuels are that this is a new technology and in order to be a feasible fuel source, bio-fuels need to be economically competitive with petroleum fuels [26]. Because of this it is highly attractive to research and develop high margin by-products that can create more revenue for a process.

## 1.3 Renewable Fuel Process at UND

At the University of North Dakota, research has been done to produce diesel and jet fuel from many different types of crop oils through the use of non-catalytic thermal

cracking. During cracking, heat is added to the process in the absence of air, specifically oxygen, to cleave chemical bonds in order to yield smaller molecules [27].

Figure 9 shows a simplified version of the overall renewable fuel process that was performed at the University of North Dakota. Many different vegetable oils and plant extracts can be used as feedstocks to make fuel, such as soy bean oil, canola oil, corn oil, algae oil, etc. This process can be done using different methods: batch autoclaves, continuously stirred tank reactors (CSTR), or other continuous processes. Different process conditions are implemented such as temperature, pressure, and residence time to produce the cracked oil, crackate. The next step is distillation of the crackate in order to remove the lighter, smaller hydrocarbons that were previously formed. Distillation can be done at atmospheric pressures or vacuum pressures. Thick, heavy residue layers,

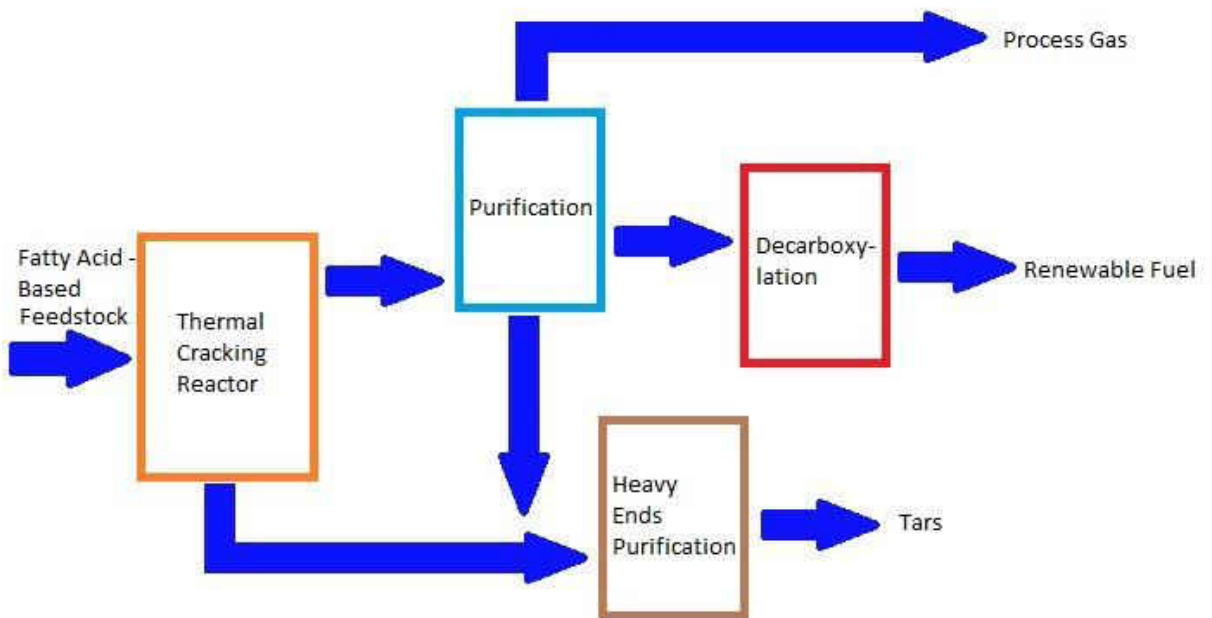


Figure 9: Simplified Process Flow Diagram of the Renewable Fuel Process at UND



known as tars, are also formed during cracking. When cracking is performed without a catalyst, the tars can be recovered and converted into a by-product.

Tars are polymers with low molecular weight and the composition of the tar is dependent upon the reaction conditions [1]. The by-product tar could be burned and used as a heat source, but these tars are a good candidate for the production of carbon materials, such as granular carbon products and carbon fiber. It is more advantageous to produce carbon products rather than burning the residual tar as a fuel source, since carbon products can add revenue to the process.

#### 1.4 Hypothesis of Research

Preliminary research and literature review have confirmed that high value carbonaceous materials can be made from the heavy, residual tars produced and recovered during crop oil cracking. However, optimum methods and process conditions will need to be explored for production and commercialization of the carbon products. Currently coal and petroleum tars are useful and valuable materials in the fabrication of carbon products and are important processes to replicate for the use of crop oil tars. Tars are made up of a chemically complex mixture of poly-aromatic hydrocarbons, which are required and necessary starting materials for the formation of polycrystalline coke solids [28].

Studies have shown that the ultimate properties and structure of carbon are formed in the early stages of carbonization. The chemical characteristics of tar such as aromaticity, aliphaticity, heteroatom content, and hydrogen distribution affect the mechanism of carbonization [28]. Key independent variables for the thermal cracking

and coking process are reaction temperature, reaction pressure, residence time, and feedstock [29].

The goals of this research are to use lab scale batch coking processes to collect overall mass balances for crop oil tars and to analyze and characterize the solid, liquid, and gas products resulting from the coking process. The overall goal of this work will be to eventually develop a continuous process for the conversion of cracked crop oil tars into high grade carbon products.

Since biomass derived coke contains less metals and impurities than petroleum coke, process conditions will be sought to optimize and maximize the production of solid coke, while also minimizing the formation of gas products. Preliminary research as well as vacuum distillation experiments performed in the lab has shown that the use of vacuum pressures may contribute to increased residual hydrocarbon removal from heavy residual tar in addition to allowing lower coking temperatures to produce solid bio-derived coke.

Thus the hypothesis that will be tested in this research is the use of vacuum pressure rather than atmospheric pressure to provide optimum coking process conditions will produce increased physical characteristics of solid coke, maximize the formation of bio-derived coke, and minimize the formation of low value gas products.

## CHAPTER II

### Experimental Methods

The first task of the project involved obtaining crop oil residual tars that are representative of residual tars accumulated from a commercial cracking process. The second task of this thesis work was to develop a process to optimize and maximize the formation of bio-derived coke, while also collecting lighter residual oil for recycle back into the process and reducing the formation of low value gas products. The third task was to characterize the solid, liquid, and gas products formed from the process.

#### 2.1 Obtaining Representative Tars

In order to study the optimization of the formation of bio-derived carbon, enough representative residual tar needed to be generated to perform lab scale testing. The challenge with this task was to identify an efficient lab-based method that provided commercially representative tars.

A continuously stirred tank reactor was used to thermally crack soy bean oil with the purpose of generating the heavy residual tars needed for this research work. Soy bean oil was fed to the CSTR reactor at 6 L/hour. Process conditions of the reactor were 410 °C and 1307.9 kPa (absolute). Reacted oil and vapors (Organic Liquid Product) were continuously removed overhead from the reactor and collected to be further processed into fuel. A difficulty with this process method was that tars would often become entrained in the OLP vapor that was collected overhead. There is a possibility for

unreacted feed to also pass through this stream. Heavy residual oil and any unreacted feed were collected from the reactor by passing a bottoms draw stream through a filter to remove solid coke particles. The reactor bottoms draw stream was gathered at a rate of 500 mL/hour.

The organic liquid product of the cracking reactor was collected and sent to a distillation column at a rate of 60 mL/min. The bottoms temperature was 240 °C for this distillation column, while the temperature of the top was operated at 125 °C. Residual oil from this first distillation column was then further processed in a second distillation column at a rate of 40 ml/min. The operating temperatures for this second distillation column were 350°C and 200 °C for the bottoms and overhead temperature, respectively. This distillation column was given the name D-300 in process diagrams. The heavy residual oil that was left in the bottom of this second distillation column was collected to be used for the research work and was labeled D-300 bottoms. The heavy residual tar left from the distillation process was selected as a better representative tar over the bottoms draw from the CSTR reactor for two reasons: 1) unknown quantities of unreacted feed oil in the reactor bottoms draw can obscure results and 2) changes were in progress to explore a new reactor design that would make the reactor bottoms obsolete. Therefore this stream was not felt to be representative of the commercial process.

## 2.2 Initial TGA Testing

Using a TA Instruments SDT Q600 TGA machine (Figure 10), D-300 bottoms oil was initially tested to find optimum coking conditions. A sample was placed in an alumina crucible which, along with an empty reference crucible, was moved into the furnace where they were heated to observe changes in the mass of the sample crucible

compared to the reference crucible. The method sequence for testing the D-300 bottoms tar with the TGA was performed using the following steps: equilibrate at 30 °C, ramp 30 °C/min to 1000 °C, isothermal for 90 minutes. The testing was done using a nitrogen purge flow of 100 mL/min through the furnace.



Figure 10: Photograph of the TA Instruments SDT Q600 TGA

Since the coking reactor would run at a lower nitrogen purge flow, tests were also performed using 90 mL/min and 30 mL/min to confirm no flow effect on the coking process. The method sequence for these tests were: equilibrate at 30 °C, isothermal for 10 minutes, ramp 30 °C/min to 430 °C, ramp 5 °C/min to 550 °C, isothermal for 15 minutes. The heating rate through the coking region was slowed down for these tests to confirm the temperature range that would be tested using the lab scale coking reactor.

There were two reasons a lab scale coker was used for the coking research rather than the TGA: 1) D-300 bottoms sample would boil over the alumina sample cups of the TGA, making the mass yields unreliable and 2) the products of the coking process (solid,

liquid, and gas products) were too small to perform characterization analysis when generated in the TGA.

### 2.3 Lab Scale Coker

A lab scale coking reactor was constructed and assembled to perform coking experiments with the D-300 bottoms using atmospheric and vacuum pressures (Figures 11,12, & 13). This process performs the removal of volatile matter and coking of tar all in one process. Based on initial TGA testing the temperature range that would be tested was 450 °C to 490 °C at 10 °C intervals. There was not a high level of temperature control inside of the reactor therefore 10 °C was the minimum temperature interval that could be comfortably tested. Some preliminary lab scale coker testing also showed that atmospheric pressures produced more char and less gas, therefore only a high and low temperature would be tested using vacuum pressures.



Figure 11: Photograph of the Lab Scale Coking Reactor

A Watlow ceramic tube furnace that operated with a maximum 120 volts and 1100 watts was used. It was six inches tall and had an outside diameter of eight inches with an inside diameter of four inches. The ceramic tube furnace was controlled by a PID controller using a thermocouple that was placed between the heater coils and reactor vessel. A half inch gap was required between the heater coils and reactor. A second thermocouple was inserted through the top of the reactor into the tar sample. Both temperatures were recorded at 1 minute intervals during the coking process for all testing.

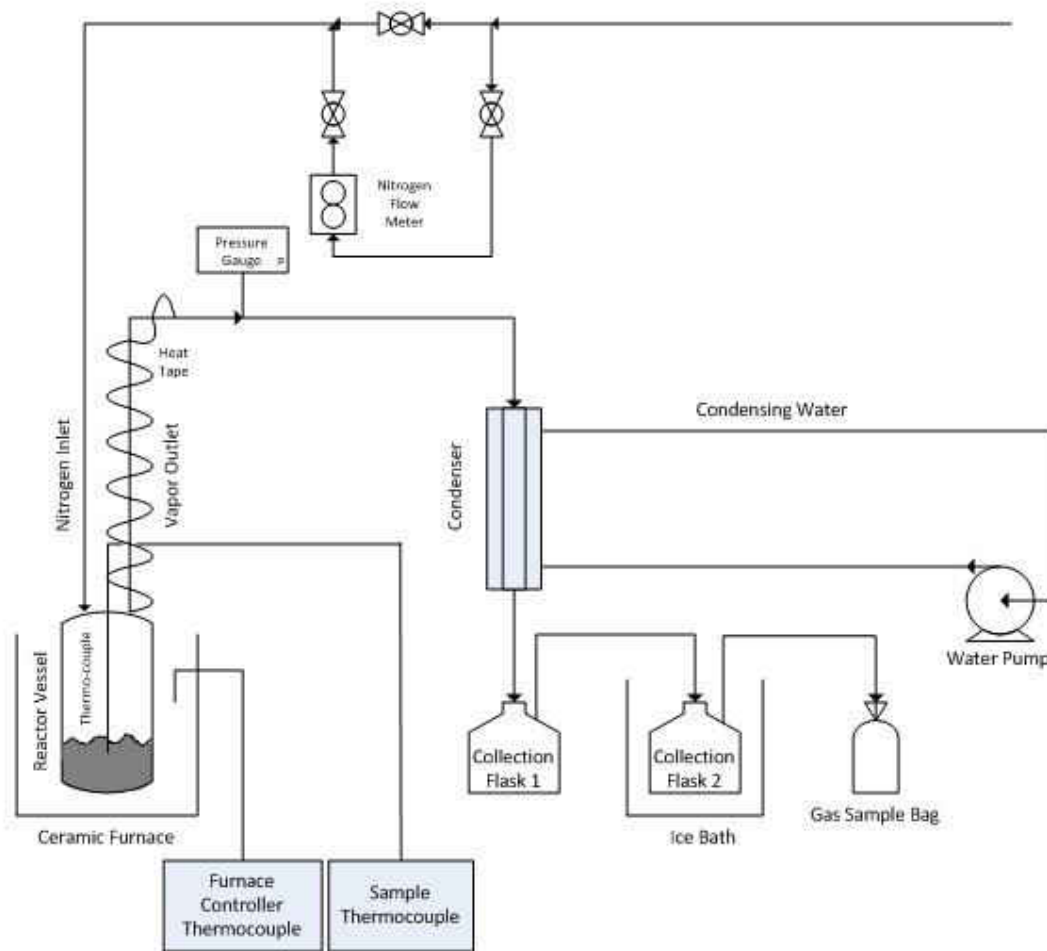


Figure 12: Process Flow Diagram of Coking Reactor Using Atmospheric Pressure

Figure 12 shows the process flow diagram of the coking reactor for atmospheric pressure testing. For atmospheric pressure testing, a constant flow of nitrogen was sent through the system to create an inert atmosphere for coking. The flow was measured at approximately 30 mL/min. The furnace heats the tar in order to boil residual volatile matter for removal. Hydrocarbon vapors are kept hot as they exit out of the top of the reactor vessel with heat tape. Then the stream was cooled through the condenser and liquid distillates were collected in a flask below. The remaining gases and vapors flowed past the first flask to a second collection flask, which was placed in an ice bath to condense additional hydrocarbons. This second flask was only necessary for the vacuum pressure testing, although it was kept in the system for all research. Remaining non-condensable gas continued past the second collection flask and was collected in a SKC one liter gas sample bag. Gas samples were only collected for atmospheric pressure testing for analysis of gas products.

Figure 13 shows the process flow diagram of the coking reactor for vacuum pressure testing. For this testing, the gas sample bag was removed from the system. A combination of two needle valves with a dampening tank and vacuum pump was connected to the system and run throughout the testing. The needle valves were used to control and stabilize the vacuum pressure being used on the system. The use of a dampening tank was needed to reduce the pulsations produced by the vacuum pump. The nitrogen inlet valves were closed for vacuum pressure testing. The vacuum pressure was monitored during this research using the pressure gauge in the system. The vacuum



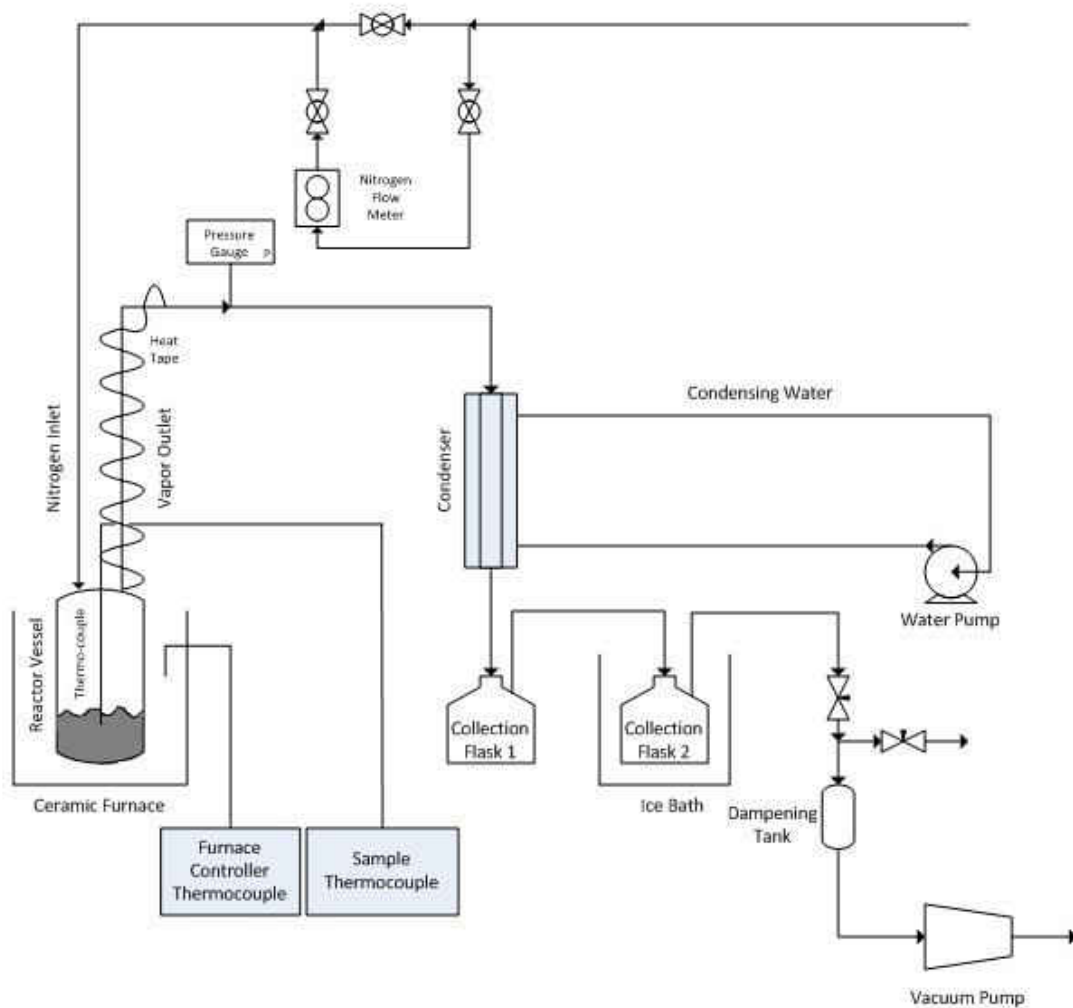


Figure 13: Process Flow Diagram of Coking Reactor Using Vacuum Pressure

pressure during testing ranged from 39.4 to 59.3 kPa (absolute). Vacuum pressure would start out at 39.4 kPa (absolute) but as the coking temperature increased more gaseous products were produced, causing the vacuum pressure to decrease to around 59.3 kPa (absolute). The gases and vapors followed the same path as the atmospheric pressure testing through the condenser and two collection flasks. Non-condensable gas passed through the vacuum pump and was vented through the hood. Mass balances were recorded for both atmospheric and vacuum pressure testing, and solid and liquid samples were collected for further characterization analysis.

## 2.4 Analysis of Solid Products

After each coking experiment, the reactor was allowed to cool back to room temperature. The remaining solid char left in the bottom of the reactor vessel was scraped out and collected for characterization.

### 2.4.1 Carbon Content

A Shimadzu TOC-V<sub>CSN</sub> Carbon Analyzer (TC Furnace, Figure 14) with a Solid Sample Module (SSM, 5000A) was used to measure the total carbon content for each coke sample. A calibration curve is made at the beginning of each day the machine is run. The standard used for total carbon (TC) testing is dextrose (C<sub>6</sub>H<sub>12</sub>O<sub>6</sub> gfw = 180.16) which is 40.00 % C by weight. The TC furnace is operated at 960 °C. Four calibration points were used, with duplicates at each point, to construct the calibration curve. Then coke samples were analyzed and carbon content was measured by the machine.



Figure 14: Photograph of the Shimadzu TOC-VCSN Carbon Analyzer and SSM 5000A

### 2.4.2 Moisture Content/Volatile Matter/Fixed Carbon/Ash Content

Analysis for moisture content, volatile matter, fixed carbon, and ash content was performed on the solid coke samples using a TA Instruments SDT Q600 TGA machine

(Figure 15). Around 10-20 mg of coke sample was placed in an alumina sample cup. Weight percent and derivative weight percent versus time were the signals that were monitored while testing to verify completion of mass loss. The method sequence for this testing was established by combining three ASTM standards into one analysis. The first step of the method sequence began by equilibrating the furnace to 30 °C. Then the moisture content was determined in the coke sample using ASTM D3173-03 (2008) [30]. The furnace was heated at 30 °C/min to 105 °C and held isothermal for 10 minutes in a nitrogen atmosphere. The next portion of analysis was to evaluate the volatile matter in the sample via ASTM D3175-07 [31]. Continuing to use a nitrogen atmosphere, the furnace was heated at 30 °C/min to 950 °C and held isothermal for 7 minutes. The final portion of analysis was to measure the ash content in the coke sample as referenced by ASTM D3174-04 [32]. Gas inside the furnace is switched to air and held isothermal at 950 °C for 20 minutes to burn off the carbon.



Figure 15: Photograph of the TA Instruments SDT Q600 TGA

## 2.5 Analysis of Liquid Products

Liquid hydrocarbon distillates collected during the coking process in collection flasks 1 and 2 were analyzed in order to characterize the products from coking. The liquid distillate samples were analyzed using a Perkin Elmer Clarus 480 Gas Chromatograph SimDist (Figure 16) to determine the boiling range distribution contained in each sample, as well as the use of a Thermo Scientific Nicolet IR 200 FT-IR (Figure 17) to measure the concentration of acids in each sample.

### *2.5.1 Liquid Analysis*

Gas chromatography was used to simulate the boiling point range distribution of hydrocarbons by distillation, for the liquid samples collected after coking. The samples are injected into the Perkin Elmer Clarus 480 gas chromatograph column and hydrocarbon components are eluted in order of increasing boiling point. Analysis procedures were performed by referencing the ASTM D2887-02 [33] test method. Helium was used as the carrier gas at a pressure of 170.2 kPa (absolute). The injector temperature was 350 °C and the detector temperature was 400 °C. The column temperature was held isothermal at 35 °C for 5 minutes. Then the temperature was raised at a linear rate of 25 °C/min until the temperature reached 325 °C and held isothermal for 20 minutes. The response of the hydrocarbon components and the area under the chromatogram were recorded by a computer throughout the analysis.



Figure 16: Photograph of the Perkin Elmer Clarus 480 Gas Chromatograph SimDist

A known mixture of hydrocarbons was used to create a calibration curve in order to assign boiling points to retention times for hydrocarbon compounds eluding from the column. The standard mixture contained the following hydrocarbons: dichloromethane (solvent), n-hexane, n-heptane, n-octane, n-nonane, n-decane, n-tridecane, n-hexadecane, n-nonadecane, and n-tricosane. At the beginning of each day that distillate samples were analyzed with the GC SimDist instrument, a blank test was run to observe the baseline of the chromatogram. Then the standard mixture was injected into the column with the purpose of constructing a calibration curve. Finally another blank test was run. Once these opening tests were performed, samples were injected to be analyzed. Two hydrocarbon samples were analyzed, one after another and then a blank sample was run to continue observation of the baseline of the chromatogram, followed by two more hydrocarbon samples and then another blank. This pattern was repeated until all samples were analyzed. The blank samples were important for the data processing because the blank chromatogram was subtracted from the sample chromatogram of each sample to perform integration of each sample chromatogram.

### 2.5.2 Acid Analysis

The liquid samples collected after coking were also analyzed using a Thermo Scientific Nicolet IR 200 FT-IR to measure the acid concentration, in order to further characterize the liquid product. Absorbance was measured by the FTIR instrument and was plotted by a computer on the y-axis along with the wave length on the x-axis to make a spectrum. Standard mixtures consisted of octanoic acid ( $\rho = 0.91$ , MW = 144.22) in dodecane ( $\rho = 0.749$ , MW = 170.34) and were combined by weight percent. The mixtures used were approximately 25, 15, 5, and 1 weight %, as well as a blank. From the FTIR spectra, peak height was measured at  $1680\text{ cm}^{-1}$ . This wave length corresponds to the C=O double bond functional group representative in carboxylic acids. The peak heights were plotted versus the concentration of the standard mixtures (mol/L) to construct the calibration curve. Using the calibration curve, acid concentrations can be found using the peak heights of the liquid distillate samples.



Figure 17: Photograph of the Thermo Scientific Nicolet IR 200 FT-IR

## 2.6 Analysis of Gas Products

When coking tests were performed at atmospheric pressures, gas samples were collected in SKC one liter gas samples bags. The first gas sample bag was connected to the system when the temperature inside the tar reached approximately 250 °C for each test. The first noticeable drip of liquid distillates would come through the condenser when the reactor temperature reached approximately 330 °C. Once a gas bag was around 80-90 % full, the bag would be swapped for an empty gas bag. Between four and five gas sample bags were needed to collect the entire gas sample released from a coking test. The purge nitrogen gas was also collected in these gas bags.

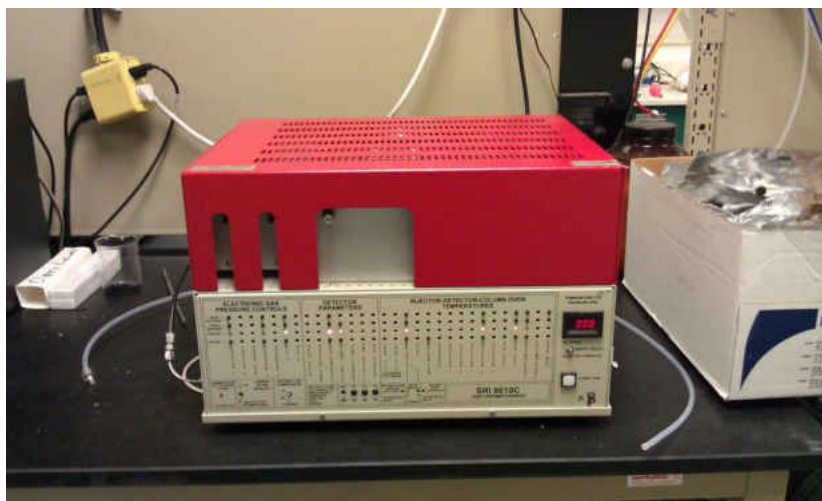


Figure 18: Photograph of the SRI 8610C Gas Chromatograph

A SRI 8610 C gas chromatograph (Figure 18) was used to measure the distribution of the light, non-condensable gases in each gas sample. The GC column installed in the machine was a Restek packed column HayeSep Q 80/100 6 ft, 2 mm ID stainless. A thermal conductivity detector (TCD) was used to measure the hydrogen concentration. A flame ionization detector (FID) was used to measure the concentration of light hydrocarbons, from C1 to C7, in addition to the concentrations of carbon

monoxide and carbon dioxide. Carbon monoxide and carbon dioxide can be measured by packing the methanizer with a catalyst that converts these gases to methane, which can be detected by the FID. Note the retention for methane is different from both the retention time of carbon monoxide and carbon dioxide. Therefore all three gases can be distinguished. The other hydrocarbons are unaffected when they pass through the methanizer.

Because coker gas was diluted with the nitrogen purge gas, nitrogen was selected as the carrier gas to operate the gas chromatography column. The pressure of the nitrogen carrier gas was 184 kPa (absolute). Hydrogen for the FID detector was at a pressure of 246.1 kPa (absolute). The temperature program used to analyze each gas sample started with the column set at 38 °C for 2 minutes. Then the column was heated at a linear rate of 20 °C/min until a final temperature of 250 °C was reached and held for 5 minutes.

A calibration bag, consisting of carbon monoxide, carbon dioxide, and propane diluted into nitrogen was used. The volume fractions for CO, CO<sub>2</sub>, and C<sub>3</sub>H<sub>8</sub> were 12 %, 20 %, and 8 %, respectively. Another calibration bag consisting of 10 % volume fraction hydrogen diluted in nitrogen was also mixed. Both of these calibration bags were used to construct calibration curves for the data analysis. The activity of the catalyst in the methanizer needed to be calculated with calibration gas each day to confirm proper conversion of the gases. All of the gas sample bags were analyzed either the same day or within 24 hours of the coking test so that the escape of any light gases would be negligible. Composition of the gas was calculated on a mole basis and took into account the volume of nitrogen purge gas that was mixed into each sample bag from testing.



## CHAPTER III

### Results & Discussion

#### 3.1 Initial TGA Testing

The first data collected for this research was initial TGA testing of the D-300 bottoms residue to identify a range of optimal coking temperatures. This is done by observing the temperature at which the weight % of the sample remains stable because this is where the sample has finished coking completely. The TGA displays the change in mass of a sample as heat is applied. The derivative weight % indicates the point where the change in the weight % has stopped.

Figure 19 shows the weight % (mass of sample over initial mass) and derivative weight % versus temperature for the D-300 bottoms sample performed on the TGA. The D-300 bottoms sample was the tar sample collected to represent a commercially representative tar to study. My observations from the weight % curve concluded that a temperature range between 450 °C and 490 °C should be tested. The heating rate of this test on the TGA was 30 °C/min and since the coking reactor heat rate would be less than 10 °C/min this seemed like an appropriate temperature range. Further testing will verify this temperature range. The derivative weight % shows where the mass loss it at its

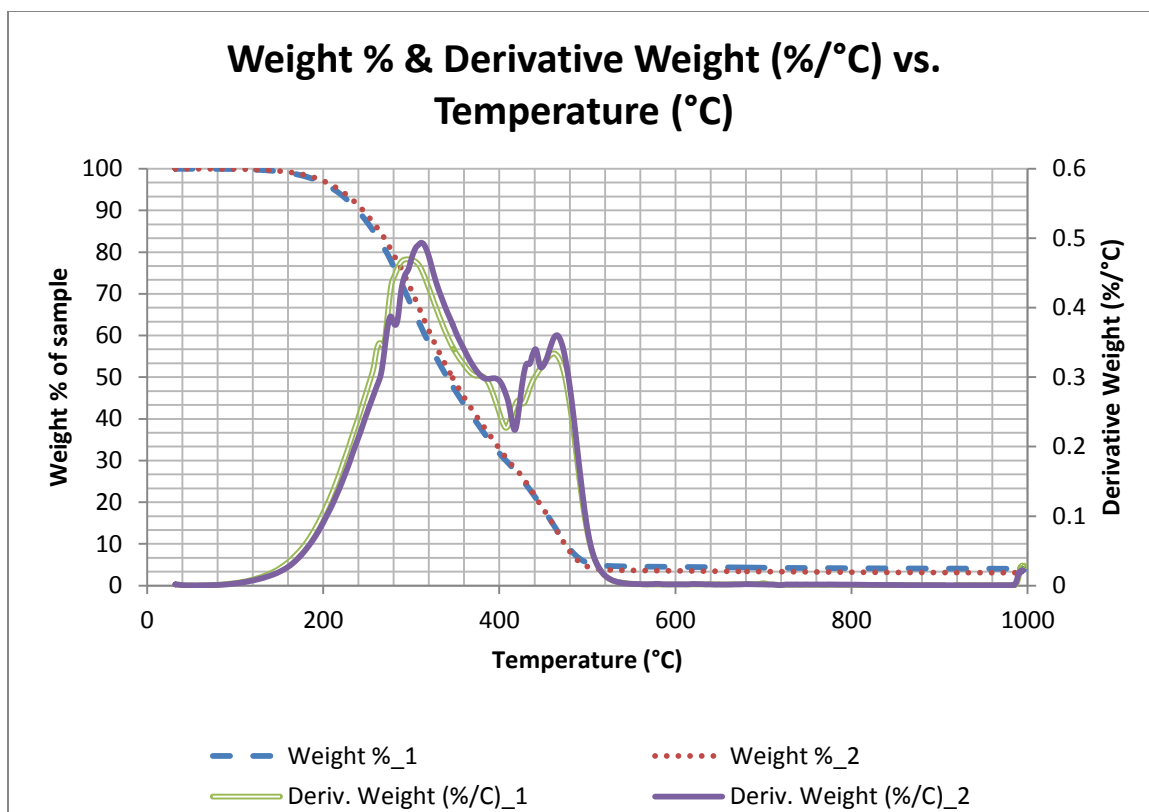


Figure 19: Initial TGA Testing on D-300 Bottoms

highest. The first peak occurs where the lighter hydrocarbons in the sample are being removed and the second peak represents either the coking of the remaining mass into a carbon product or possibly thermally cracked unreacted feed oil.

After this first test, a second test was performed to confirm that the flow of nitrogen purge gas through the furnace would not affect the coke yield or temperature of coke formation. This was tested because the lab scale coking reactor would be operated at a nitrogen flow of 30 mL/min.

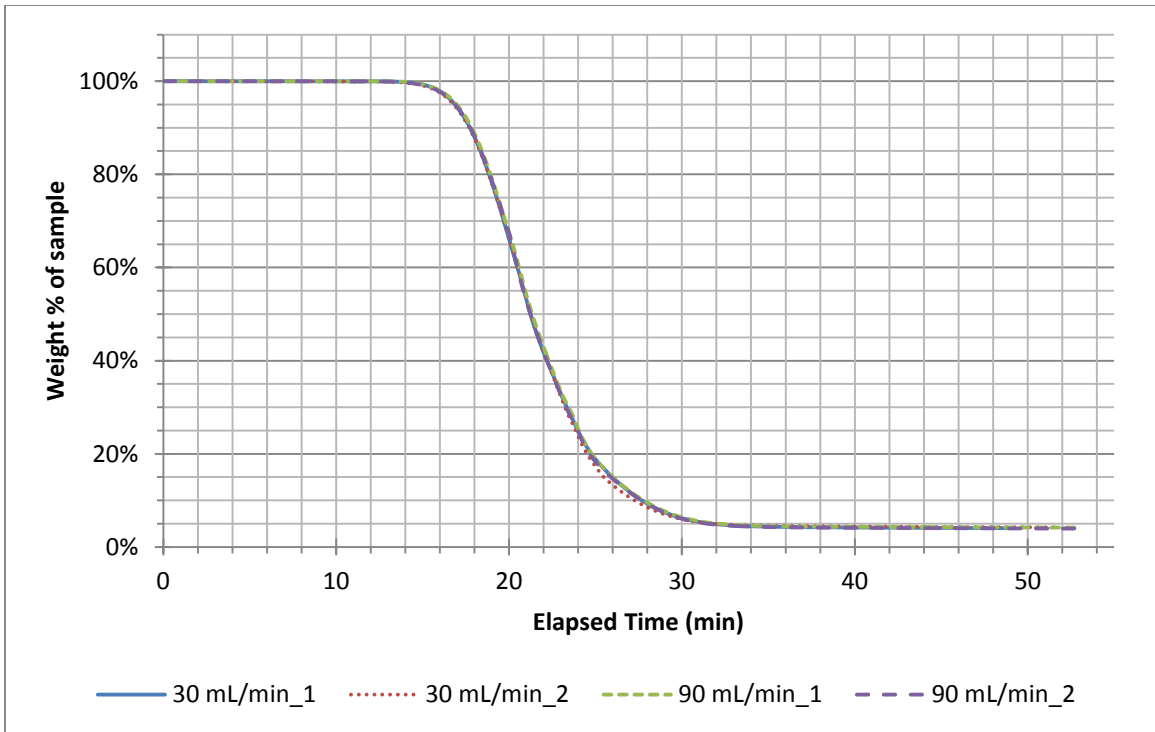


Figure 20: Coke Formation for Varied Nitrogen Flow Rates Based on Time

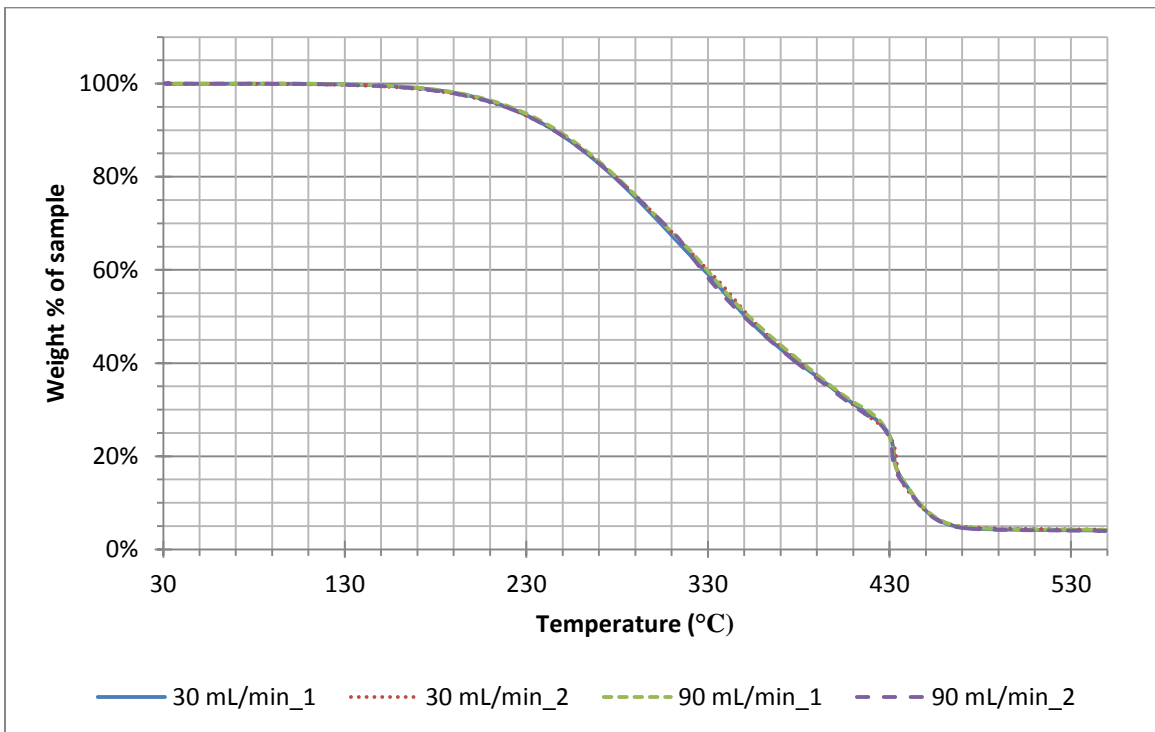


Figure 21: Coke Formation for Varied Nitrogen Flow Rates Based on Temperature

Both Figures 20 and 21 show that a slower flow rate of nitrogen did not affect the formation of coke since the graphs are all similar. Figure 21 has the slight hump right around the coking conditions that was not seen in Figure 20. This is because of the method sequence used for testing since Figure 20 shows weight % of sample versus elapsed time and Figure 21 shows weight % of sample versus temperature. The ramp rate was lowered from 30 °C/min to 5 °C/min at 430 °C to better observe this coking region in the second set of experiments (Figure 21). My observations from the weight % curve in Figure 21 confirmed the temperature range that would be tested between 450 °C and 490 °C.

### 3.2 Lab Scale Coking Experiments

D-300 bottoms sample was heated in the coking reactor following the procedure described in 2.3 experimental methods - lab scale coker section. Figure 22 shows the temperature inside the coking reactor recorded every minute. This graph shows a point when the heating rate slows down at around 330 °C for all of the coking tests. At this temperature the first distillates start exiting the reactor and therefore heating of the sample slows down.

In preliminary coking tests it was observed that the lower limit of testing (450 °C) didn't allow for complete coking of the D-300 bottoms sample. Inside the reactor would be a mixture of solid coke formation surrounded by a heavy residue. This testing revealed that 460 °C was the temperature at which D-300 bottoms completely formed a solid coke and produced the highest yield of solid, as shown in the mass balances in Table 1. This temperature was considered to be the optimum coking temperature for

processing the heavy tar residual and was therefore tested in triplicate throughout this research. The 460 °C coking test will be represented by a \_1, \_2, or \_3 in the results.

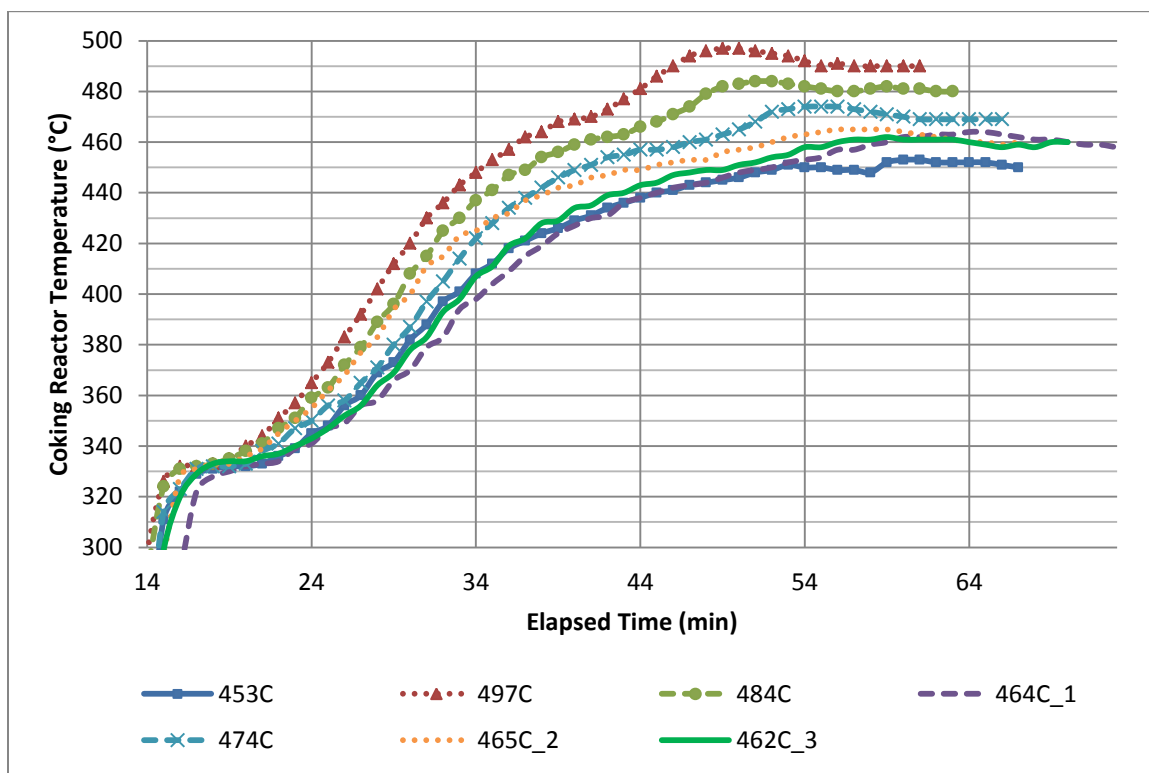


Figure 22: Coking Reactor Temperature Versus Time for Atmospheric Pressure Coking of D-300 Bottoms

Preliminary testing also showed that vacuum pressures produce less char and that 450 °C wasn't hot enough to completely coke the sample. Therefore, only the temperatures 460 °C and 490 °C were tested under vacuum pressures to compare to the mass balance of the same temperature preferred at an atmospheric pressure. The value represented in the results is the maximum temperature reached during that particular coking test.

Figure 23 shows the reactor temperature of the vacuum pressure tests over time. The first portion was heated at atmospheric pressure, up until between 360 °C and 370 °C

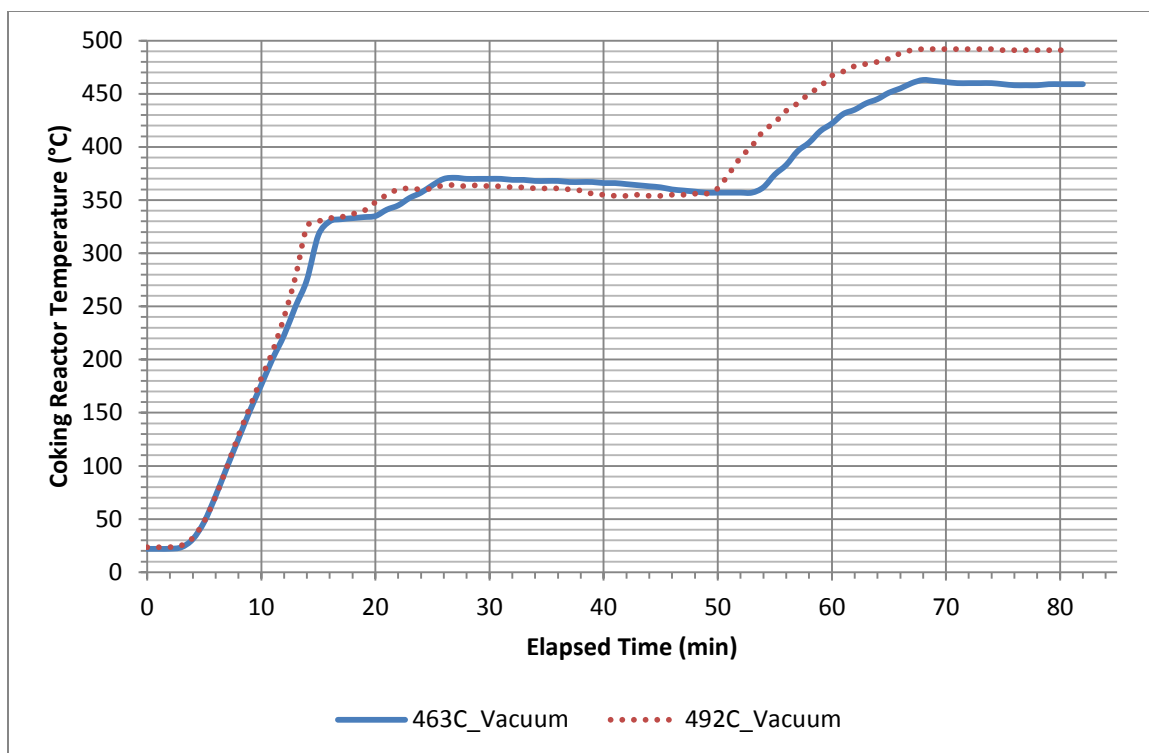


Figure 23: Coking Reactor Temperature Versus Time for Vacuum Pressure Coking of D-300 Bottoms (cracking temperature is 370 °C), and then the system was switched to vacuum pressures and further heated. Details of this procedure can be found in Appendix A.

Table 1: Mass Balance for Coking Reactor Batch Experiments in Weight %

Max Temperature	Solid (coke)	Liquid	Gas (by difference)
453 °C	13.0	82.7	4.3
464 °C_1	10.1	85.3	4.6
465 °C_2	10.1	85.4	4.4
462 °C_3	10.7	84.8	4.5
Vacuum 463 °C	7.5	88.9	3.6
474 °C	9.4	86.4	4.2
484 °C	8.9	86.8	4.3
497 °C	8.2	87.4	4.4
Vacuum 492 °C	6.7	89.1	4.2

Table 1 shows the mass balances that were calculated from batch coking reactions at various temperatures. The solid portion is evaluated by weighing the mass of coke

remaining in the reactor as well as any residual coke that built up on the gasket, thermocouple, and top flange of the reactor. The results show that reactions at vacuum pressure produced 3.2 to 1.5 percent less char than reactions conducted at atmospheric pressure at the same temperature. The liquid portion is evaluated by simply weighing the distillates and subtracting the weight of the clean flask.

By subtraction, the gas fraction is calculated from the solid and liquid fraction. Since the gas fraction is calculated from this subtraction method, a source of error is any light residual hydrocarbons that accumulate on the walls of the vapor outlet or condenser that aren't collected in the flask. Note that the gas fraction remains similar for all tests. This is significant because the reactions at vacuum pressure produce more liquid product.

The mass of solid seems to get smaller while the liquid fraction increases as the coking temperature increases. The reason for this is because higher temperature induces the removal of more semi-volatile matter, and in return less mass of solid coke. The mass is moved from the solid fraction to the liquid fraction as the temperature increases. This is noteworthy because it suggests that there will still be volatile matter in the coke that will need to be removed, depending upon the application for this coke.

Figure 24 combines the mass balances shown in Table 1 with mass balances that were collected from some preliminary coking testing (Appendix B). As shown, solid fraction decreases as temperature increases over this temperature range. The graph gives a good estimate of coke formation for coking temperatures between 460 °C and 500 °C. The preliminary coking tests only provided mass balance data. None of the products were saved for further analysis.

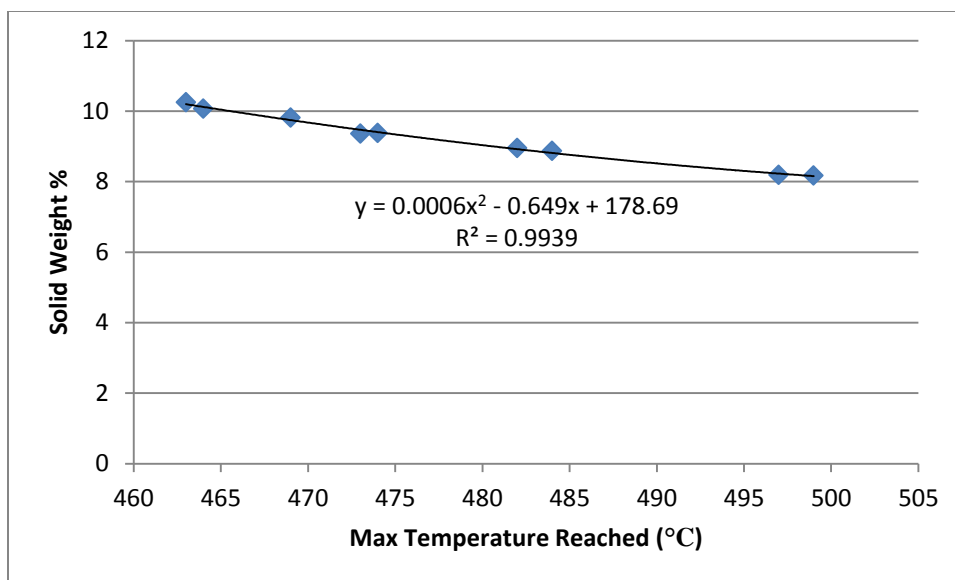


Figure 24: Coke Formation Versus Temperature from Batch Atmospheric Pressure Coking Reactions of Crop Oil Cracking Derived Tars

### 3.3 Analysis of Solid Products

#### 3.3.1 Carbon Content

The concentration of carbon in each coke sample was measured using the Shimadzu TOC-V<sub>CSN</sub> Carbon Analyzer and Solid Sample Module (SSM) 5000A. Standard solutions are measured to calibrate the machine. The total carbon of each standard is plotted versus the area under the curve to make a calibration curve. Using this calibration curve and the measured area from the sample, the instrument calculates a carbon concentration (wt %) for each unknown coke sample. For a more detailed explanation refer to Appendix C. The results can be seen in Table 2.



Table 2: Carbon Content in Coke Samples

Condition	Temp. (°C)	Carbon (wt %)	Avg C (wt %)
Atmospheric Pressure Coking	497 °C	92.94	91.6
		90.26	
	484 °C	93.30	93.0
		92.60	
	474 °C	91.53	93.3
		93.25	
		97.04	
		91.33	
	464 °C_1	91.38	91.3
		88.59	
		94.81	
	465 °C_2	90.56	91.8
91.7			
92.43			
92.22			
462 °C_3	91.00	91.6	
	91.81		
	91.15		
	91.19		
Vacuum Pressure Coking	492 °C	88.21	88.1
		88.05	
	463 °C	91.21	92.3
		93.33	

Carbon content was measured for the 464 °C\_1, 465 °C\_2, and 462 °C\_3 coke samples a total of four times each to assess the variability in the results. The 474 °C coke sample was also measured four times since it was the next closest coking temperature to the considered optimum coking temperature, 460 °C. All other coke samples were measured twice. No trends are seen in the relationship between the coking temperature

and the concentration of carbon in the coke produced. This is most likely due to the narrow range of coking temperatures tested in relation to the broad coking temperature range that exists between green coke (460 °C) and calcined coke (above 1000 °C).

Overall, the green coke that is produced from D-300 bottoms (commercially representative tar) at the optimum temperature of 460°C will contain approximately 92 % carbon. However, this property is dependent upon the process conditions and original feedstock used for thermal cracking.

### 3.3.2 Moisture Content/Volatile Matter/Fixed Carbon/Ash Content

A TA Instruments SDT Q600 TGA instrument was used to measure the moisture content, volatile matter, fixed carbon, and ash content of each coke sample. Procedures were followed as explained in section 2.4.2. Analysis of the data was performed using the Universal Analysis software provided with the instrument.

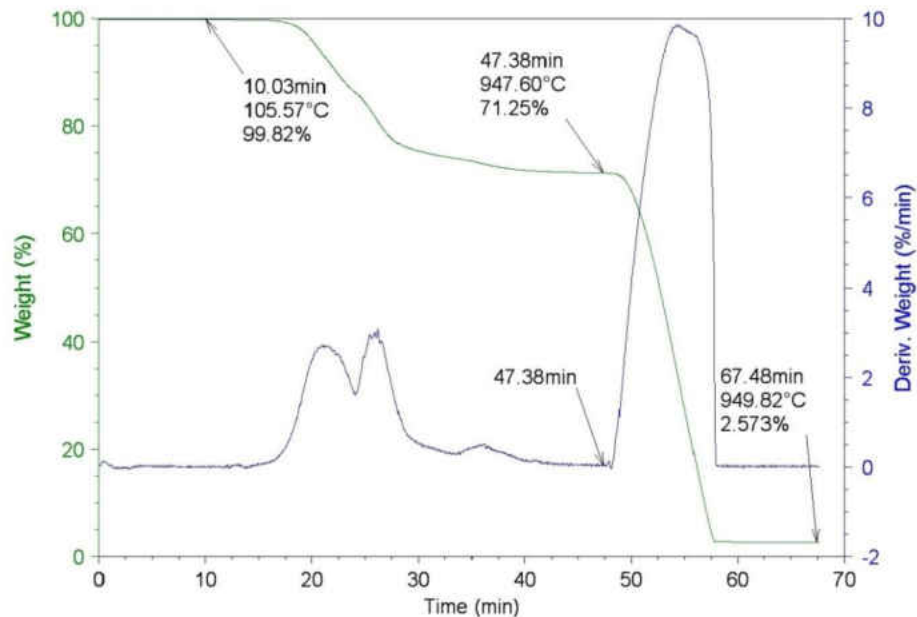


Figure 25: Moisture Content/Volatile Matter/Fixed Carbon/Ash Content Evolution for a 464 °C\_1 (test 1) Coke Sample

Figure 25 shows a graph from the analysis of moisture content, volatile matter, fixed carbon, and ash content for the 464 °C\_1 (test 1) coke sample. The weight % of all three components can be calculated using this analysis. Weight % of the sample and the derivative weight %/min are graphed versus time. The derivative weight %/min shows where majority mass loss occurs and indicates when the mass has been essentially all removed from the sample for each step.

The first point labeled in the graph is the mass remaining after the moisture content has been removed. This is obtained by heating the coke to 105 °C in an inert atmosphere (nitrogen). In order to calculate the moisture content for the sample, this point is subtracted from 100 wt % to find the mass of moisture that was volatilized and removed from the sample.

Volatile matter is represented by the second plateau. The volatile matter is removed by heating the coke sample to 950 °C in an inert atmosphere. This point is labeled in the analysis on both the wt % curve and derivative wt % curve to show the mass loss is finished. The volatile matter is calculated by subtracting this second labeled point in the graph from the wt % before volatile matter was removed (the first point labeled in the graph). The volatile matter consists of any residual oil entrapped in the coke sample.

Finally, the last point labeled in the graph is the remaining mass after the fixed carbon has been burned off by air and is the amount of ash in the coke sample. This step is performed by holding the sample isothermal at 950 °C while switching the gas to breathing air. This gas contains oxygen, which burns away the fixed carbon, leaving the remaining mass as ash. These calculations are performed for analysis of the graphs for

all coke samples. The remaining moisture content/volatile matter/fixed carbon/ash content graphs can be observed in Appendix D.

Table 3: Moisture Content/Volatile Matter/Fixed Carbon/Ash Content of Coke Samples

Condition	Sample	Moisture Content (wt %)	Volatile Matter (wt %)	Fixed Carbon (wt %)	Ash Content (wt %)
Atmospheric Pressure Coking	464 °C_1	0.18	28.57	68.68	2.57
		0.21	32.06	66.81	0.92
		0.08	30.49	69.10	0.33
		0.04	28.22	70.06	1.68
		0.05	28.90	68.38	2.67
	Average 464 °C_1	0.11	29.65	68.61	1.63
	465 °C_2	0.08	30.71	68.80	0.41
		0.03	29.76	67.13	3.08
		0.07	32.10	64.32	3.52
	Average 465 °C_2	0.06	30.86	66.75	2.33
	462 °C_3	0.22	29.62	68.45	1.71
		0.16	32.82	66.91	0.11
		0.06	30.71	67.65	1.58
	Average 462 °C_3	0.15	31.05	67.67	1.13
	474 °C	0.10	22.68	74.83	2.40
0.07		22.69	75.04	2.20	
Average 474 °C	0.09	22.69	74.93	2.30	
484 °C	0.21	16.85	80.28	2.67	
	0.06	16.05	81.48	2.41	
Average 484 °C	0.14	16.45	80.88	2.54	
497 °C	0.10	11.56	85.44	2.90	
	0.09	12.53	84.03	3.35	
Average 497 °C	0.10	12.05	84.74	3.13	
Vacuum Pressure Coking	463 °C_Vac	0.36	14.40	82.31	2.94
		0.30	15.76	81.74	2.20
	Average 463 °C_Vac	0.33	15.08	82.02	2.57
	492 °C_Vac	0.33	11.14	84.74	3.79
		0.10	13.85	82.20	3.85
Average 492 °C_Vac	0.21	12.50	83.47	3.82	

Table 3 shows all the data collected for the analysis of moisture content, volatile matter, fixed carbon, and ash content in the coke samples. The samples were tested multiple times and averages were calculated for each individual sample. Moisture content and ash content should be relatively consistent between each sample. The moisture content fluctuates slightly depending on the day of testing but is in the range of 0.36-0.03 %. A possible cause for this is the humidity on the particular day of testing.

The weight of ash in a sample is observed to differ even more from sample to sample in the range of 3.85-0.11 %. Possible reasons for this are that the sample size may be too small compared to the overall coke sample and is not well mixed. Another possible reason is that over time the instrument and its components degrade from the extreme heat and do not provide results with the extreme precision that is needed for this analysis. The ash content measured in the coke samples is less than 5 % and it is very difficult to get repeatable precise results. The beams inside the furnace of the TGA that monitor the weight of the sample needed to be replaced in the middle of all of these tests. All of these possibilities can contribute to the reproducibility of the results.

Due to variations in volatile matter, the coke yield can be misleading, as volatile matter is a function of previous processing conditions, not coking. To set a true coke yield, the coke yield was normalized using the fixed carbon. Table 4 shows the coke yield normalized to fixed carbon calculated from each coking test. The amount of fixed carbon for vacuum pressure samples is smaller than the amount of fixed carbon for atmospheric pressure samples. This continues to confirm that atmospheric pressure provides better coking conditions than vacuum pressure. A source from literature

suggests that increased pressure up to 0.6 MPa can produce higher amounts of coke [34]. Exploration of these conditions in future work is recommended.

Table 4. Coke Yield Normalized to Fixed Carbon Fraction (wt %)

464 °C_1	465 °C_2	462 °C_3	Vacuum 463 °C	474 °C	484 °C	497 °C	Vacuum 492 °C
6.9	6.8	7.2	6.1	7.0	7.2	6.9	5.6

Table 5 shows the coke properties sought for aluminum anode-grade applications to give a comparison to the coke produced in this research. Birghila [17] reported results from three coke samples. The moisture content of the samples ranged between 0.28 - 0.37 %, which was stated as being low in moisture. The amount of volatile matter under all conditions obtained in my experiments (Table 3) is quite a bit higher than the amount sought for aluminum anode-grade coke. The coke from the UND cracking process is comparable to green coke and depending upon the application, will have to be calcined for use as high grade carbon.

Table 5: Coke Properties for Aluminum Anode-Grade Carbon Products [17]

Property	Calcined
Ash wt %	0.1 – 0.3
Volatile Matter wt %	< 0.25

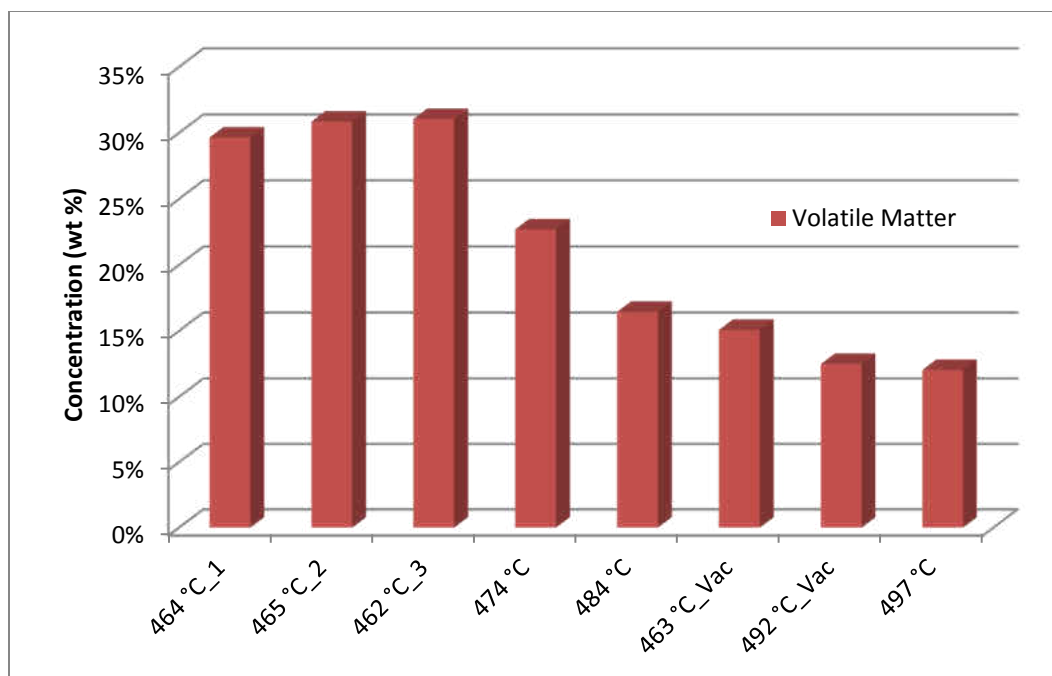


Figure 26: The Volatile Matter Content in Coke Samples

Figure 26 shows the volatile matter and how it compares between samples. In general, as the coking temperature increases, the amount of volatile matter decreases. This is because the higher temperature vaporizes and drives off more of the semi-volatile matter caught between the pores of the coke during formation. The volatile matter can then be either collected in the liquid stream or removed in the gas stream. Another observation is that the use of vacuum pressure removes more of the volatile matter at 463 °C\_Vac testing compared to coking at atmospheric pressure.

### 3.4 Analysis of Liquid Products

#### 3.4.1 Liquid Analysis

A Perkin Elmer Clarus 480 gas chromatograph with a SimDist column was used to simulate the boiling point range distribution of hydrocarbons by distillation, for the liquid samples collected after coking. A standard mixture was injected for calibration at

the beginning of each day of analysis. Procedures were followed as explained in section 2.5.1.

Analysis is performed by subtracting a chromatogram produced from the blank injection from the chromatogram of the unknown sample. Then fractions are calculated for the following hydrocarbon fuel cuts: lights (boiling point  $< 68.8$  °C), naphtha (boiling point range  $68.8 - 160$  °C), jet fuel (boiling point range  $160 - 210$  °C), diesel (boiling point range  $210 - 350$  °C), and heavy fuel oil (boiling point  $> 350$  °C). Using the calibration curve, the retention time corresponding to these temperatures can be calculated. The calibration curves and chromatographs can be found in Appendix E.

It is noted that since the GC baseline was not adjusted for unresolved compounds (the “hump” seen in Figure E.2 and other chromatographs in Appendix E), acid mixtures and other compounds could be included in these values. The analysis was calculated by integrating the chromatograph of the sample to the blank chromatograph.

Table 6 shows the data from this liquid analysis in the liquid samples collected from the coking reaction experiments, classified by fuel cut (wt% C). These values were calculated based on the boiling point ranges. Observing the data from Table 6 and Figure 27, the samples mostly contain the diesel and heavy fuel oil cuts. This is expected because the tar used for coking contains an abundance of high boiling point hydrocarbons, which are removed and collected during the coking process to allow the formation of solid coke. For atmospheric pressure coking these two oil cuts account for over 91 % of the sample, while for the vacuum pressure coking samples this amount is



Table 6: The Concentration of Fuel Cuts in Liquid Samples Collected After Coking (wt % C)

Sample Name		Lights (<68.8 °C)	Naphtha (68.8-160 °C)	Jet Fuel (160-210 °C)	Diesel (210-350 °C)	Heavy Fuel Oil (>350 °C)
Atmospheric Pressure Coking	453 °C	0.1	3.9	4.7	58.1	33.2
	464 °C_1	0.7	3.6	4.2	53.9	37.6
		0.6	4.3	4.3	55.4	35.3
	Average 464 °C_1	0.6	3.9	4.3	57.5	33.7
	465 °C_2	0.6	3.9	4.3	55.6	35.6
		0.5	3.9	4.3	52.7	38.6
		0.5	4.0	4.5	54.9	36.1
	Average 465 °C_2	0.4	4.0	4.5	55.2	35.9
	462 °C_3	0.5	3.9	4.4	54.3	36.9
		0.3	3.8	4.7	52.9	38.3
		0.3	3.8	4.6	54.7	36.7
	Average 462 °C_3	0.2	3.5	4.3	56.7	35.2
474 °C	0.3	3.7	4.5	54.8	36.7	
484 °C	0.6	3.5	4.3	54.2	37.4	
497 °C	0.7	3.3	4.0	51.9	40.2	
Vacuum Pressure Coking	463 °C_Vac	0.7	3.4	4.1	51.5	40.4
		0.1	1.1	2.0	29.9	66.9
		0.0	0.9	1.8	27.4	69.8
	Average 463 °C_Vac	0.1	1.1	1.7	25.7	71.4
	492 °C_Vac	0.1	1.1	1.8	27.7	69.4

over 95 % of the sample. The reason that vacuum pressure coking produces a higher amount is because the lower pressure allows for additional higher boiling point hydrocarbons to be removed compared to lower temperatures. For atmospheric pressure coking, the concentration of the diesel cut decreases and the heavy fuel oil increases as the temperature of coking increases because additional higher boiling point compounds are volatilized out of the tars. The vacuum pressure coking results follow the opposite pattern.

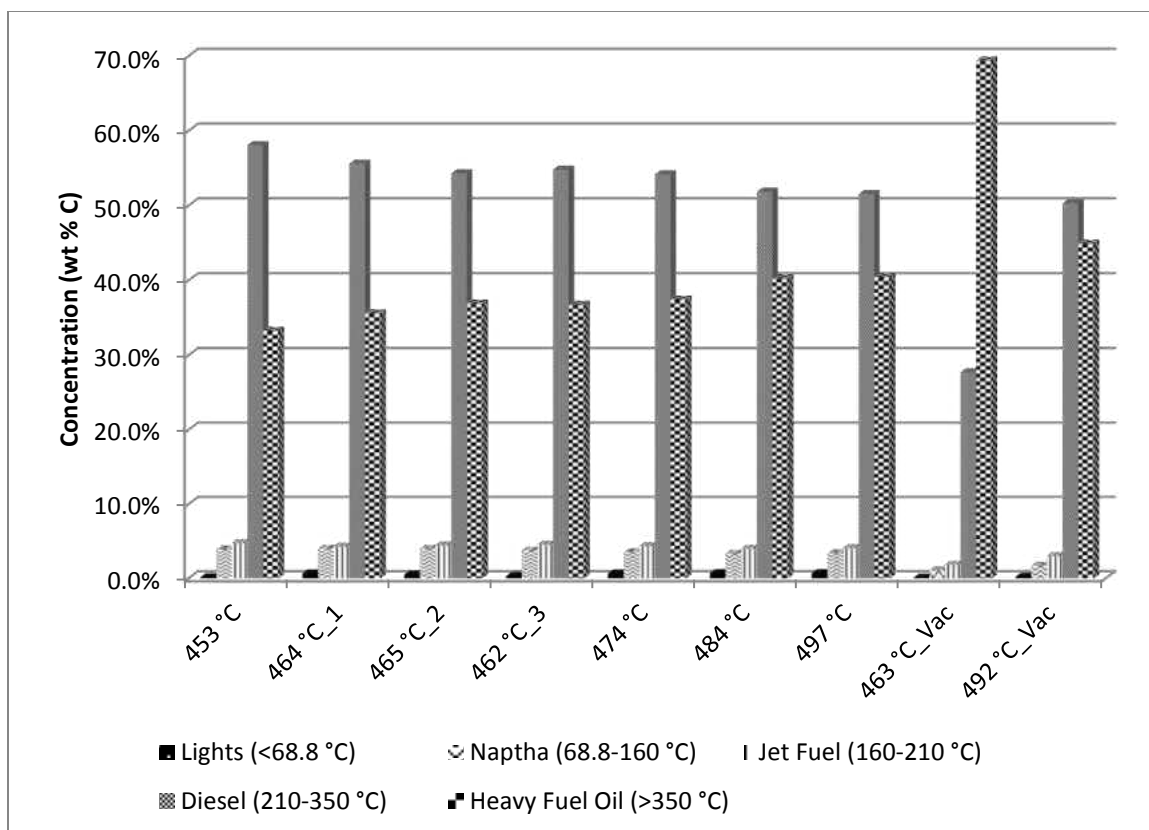


Figure 27: Fuel Cut Concentrations in Liquid Samples Collected After Coking

Figure 27 shows the hydrocarbon cuts that were contained in each sample compared to the other samples. The significance of this analysis is to observe and have an understanding of the content contained in the liquid samples as coking conditions are changed so that this liquid stream can be recycled back through the process.

### 3.4.2 Acid Analysis

The main constituents in vegetable oil are triglycerides (TG's), which contain three carboxylic acid groups and the tars generated during the thermal cracking process originated from these TG's. It is important to know where the acid concentration is distributed during the process. Acids in the diesel and jet fuel can cause corrosion and form engine deposits during combustion and therefore are separated from the product fuel

during processing. The acid concentration was analyzed using a Thermo Scientific Nicolet IR 200 FT-IR in order to further characterize the liquid sample collected after coking. The spectrum produced by the FTIR instrument consists of the absorbance of the liquid (peak height) versus the wave length. A more detailed analysis of the calculations and calibration data can be found in Appendix F.

Table 7: Peak Heights and Total Acid Concentrations of Liquid Samples Collected After Coking

Sample	Peak Height (abs units)	Acid Conc. (mol/L)	Wt % Acid (Octanoic Acid)	Wt % Acid (Stearic Acid)
D-300 Bottoms	0.981	1.37E+04	10.32%	6.85%
453 °C	0.590	8.27E+03	6.23%	4.14%
464 °C_1	0.585	8.20E+03	6.18%	4.10%
465 °C_2	0.617	8.65E+03	6.52%	4.33%
462 °C_3	0.603	8.45E+03	6.37%	4.23%
474 °C	0.607	8.51E+03	6.41%	4.26%
484 °C	0.617	8.65E+03	6.52%	4.33%
497 °C	0.637	8.93E+03	6.73%	4.47%
463 °C_Vac	0.577	8.08E+03	6.09%	4.04%
492 °C_Vac	0.567	7.94E+03	5.98%	3.97%

Table 7 shows the peak heights and calculated acid concentrations for the unknown liquid samples collected after coking. The D-300 bottom (original starting tar) is also analyzed to observe the initial acid concentration and differences in the liquid samples. D-300 bottoms had an initial acid concentration of 1.37E+04 mol/L while the liquid samples contained acid concentrations between 8E+03 mol/L and 9E+03 mol/L. These data are shown graphically in Figure 28.

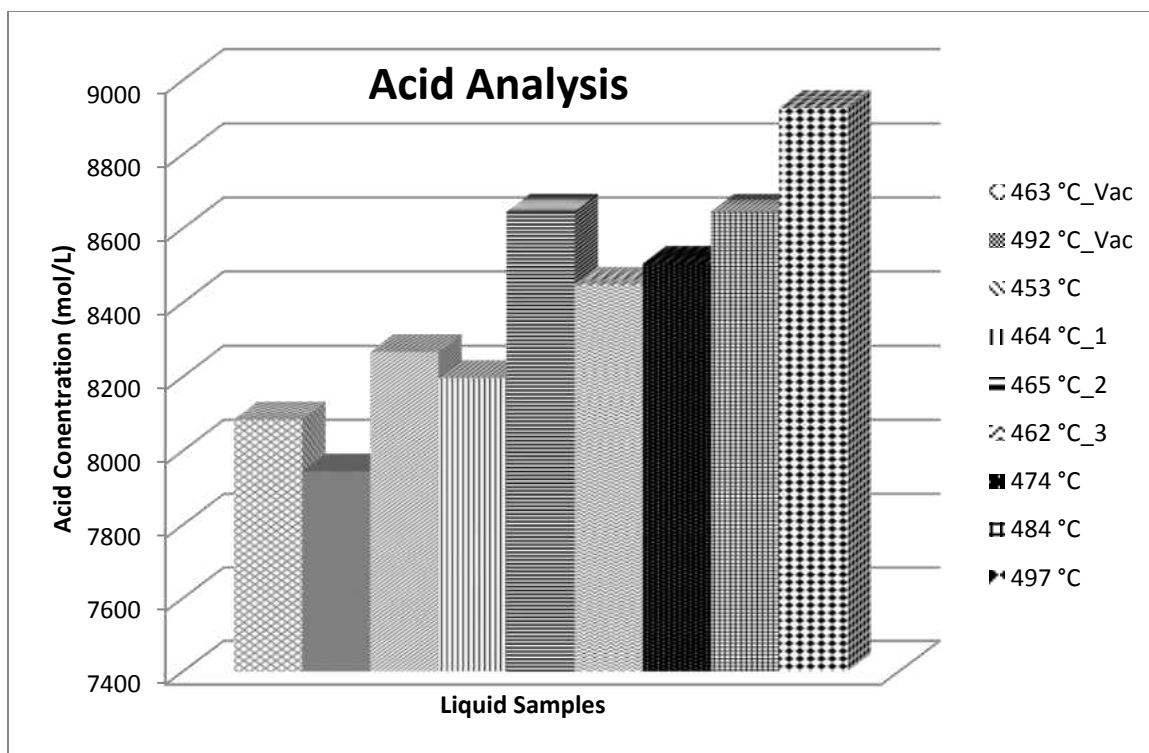


Figure 28: Acid Concentration of Liquid Samples Collected After Coking

For an estimation of the quantity of acid present in the liquid samples a linear relationship is observed between acid concentration and the wt % acid from the calibrations. However, this isn't the most accurate representation of the quantity of acid because the acid compounds in the samples are complex and not known. The calibration was executed using octanoic acid since the FT-IR instrument only measures the C=O double bond functional group in the acid. Back calculations were performed for both octanoic acid and stearic acid (octadecanoic acid) to get an idea of the weight % acid contained in the liquid samples. Therefore, if acid concentrations are back calculated to a wt % of acid, the D-300 bottoms contains 6.9-10.3 wt % acid and all other liquid samples contain anywhere from 3.97 wt % to 6.73 wt % acid for stearic acid and octanoic acid, respectively. However, the wt % acid is closer to the values represented by stearic acid.

The acid concentration is lowest among the samples that used vacuum pressure for coking. Also, the acid concentration gets larger as the coking temperature increased amongst the atmospheric pressure coking samples. Although, compared to the acid concentration in the D-300 bottoms tar sample the acid concentrations were all lower in the liquid samples. Overall, the acid concentration is rather low in comparison to other streams in the process and this analysis gives insight into where this liquid stream from coking will be best recycled back into the process.

Taking into consideration the concentration of hydrocarbons and the acid concentration, in the overall renewable fuel process this liquid stream will be recycled, first removing the heavy fuel oil product. The remaining liquid stream will then be mixed with the organic liquid product (OLP) stream that exits the thermal cracking unit.

### 3.5 Analysis of Gas Products

A SRI 8610 C gas chromatograph was used to measure the distribution of the light, non-condensable gases in each gas sample bag collected during atmospheric pressure coking. Calibrations were performed before analysis of the unknown gas took place. More details of the calibration calculations and additional gas chromatography data can be found in Appendix G.

During atmospheric pressure coking, between four and five gas sample bags were needed to collect the entire gas sample released from a coking test. All of the gas sample bags were analyzed either the same day or within 24 hours of the coking test so that the escape of any light gases would be negligible. The composition of the gas was calculated using mol % (also = vol %) and took into account the volume of nitrogen purge gas that was mixed into each sample bag from testing. During analysis, the injection volume was

known. The volume of measured gas could be calculated from the FID and TCD signal responses and therefore the remaining injection volume that is not measured by the instrument is considered to be the nitrogen purge gas from testing.

Table 8 - 14 show the distribution of the light, non-condensable gases collected during atmospheric pressure coking for the coking temperatures researched. The temperature range seen at the left end of each table represents the temperature range at which each gas sample bag was connected to the system for that particular coking temperature as it ramped up. The last row of each table that lists a temperature hold (ie. 450 °C hold) represents the 15 minute attempted isothermal hold each sample was given during coking to ensure complete vaporization of hydrocarbons at that particular temperature. For this analysis, each gas sample bag was analyzed twice since differences in the results were small. The average is presented in the tables below. With the exception of table 12 & 13, where the analysis was performed in triplicate and averaged since this was found to be the optimum coking temperature. The calibration bag containing carbon monoxide, carbon dioxide and propane was analyzed at the beginning of every analysis to ensure the catalyst packed inside the methanizer was working properly and didn't need to be replaced.

Table 8: Gas Components from 497 °C Atmospheric Pressure Coking (mol %)

	H <sub>2</sub>	CO	CH <sub>4</sub>	CO <sub>2</sub>	C <sub>2</sub> H <sub>4</sub>	C <sub>2</sub> H <sub>6</sub>	C <sub>3</sub> H <sub>6</sub>	C <sub>3</sub> H <sub>8</sub>	C <sub>4</sub> H <sub>x</sub>	C <sub>5</sub> H <sub>x</sub>	C <sub>6</sub> H <sub>x</sub>	C <sub>7</sub> H <sub>x</sub>	N <sub>2</sub>
250 - 392 °C	0.26	7.28	1.13	2.25	0.04	0.09	0.04	0.05	0.05	0.01	0.00	0.00	88.79
392 - 453 °C	1.75	25.06	3.95	11.43	0.49	1.57	1.25	0.97	0.97	0.43	0.14	0.00	51.98
453 - 473 °C	4.61	17.58	14.09	4.67	2.51	9.39	4.00	5.29	5.00	2.06	0.64	0.07	30.08
473 - 490 °C	7.24	9.34	23.35	1.73	3.11	12.81	4.22	6.29	5.35	2.38	0.79	0.08	23.31
490 °C hold	9.59	4.57	26.89	0.82	3.09	11.12	3.32	4.79	3.86	1.92	0.77	0.10	29.17

Table 9: Gas Components from 484 °C Atmospheric Pressure Coking (mol %)

	H <sub>2</sub>	CO	CH <sub>4</sub>	CO <sub>2</sub>	C <sub>2</sub> H <sub>4</sub>	C <sub>2</sub> H <sub>6</sub>	C <sub>3</sub> H <sub>6</sub>	C <sub>3</sub> H <sub>8</sub>	C <sub>4</sub> H <sub>x</sub>	C <sub>5</sub> H <sub>x</sub>	C <sub>6</sub> H <sub>x</sub>	C <sub>7</sub> H <sub>x</sub>	N <sub>2</sub>
252 - 389 °C	0.29	6.32	0.78	2.09	0.04	0.10	0.06	0.06	0.09	0.11	0.02	0.00	90.04
389 - 449 °C	1.89	28.41	3.92	12.40	0.50	1.62	1.24	0.97	0.93	0.45	0.16	0.01	47.48
449 - 463 °C	4.37	22.11	14.04	6.63	2.48	9.31	4.03	5.22	4.70	1.84	0.57	0.06	24.63
463 - 479 °C	5.62	12.96	19.96	2.36	2.81	11.89	4.22	6.08	5.27	2.21	0.72	0.09	25.80
480 °C hold	8.02	6.78	27.01	1.21	3.01	12.74	3.79	5.85	4.72	2.25	0.91	0.14	23.57

Table 10: Gas Components from 474 °C Atmospheric Pressure Coking (mol %)

	H <sub>2</sub>	CO	CH <sub>4</sub>	CO <sub>2</sub>	C <sub>2</sub> H <sub>4</sub>	C <sub>2</sub> H <sub>6</sub>	C <sub>3</sub> H <sub>6</sub>	C <sub>3</sub> H <sub>8</sub>	C <sub>4</sub> H <sub>x</sub>	C <sub>5</sub> H <sub>x</sub>	C <sub>6</sub> H <sub>x</sub>	C <sub>7</sub> H <sub>x</sub>	N <sub>2</sub>
261 - 387 °C	0.27	7.47	1.18	2.42	0.05	0.10	0.06	0.07	0.07	0.07	0.04	0.00	88.20
387 - 446 °C	1.75	26.68	3.90	12.08	0.44	1.44	1.20	0.90	0.91	0.45	0.18	0.00	50.07
446 - 458 °C	4.01	19.05	12.13	5.59	2.10	8.23	3.64	4.75	4.59	1.97	0.66	0.07	33.22
458 - 472 °C	5.67	13.10	19.42	2.37	2.57	11.65	4.17	6.20	5.55	2.50	0.88	0.11	25.80
470 °C hold	7.37	6.77	23.92	1.21	2.46	12.01	3.48	5.75	4.72	2.32	0.95	0.13	28.90

Table 11: Gas Components from 464 °C\_1 Atmospheric Pressure Coking (mol %)

	H <sub>2</sub>	CO	CH <sub>4</sub>	CO <sub>2</sub>	C <sub>2</sub> H <sub>4</sub>	C <sub>2</sub> H <sub>6</sub>	C <sub>3</sub> H <sub>6</sub>	C <sub>3</sub> H <sub>8</sub>	C <sub>4</sub> H <sub>x</sub>	C <sub>5</sub> H <sub>x</sub>	C <sub>6</sub> H <sub>x</sub>	C <sub>7</sub> H <sub>x</sub>	N <sub>2</sub>
257 - 383 °C	0.28	6.75	1.04	2.28	0.05	0.12	0.07	0.08	0.10	0.59	0.05	0.00	88.60
383 - 431 °C	1.78	25.95	3.07	12.00	0.36	1.15	1.07	0.73	0.77	0.55	0.16	0.00	52.43
431 - 449 °C	3.13	19.10	9.38	6.78	1.64	6.58	3.12	3.93	3.97	1.90	0.63	0.07	39.78
449 - 460 °C	4.51	14.19	15.81	2.40	2.31	10.15	4.04	5.64	5.36	2.49	0.89	0.11	32.11
460 °C hold	5.88	7.76	20.87	1.18	2.19	11.30	3.48	5.73	4.89	2.42	0.96	0.12	33.24

Table 12: Gas Components from 465 °C\_2 Atmospheric Pressure Coking (mol %)

	H <sub>2</sub>	CO	CH <sub>4</sub>	CO <sub>2</sub>	C <sub>2</sub> H <sub>4</sub>	C <sub>2</sub> H <sub>6</sub>	C <sub>3</sub> H <sub>6</sub>	C <sub>3</sub> H <sub>8</sub>	C <sub>4</sub> H <sub>x</sub>	C <sub>5</sub> H <sub>x</sub>	C <sub>6</sub> H <sub>x</sub>	C <sub>7</sub> H <sub>x</sub>	N <sub>2</sub>
265 - 383 °C	0.22	5.84	1.18	2.06	0.04	0.09	0.05	0.06	0.07	0.17	0.02	0.00	90.20
383 - 430 °C	1.45	26.65	3.47	11.29	0.29	0.87	0.94	0.57	0.62	0.47	0.11	0.00	53.28
430 - 449 °C	2.89	21.51	8.63	9.52	1.43	5.52	2.84	3.36	3.48	1.73	0.47	0.05	38.57
449 - 460 °C	4.47	15.43	15.93	2.88	2.36	10.15	4.10	5.71	5.53	2.55	0.77	0.09	30.03
460 °C hold	6.25	8.05	22.15	1.28	2.31	11.74	3.60	5.95	5.12	2.53	0.89	0.12	30.01

Table 4: Gas Components from 462 °C\_3 Atmospheric Pressure Coking (mol %)

	H <sub>2</sub>	CO	CH <sub>4</sub>	CO <sub>2</sub>	C <sub>2</sub> H <sub>4</sub>	C <sub>2</sub> H <sub>6</sub>	C <sub>3</sub> H <sub>6</sub>	C <sub>3</sub> H <sub>8</sub>	C <sub>4</sub> H <sub>x</sub>	C <sub>5</sub> H <sub>x</sub>	C <sub>6</sub> H <sub>x</sub>	C <sub>7</sub> H <sub>x</sub>	N <sub>2</sub>
256 - 378 °C	0.28	5.48	1.08	2.38	0.04	0.10	0.05	0.07	0.08	0.28	0.03	0.00	90.14
378 - 428 °C	1.30	25.59	3.34	10.55	0.25	0.74	0.79	0.49	0.54	0.48	0.10	0.00	55.83
428 - 448 °C	2.78	21.27	8.25	9.50	1.32	5.19	2.65	3.17	3.29	1.61	0.47	0.05	40.45
448 - 458 °C	4.35	15.98	15.56	3.16	2.28	9.92	4.02	5.61	5.39	2.43	0.74	0.09	30.48
460 °C hold	5.96	9.21	21.10	1.51	2.26	11.64	3.70	6.03	5.29	2.58	0.92	0.13	29.68

Table 5: Gas Components from 453 °C Atmospheric Pressure Coking (mol %)

	H <sub>2</sub>	CO	CH <sub>4</sub>	CO <sub>2</sub>	C <sub>2</sub> H <sub>4</sub>	C <sub>2</sub> H <sub>6</sub>	C <sub>3</sub> H <sub>6</sub>	C <sub>3</sub> H <sub>8</sub>	C <sub>4</sub> H <sub>x</sub>	C <sub>5</sub> H <sub>x</sub>	C <sub>6</sub> H <sub>x</sub>	C <sub>7</sub> H <sub>x</sub>	N <sub>2</sub>
260 - 382 °C	0.30	6.26	0.95	2.10	0.04	0.09	0.05	0.06	0.07	0.05	0.02	0.00	90.01
382 - 429 °C	1.44	25.25	2.58	10.87	0.29	0.91	0.88	0.58	0.61	0.30	0.14	0.00	56.15
429 - 448 °C	2.81	18.38	8.25	6.82	1.41	5.70	2.72	3.37	3.37	1.49	0.52	0.06	45.10
450 °C hold	4.47	13.28	15.70	2.25	2.14	9.87	3.79	5.38	5.02	2.23	0.80	0.11	34.95

There are some trends that can be observed in the data. First, as the temperature of an individual coking test increases the amount of measurable gas also increases. The first gas collection bag contains approximately 10 % measurable gas in all the coking tests and as the temperature increases the amount of measurable gas increases to around 70 %. Next, the amount of carbon monoxide and carbon dioxide are the highest in the de-oxygenation region (370 – 460 °C). Another observation is as the temperature increases for an individual coking test, the amount of hydrogen increases and more hydrogen is produced at higher coking temperatures. Lastly, for the 460 °C coking tests a wide range of hydrocarbons exist in the last collection bag at the coking range (above 460 °C). The highest amounts of desirable product gas produced in this coking range are methane, ethane, and hydrogen.

The results of this analysis give a composition of the gas phase that develops from coking D-300 bottoms tar. Even though an objective for coking was to limit the gas



formation from coking and the gas phase only represents less than 5 wt % of the mass balance, the gas produces useful syn gas and hydrogen products.

Since the overall goal of this research is to eventually turn the formation of coke into a continuous process for the commercialization of coke at a pilot crop oil refinery plant, it is important to draw implications for the gas composition expected from a steady state continuous coking process.

Table 6: Gas Components of Measurable Gas for 464 °C\_1, 465 °C\_2, and 462 °C\_3 Coking (mol %)

	H <sub>2</sub>	CO	CH <sub>4</sub>	CO <sub>2</sub>	C <sub>2</sub> H <sub>4</sub>	C <sub>2</sub> H <sub>6</sub>	C <sub>3</sub> H <sub>6</sub>	C <sub>3</sub> H <sub>8</sub>	C <sub>4</sub> H <sub>x</sub>	C <sub>5</sub> H <sub>x</sub>	C <sub>6</sub> H <sub>x</sub>	C <sub>7</sub> H <sub>x</sub>
464 °C_1	5.37	35.60	17.14	12.36	2.11	9.24	3.83	5.13	4.85	3.36	0.91	0.09
465 °C_2	5.08	37.03	17.58	13.32	2.01	8.61	3.63	4.80	4.59	2.56	0.72	0.07
462 °C_3	5.03	37.06	16.94	14.14	1.94	8.44	3.56	4.75	4.57	2.76	0.74	0.08

The concentration (mol %) of measurable process gas (not including the N<sub>2</sub> purge gas) is totaled from the batch process for the 464 °C\_1, 465 °C\_2, and 462 °C\_3 coking tests and is seen in Table 15. Although it is difficult to predict the gas composition from a steady state continuous coking process at an optimum 460 °C coking temperature, this gives a good estimation. However, this composition is highly dependent on process conditions (temperature and pressure) of thermal cracking, distillation (atmospheric pressure vs. vacuum pressure), and feed oil.

Approximately 50 mol % of the measurable gas consists of carbon monoxide and carbon dioxide. This is not a huge surprise since bio feedstocks (such as soybean oil) contain higher amounts of oxygen than fossil fuels and the oxygen needs to be removed for carbonization to occur. The remaining 50 mol % of measurable gas contains a mixture of light hydrocarbons and hydrogen with the three major components being methane, ethane, and hydrogen. In a continuous coking process this gas stream will be

mixed with other non-condensable process gas and further processed into syngas, hydrogen, liquefied petroleum gas (LPG), and pentanes.

## CHAPTER IV

### Conclusion

#### 4.1 Research of Lab Scale Coking

High value carbonaceous materials were successfully produced from the heavy, residual tars produced and recovered during crop oil cracking. This carbonization of tars was effectively performed using a lab scale batch coking process for the collection of an overall mass balance as well as the analysis and characterization of the coke, liquid phase, and gas phase products that resulted.

Research found that coking of the heavy, residual tars using a temperature above 460 °C and at atmospheric pressure resulted in the maximum formation of bio-derived coke, while also minimizing the formation of low value gas products. These process conditions produced a little more than 10 wt % coke. Further analysis found that this coke contains 92 wt % carbon. However, this coke also contains significant quantities of volatile matter and therefore would need to be further processed using a calcination process for use as high grade carbon. This calcination process step depends on the applications sought for this coke.

From analysis of the liquid phase, it was found that over 91 wt % of the liquid phase is heavy fuel oil and diesel fuel cuts. This phase contained between 4.0-6.7 wt % acid. However, this liquid stream will be recycled back into the process and intermixed with the organic liquid product resulting from thermal cracking to process into numerous

fuels. Analysis of the non-condensable gas phase displayed a mixture of light hydrocarbons, carbon monoxide, carbon dioxide, and hydrogen. This stream will be combined with other process gas for the production of gas products.

#### 4.2 Future Work

The next step for research in this area is to develop a continuous coking process for the carbonization of cracked crop oil tars into high grade carbon products. This will be used in the commercialization of crop oil thermal cracking in a pilot plant. Difficulties for the development of a continuous process are to apply enough heat for residual tars to lower the viscosity enough for flow or designing a mechanical system to move the tars through the process. Process conditions from literature suggest that pressures above atmospheric pressure can provide increased coke yields, although for safety reasons they weren't tested in this research.

Another area of research involving the use of cracked crop oil tars to produce carbon products is to process the tars into a mesophase pitch from which carbon fibers could be spun. Some research has been done for this topic to determine feasibility of this process. Although, optimum process conditions would need to be researched in order to produce the highest quality pitch for spinning carbon fibers, preliminary results are promising.

## APPENDICES

## Appendix A Lab Scale Coker Operation

To set up and run the lab scale coking reactor, the equipment was weighed prior to use. Items weighed were: a clean reactor vessel, the top of the reactor with thermocouple attached, spiral wound gasket, and clean distillate flask. The gasket used was a Flexitallic spiral wound, thermiculite gasket, type CG – 316L. Once the clean reactor vessel was weighed, sample tar was added and then the vessel was weighed again to obtain the sample weight. Approximately 100 g of sample tar was used for each coking experiment.

Vacuum grease was applied to both sides of the gasket for all testing to properly seal the reactor and prevent distillates from escaping between the flanges. The gasket was then placed on top of the flange of the reactor vessel and the top flange with thermocouple was placed above the gasket, aligning the bolt holes. Some vacuum grease was also applied to the glass connection between the distillate flask and condenser. Loctite C5-A copper based anti-seize lubricant was applied inside the threads of the four nuts used to seal the reactor. The nuts were initially hand tightened on the four bolts to seal the reactor and excess anti-seize was wiped off. A torque wrench was then used to evenly tighten the bolts 33.9 Newton meters.



Figure A.1: Photograph of the Coking Reactor Vessel

The reactor vessel (Figure A.1) was lifted and placed inside the ceramic heater. This reactor was roughly 0.5 L. The Swagelok fittings for the nitrogen inlet and vapor outlet lines were connected to the top of the vessel and tightened. Then the nitrogen tank was opened to start flowing nitrogen through the system. Nitrogen was sent through the system for about 20 minutes before each test to ensure all oxygen was removed. The ball valve for the nitrogen was operated at a setting of 40, which was calibrated at approximately 30 mL/min. If atmospheric pressure testing was being performed and a gas sample was collected for analysis, the proper fitting for the gas sample bag was connected following the second collection flask. The thermo-couple wire was also connected to the thermo-couple reader at this time. Insulation was pieced together in and around the Swagelok fittings and thermo-couple to cover the top of the reactor. The heat tape surrounding the vapor outlet line was plugged in at this time to start warming the metal.

Once the nitrogen flow had sufficient time to purge the system of any oxygen, the furnace controller was set to a set point temperature above that of the goal for the experiment. The reason the controller temperature needs to be set higher is because the thermo-couple for the furnace controller is on the outside of the reactor and is representative of the wall temperature of the reactor. For this research, the controller temperature was set at 50 °C above the desired reactor temperature. The pump for the condenser water and pressure gauge were also turned on at this time.

As the temperature rises, liquid and gas were observed flowing through the condenser. If a gas sample was collected, the first gas sample bag was connected around 250 °C to start collecting the gas sample. The gas sample bag was changed out once it was about 80 % full with an empty gas sample bag and the temperature range for each bag was recorded. The first drips of distillate were observed at around 330 °C for the D-300 bottoms sample, although this temperature varied depending on the tar samples being coked. When the reactor temperature was within 5 °C of the desired temperature, the controller temperature was lowered to a set point 10 °C above the desired reactor temperature. Once the reactor temperature reached its desired temperature, it was held isothermal for 15 minutes to ensure complete vaporization of hydrocarbons at that temperature.

After the experiment was run at the necessary temperature for adequate time, the furnace controller was turned off and the heat tape was unplugged. The insulation around the top of the reactor was then removed and a fan placed above the reactor to shorten the cooling time. The nitrogen purge continued flowing through the reactor until the reactor



temperature was below 250 °C to be sure none of the carbon was burned off due to oxygen entering the system.

When testing was performed under vacuum pressures, the second collection flask was cleaned and weighed. This second collection flask was placed in an ice bath and the flask was connected to the dampening tank and vacuum pump. Start-up procedures were the same as for the atmospheric pressure testing. The controller temperature was heated to 370 °C for all of the vacuum testing under nitrogen first to remove the lightest hydrocarbons. This prevents the system from creating a siphon from violent boiling and prevents the removal of heavy residual hydrocarbons. Once the reactor temperature reached between 360 °C – 370 °C (under the 370 °C cracking temperature) and held for 15 minutes, procedures were started to switch the system to vacuum pressure. First the two ball valves directly before and after the flow meter were closed to shut off the nitrogen flow. Then the two needle valves connected to the dampening tank were closed and the vacuum pump started. The needle valve controlling the system was slowly opened while monitoring the pressure gauge so that the vacuum pressure is gently applied to the system and flashing of the sample tar was avoided.

After the vacuum pressure was slowly increased, the controller temperature was set at 50 °C above the desired reactor temperature. The same procedure was followed for heating the reactor as with the atmospheric pressure testing. The vacuum pressure testing often produced a distillate that was very waxy and would solidify in the condenser. This was resolved by placing the beaker of condenser water on a hot plate to cycle warm water through the condenser in order to melt away the waxy distillates. Also, sometimes a heat

gun was used to gently heat the walls of the condenser to get the waxy distillates to flow down into the collecting flask. Even though the final reactor temperature was reached and the furnace controller was shut off, the vacuum pump remained running. The vacuum pump was allowed to run until the reactor cooled to below 250 °C to ensure no carbon was burned off.

Following the coking tests, the reactor was given enough time to cool so that it could be handled safely. The fittings for the nitrogen inlet and vapor outlet were then disconnected and the reactor removed from the furnace. The reactor was opened up and residual vacuum grease was wiped clean. This cleaning should be meticulous to make sure none of the residual coke is wiped away. The reactor vessel, spiral wound gasket, and top of the reactor were weighed to calculate the weight of solid coke produced. The collection flasks were also disconnected so that the distillates could be weighed for the final mass balance.



Figure A.2: Photograph looking into the Coking Vessel



Figure A.3: Photograph of Green Coke

After the equipment was weighed, the coking vessel was scraped to remove the solid coke formed from the testing. Figure A.2 shows a photograph of how the inside of the coking vessel looks after a coking experiment. Figure A.3 shows some green coke that was produced from the coking process. The coking vessel, gasket, and top of the reactor were cleaned after each use.

Appendix B  
Mass Balances from Preliminary Coking Testing

Table B-1: Preliminary Coking Testing Mass Balances

Max Temperature	463 °C	469 °C	473 °C	482 °C	499 °C
Solid (coke)	10.3	9.8	9.4	8.9	8.2
Liquid	85.5	85.8	85.8	86.9	87.3
Gas	4.3	4.4	4.8	4.2	4.5

## Appendix C Carbon Content Calibrations

A Shimadzu TOC-V<sub>CSN</sub> Carbon Analyzer with a Solid Sample Module (SSM, 5000A) was used to measure the carbon content for each coke sample. A calibration curve is made at the beginning of each day the machine is run. The standard used for total carbon (TC) testing is dextrose (C<sub>6</sub>H<sub>12</sub>O<sub>6</sub> gfw = 180.16) which is 40.00 % C by weight. Four standards (0, 5, 10, and 15 mg) were measured, with duplicates at each point, and placed in the sample boats. The machine would measure the area of the response to build the calibration curve.

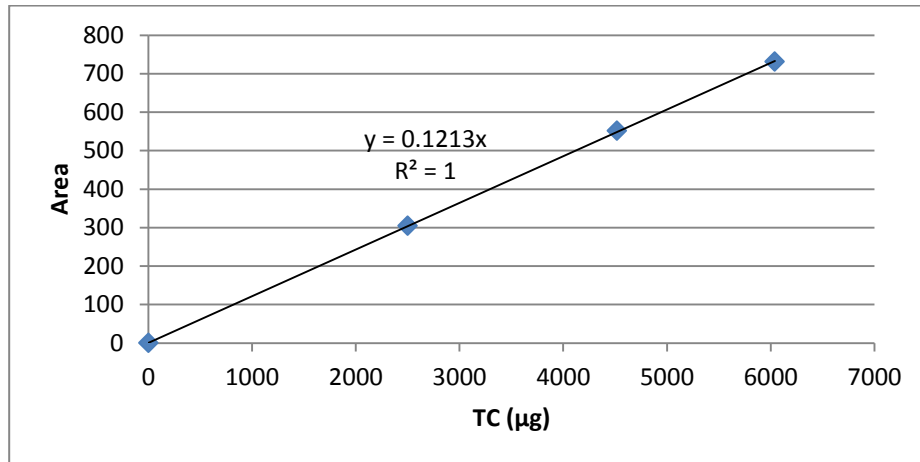


Figure C-1: Calibration Curve for Carbon Content Analysis from 5-23-12

The calibration curve for carbon content analysis from 5-23-12 can be seen in Figure C-1. The area of the response for unknown samples can then be measured and the carbon in the sample can be found. Since previous carbon content analysis measured 90 % - 95 % C, the mass of unknown samples was kept below approximately 6 mg to ensure the area of the response would be in the range of the calibration curve. Coke samples were weighed out and the carbon content was measured.

Table C-1: Results of Carbon Content Analysis for Atmospheric Pressure Coking

Sample name: 4-24-497-N2				
#	Area	CNV	% C	amount (mg)
1	575.1	575.1	92.94	5.1
2	646.0	558.4	90.26	5.9
MN	610.6	566.8	91.60	
SD		11.8	1.9	
CV		2.08%	2.07%	

Sample name: 4-26-484-N2				
#	Area	CNV	% C	amount (mg)
1	554.7	554.7	93.3	4.9
2	696.4	550.4	92.6	6.2
MN	625.6	552.5	92.95	
SD		3.05	0.5	
CV		0.55%	0.53%	

Sample name: 5-3-474-N2				
#	Area	CNV	% C	amount (mg)
1	610.7	610.7	91.53	5.5
2	633.5	622.2	93.25	5.6
3	518.1	647.6	97.04	4.4
4	664.7	609.3	91.33	6.0
MN	606.8	622.5	93.29	
SD		17.7	2.65	
CV		2.85%	2.84%	

Sample name: 5-2-464_1-N2				
#	Area	CNV	% C	amount (mg)
1	609.7	609.7	91.38	5.5
2	558.9	591.1	88.59	5.2
3	632.6	632.6	94.81	5.5
4	637.2	604.2	90.56	5.8
MN	609.6	609.4	91.33	
SD		17.3	2.6	
CV		2.84%	2.84%	

Table C-2: Results of Carbon Content Analysis for Vacuum Pressure Coking

Sample name: 5-8-463-VAC				
#	Area	CNV	%	amount (mg)
1	464.9	464.9	91.21	4.2
2	566.2	475.6	93.33	5.0
MN	515.6	470.3	92.27	
SD		7.57	1.5	
CV		1.61%	1.63%	

Sample name: 5-10-492-VAC				
#	Area	CNV	%	amount (mg)
1	610	610	88.21	5.7
2	555.5	608.9	88.05	5.2
MN	582.8	609.5	88.13	
SD		0.77	0.12	
CV		0.13%	0.13%	

The data collected for carbon content analysis of atmospheric (Table C-1) and vacuum pressure coking samples (Table C-2) can be seen above.

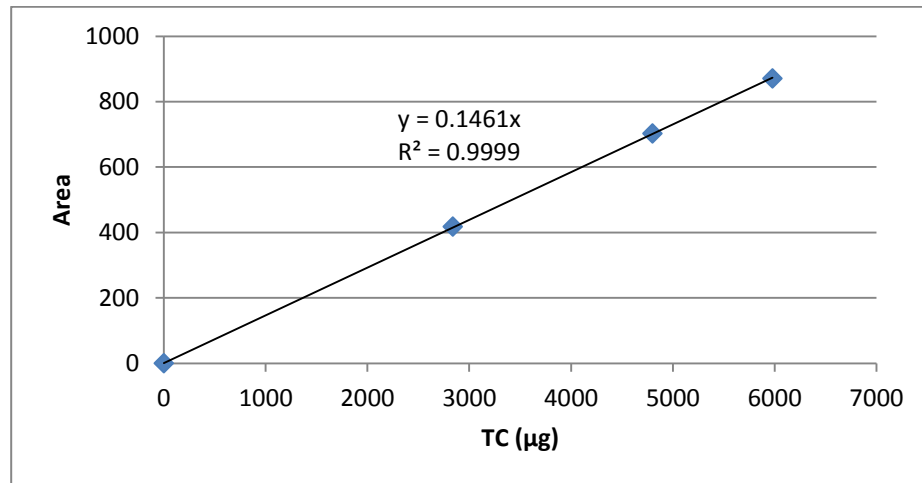


Figure C-2: Calibration Curve for Carbon Content Analysis from 6-15-12

The calibration curve from 6-15-12 can be seen in Figure C-2. This curve was used to measure the carbon content of the final two coking tests at 460 °C.

Table C-3: Results of Carbon Content Analysis for Atmospheric Pressure Coking

Sample name: 6-5-465_2-N2				
#	Area	CNV	% C	amount (mg)
1	790.0	790.0	91.70	5.9
2	850.1	796.1	92.43	6.3
3	727.3	794.6	92.22	5.4
4	638.1	784.3	91.00	4.8
MN	751.4	791.3	91.84	
SD		5.31	0.64	
CV		0.67%	0.69%	

Sample name: 6-7-462_3-N2				
#	Area	CNV	% C	amount (mg)
1	710.7	710.7	91.81	5.3
2	838.4	705.3	91.15	6.3
3	599.6	706.2	91.19	4.5
4	713.9	713.9	92.23	5.3
MN	715.7	709.0	91.60	
SD		4.01	0.52	
CV		0.57%	0.57%	

Table C-3 shows the data collected for carbon content analysis of the final two atmospheric pressure coke samples at 460 °C.



APPENDIX D

Moisture Content/Volatile Matter/Fixed Carbon/Ash Content Graphs

The graphs were constructed from the TA Instruments SDT Q600 TGA instrument

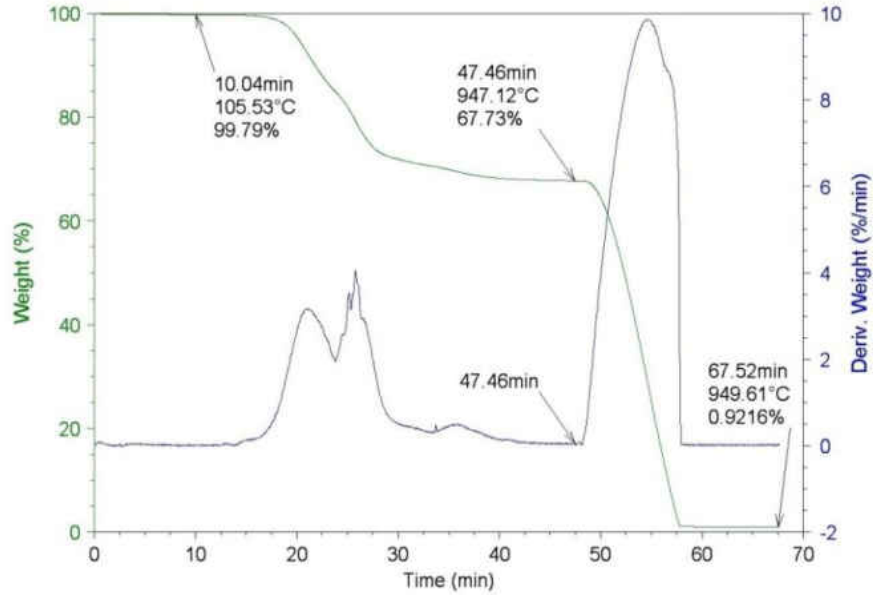


Figure D-1: Moisture Content/Volatile Matter/Fixed Carbon/Ash Content Evolution for 464 °C\_1 (test 2) Coke Sample

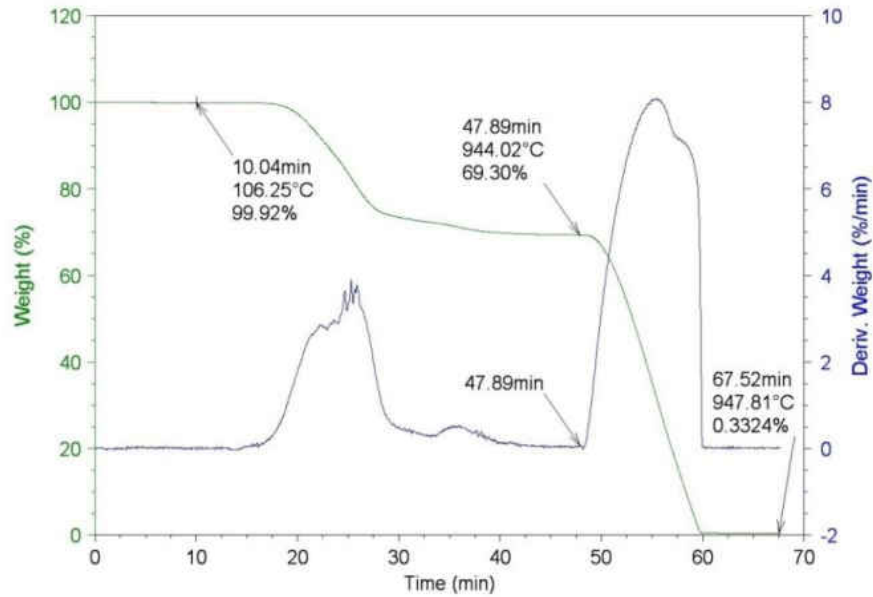


Figure D-2: Moisture Content/Volatile Matter/Fixed Carbon/Ash Content Evolution for 464 °C\_1 (test 3) Coke Sample

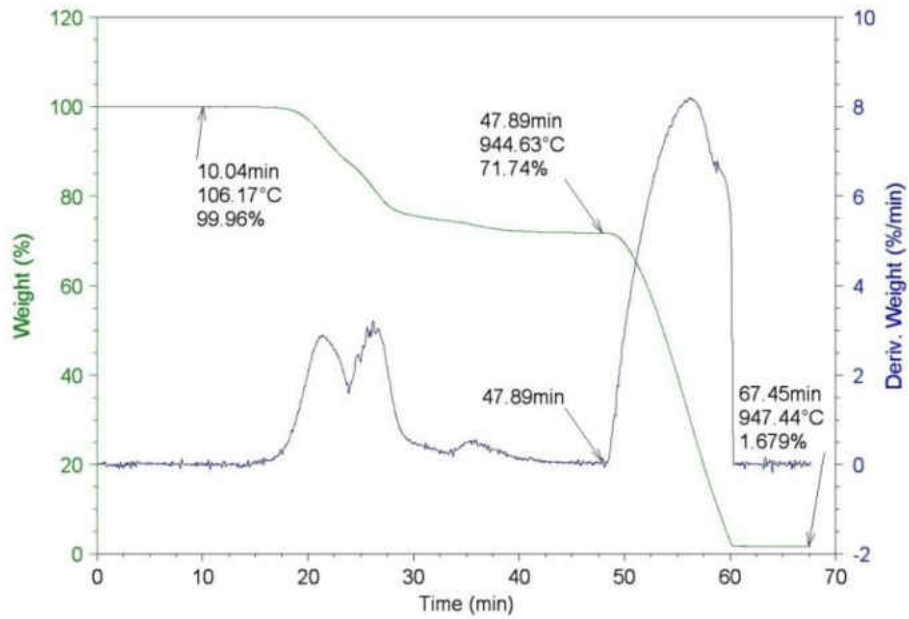


Figure D-3: Moisture Content/Volatile Matter/Fixed Carbon/Ash Content Evolution for 464 °C\_1 (test 4) Coke Sample

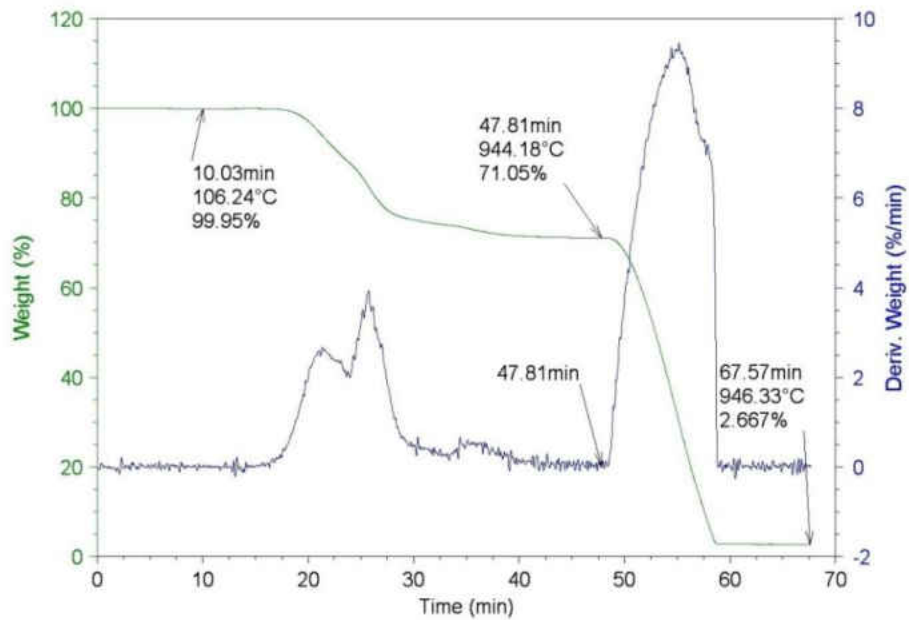


Figure D-4: Moisture Content/Volatile Matter/Fixed Carbon/Ash Content Evolution for 464 °C\_1 (test 5) Coke Sample

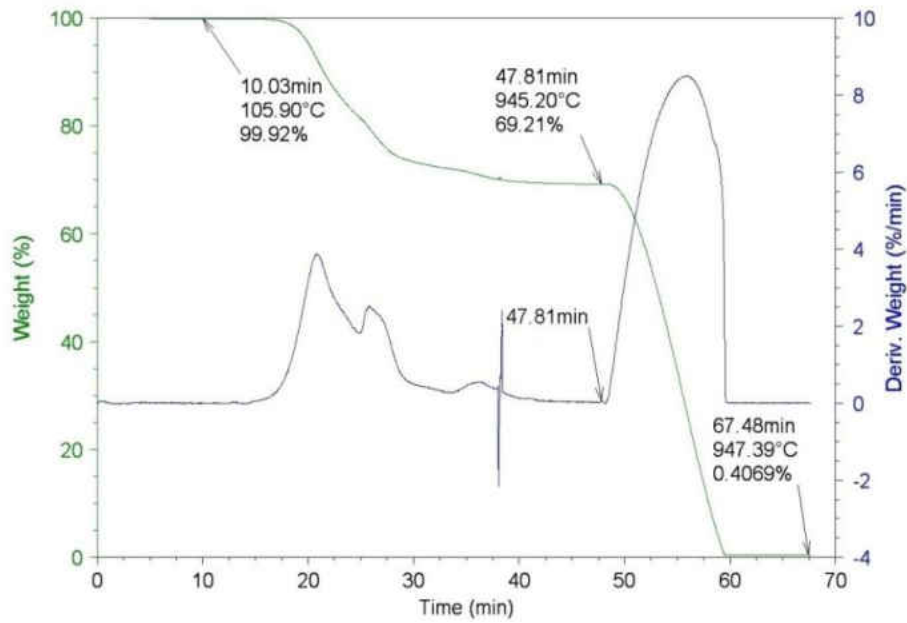


Figure D-5: Moisture Content/Volatile Matter/Fixed Carbon/Ash Content Evolution for 465 °C\_2 (test 1) Coke Sample

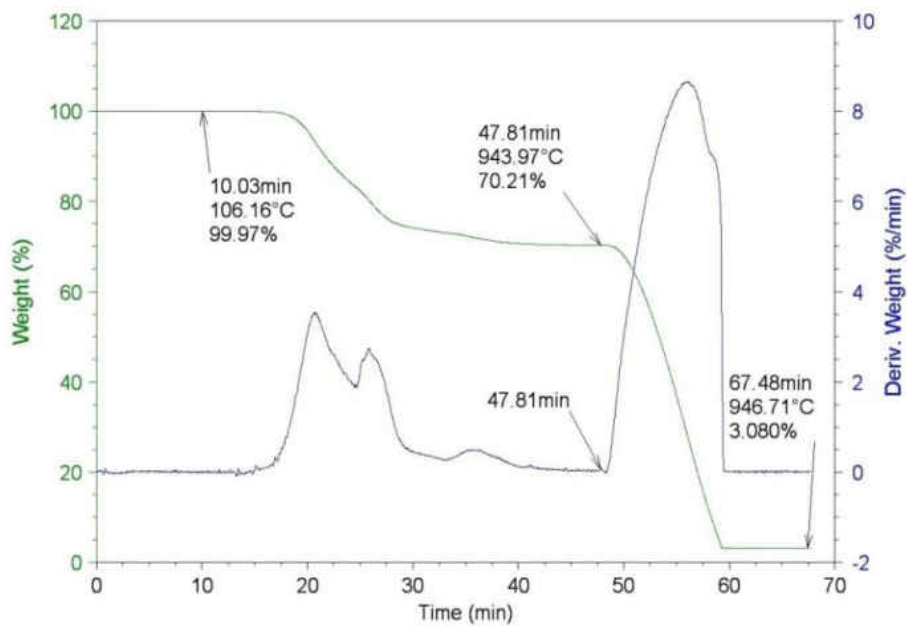


Figure D-6: Moisture Content/Volatile Matter/Fixed Carbon/Ash Content Evolution for 465 °C\_2 (test 2) Coke Sample

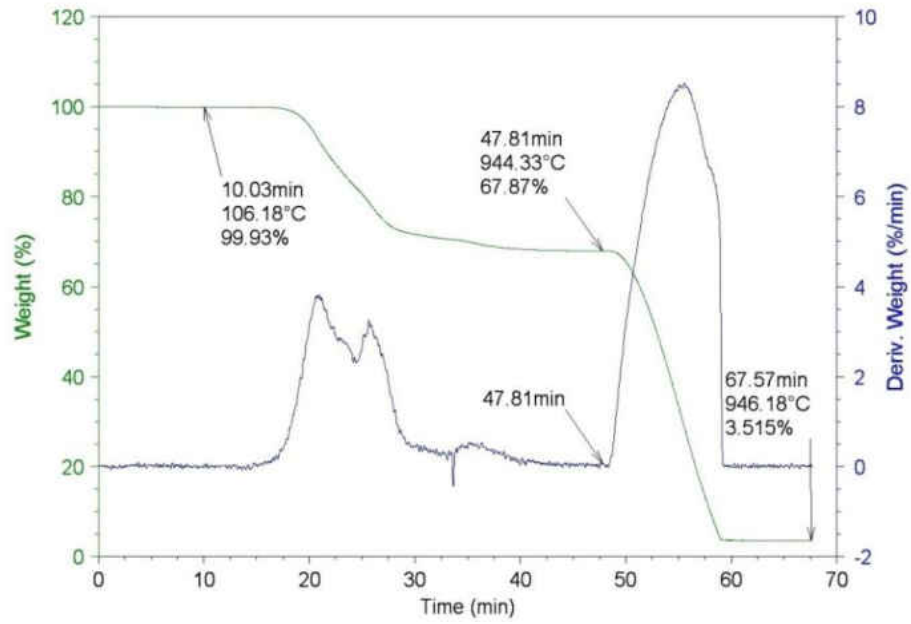


Figure D-7: Moisture Content/Volatile Matter/Fixed Carbon/Ash Content Evolution for 465 °C\_2 (test 3) Coke Sample

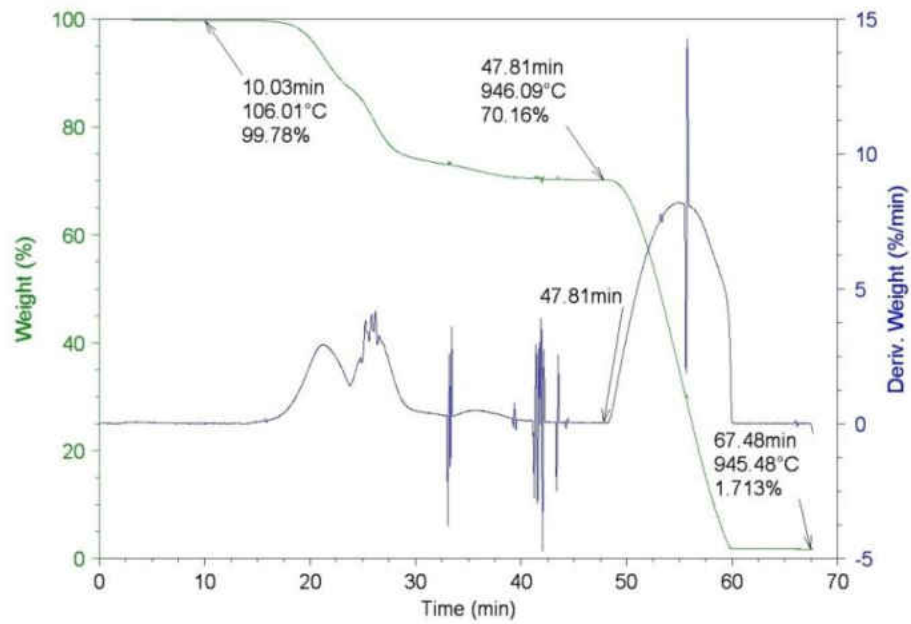


Figure D-8: Moisture Content/Volatile Matter/Fixed Carbon/Ash Content Evolution for 462 °C\_3 (test 1) Coke Sample

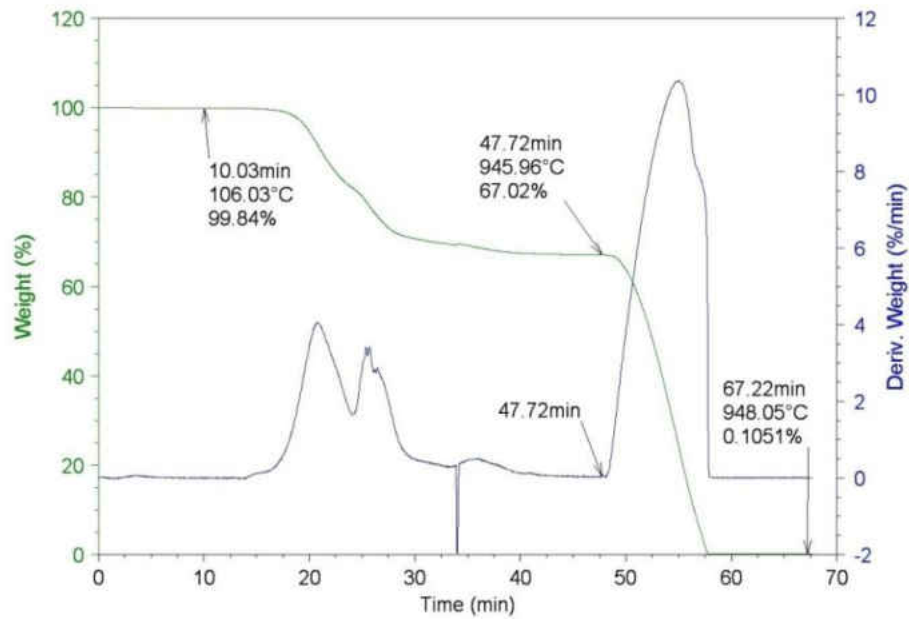


Figure D-9: Moisture Content/Volatile Matter/Fixed Carbon/Ash Content Evolution for 462 °C\_3 (test 2) Coke Sample

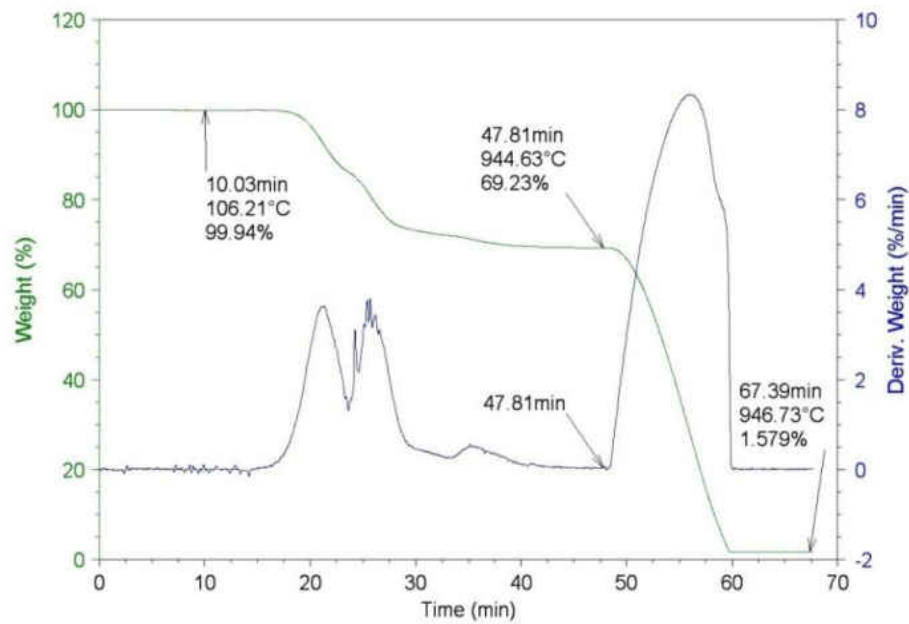


Figure D-10: Moisture Content/Volatile Matter/Fixed Carbon/Ash Content Evolution for 462 °C\_3 (test 3) Coke Sample

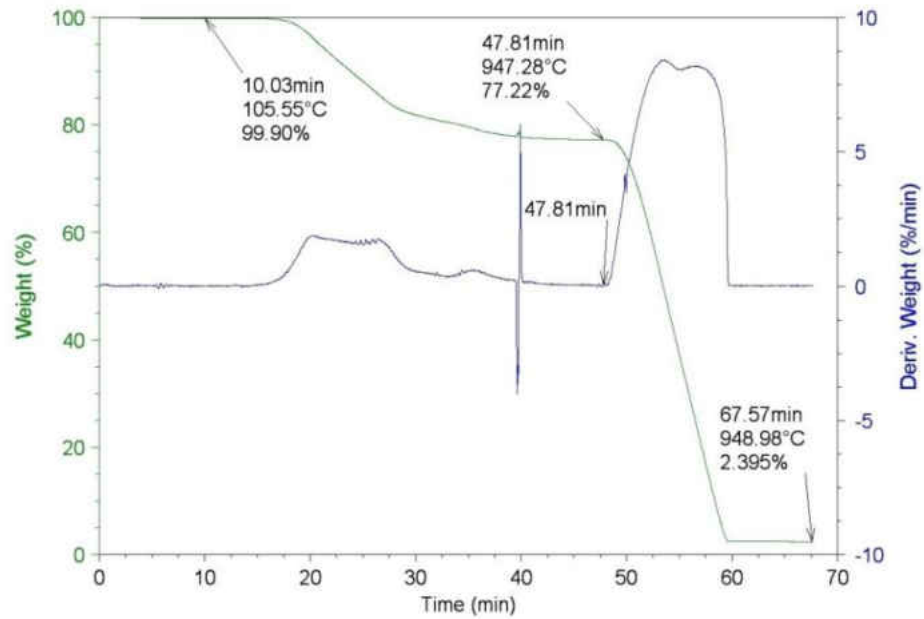


Figure D-11: Moisture Content/Volatile Matter/Fixed Carbon/Ash Content Evolution for 474 °C (test 1) Coke Sample

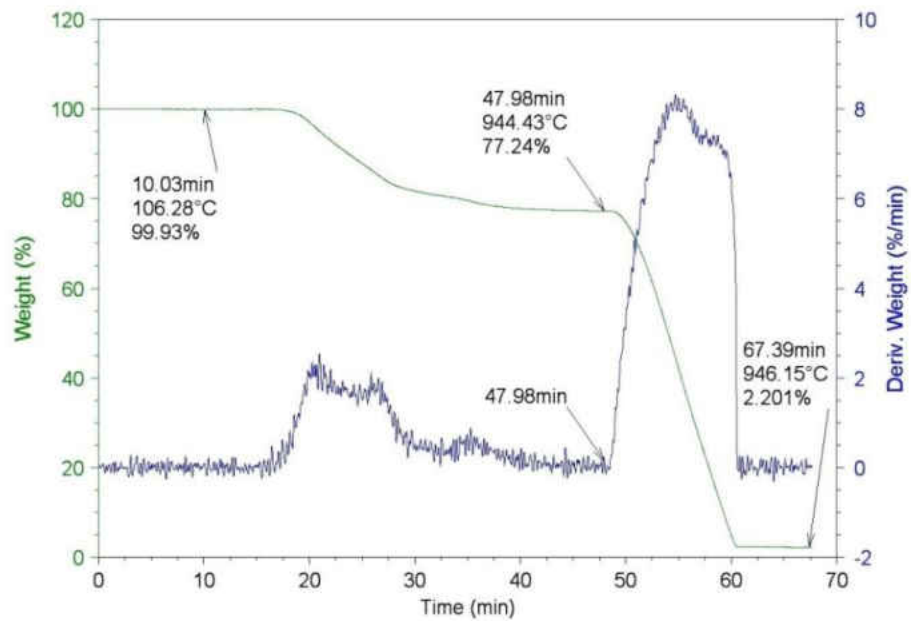


Figure D-12: Moisture Content/Volatile Matter/Fixed Carbon/Ash Content Evolution for 474 °C (test 2) Coke Sample

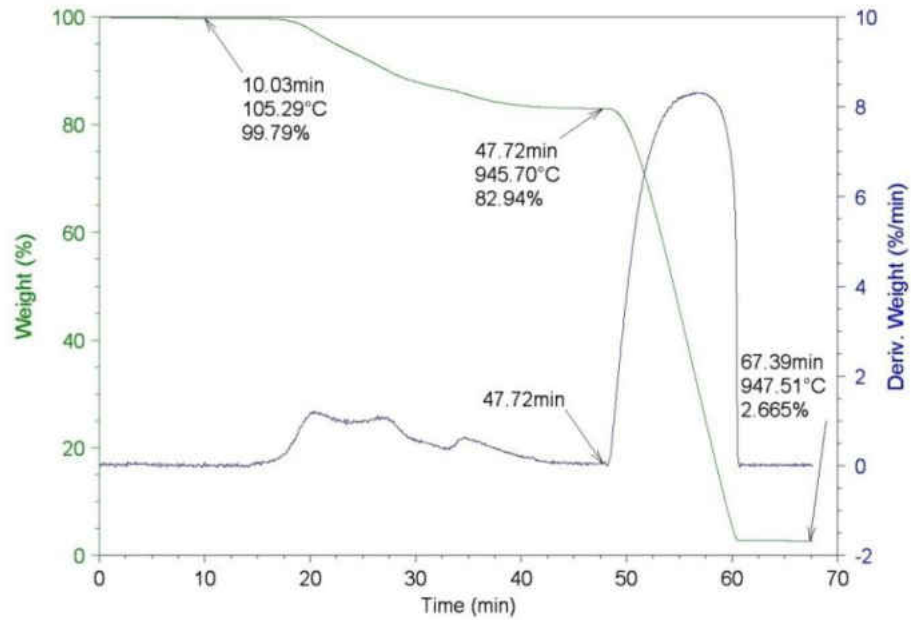


Figure D-13: Moisture Content/Volatile Matter/Fixed Carbon/Ash Content Evolution for 484 °C (test 1) Coke Sample

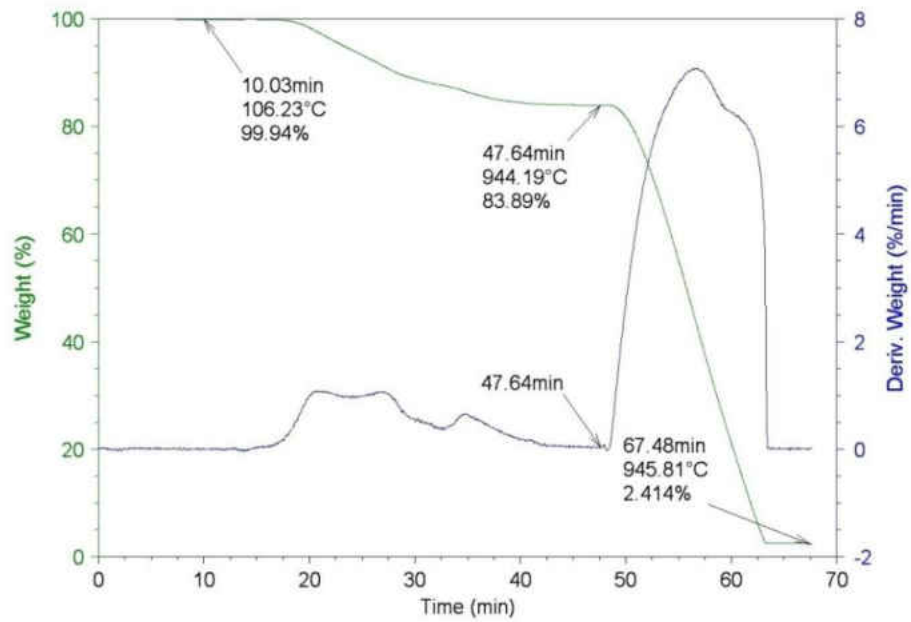


Figure D-14: Moisture Content/Volatile Matter/Fixed Carbon/Ash Content Evolution for 484 °C (test 2) Coke Sample

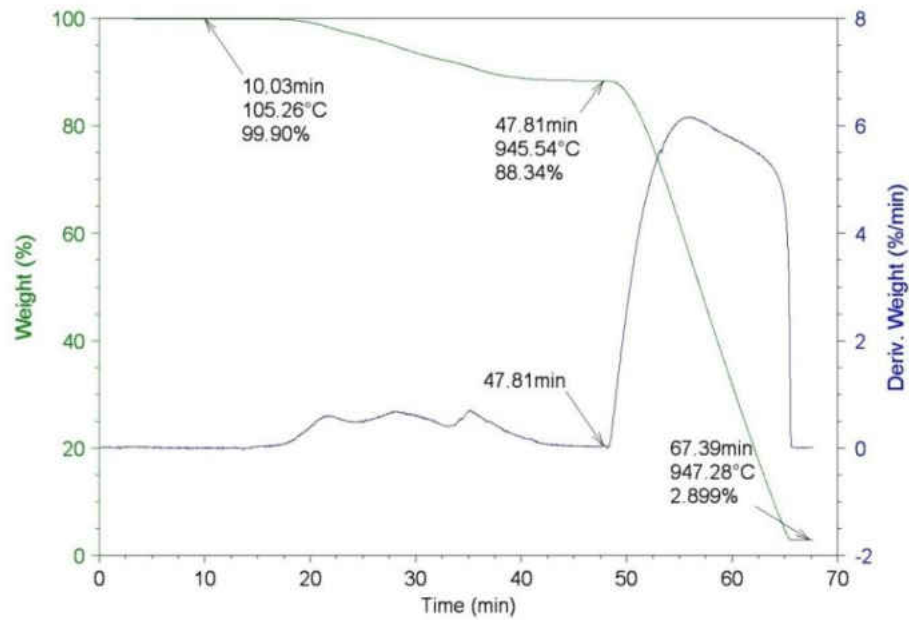


Figure D-15: Moisture Content/Volatile Matter/Fixed Carbon/Ash Content Evolution for 497 °C (test 1) Coke Sample

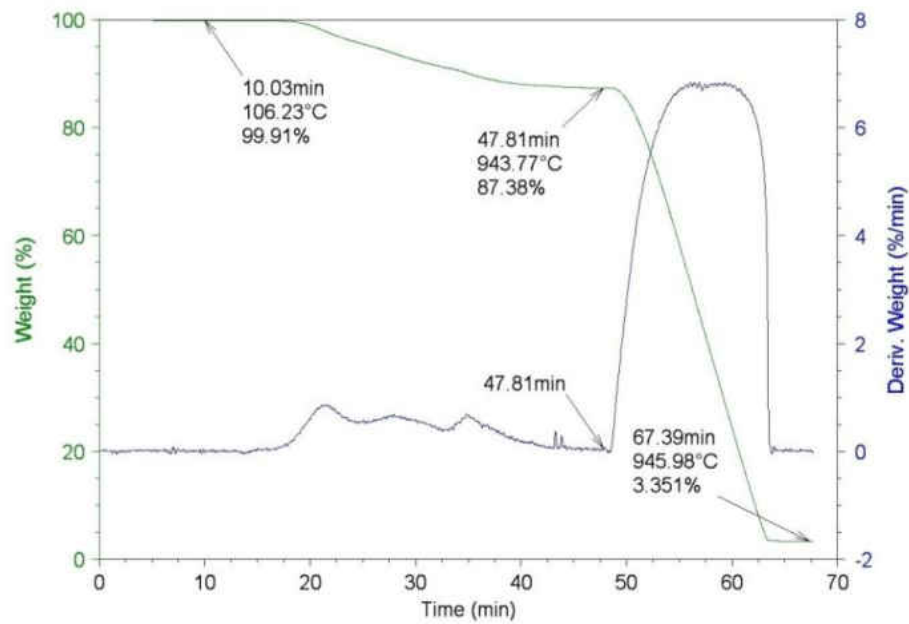


Figure D-16: Moisture Content/Volatile Matter/Fixed Carbon/Ash Content Evolution for 497 °C (test 2) Coke Sample



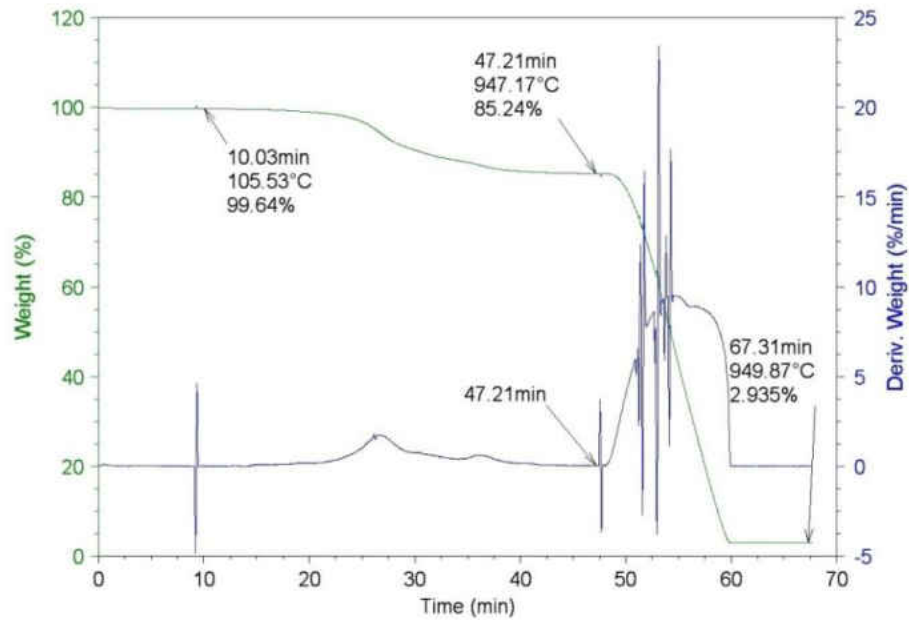


Figure D-17: Moisture Content/Volatile Matter/Fixed Carbon/Ash Content Evolution for 463 °C\_Vac (test 1) Coke Sample

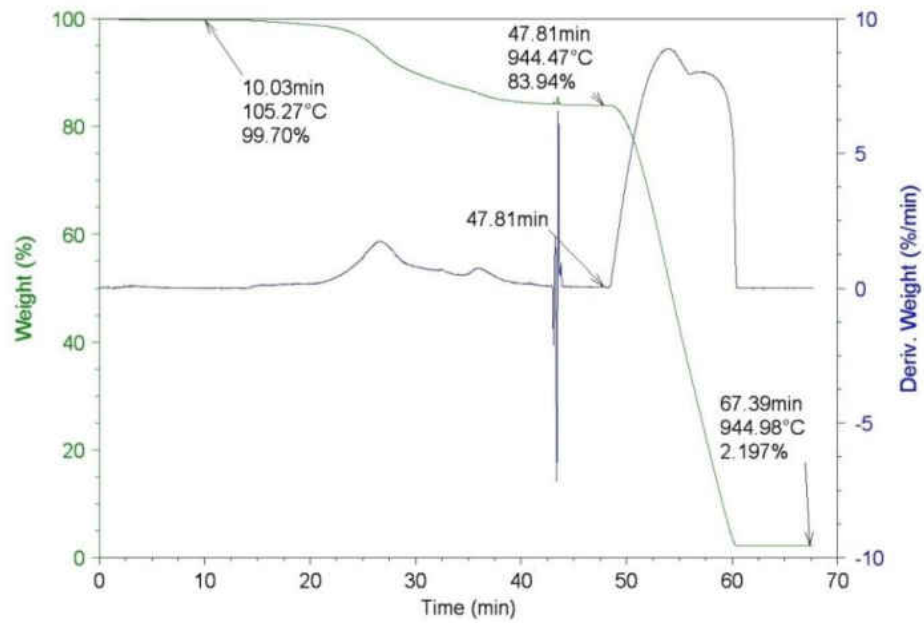


Figure D-18: Moisture Content/Volatile Matter/Fixed Carbon/Ash Content Evolution for 463 °C\_Vac (test 2) Coke Sample

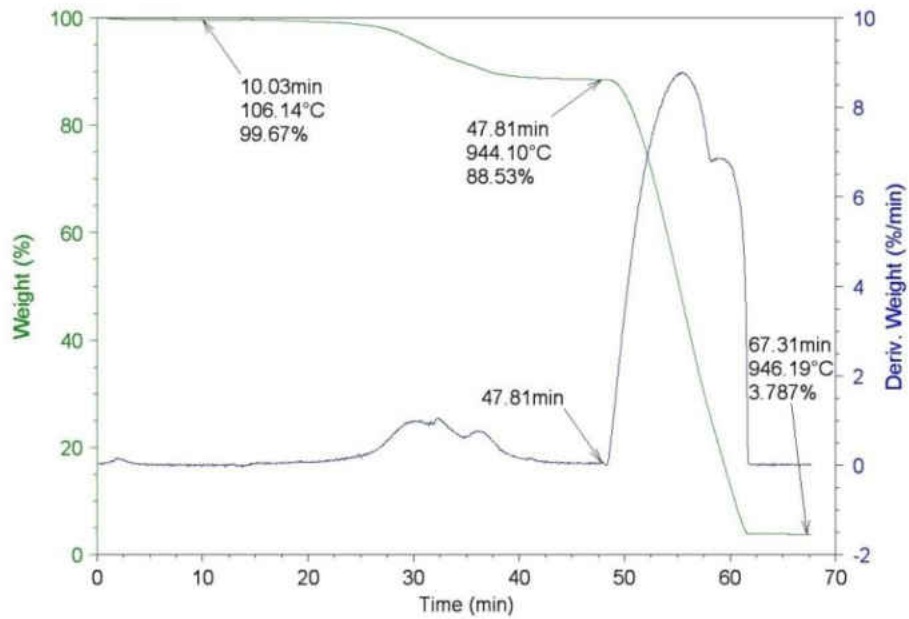


Figure D-19: Moisture Content/Volatile Matter/Fixed Carbon/Ash Content Evolution for 492 °C\_Vac (test 1) Coke Sample

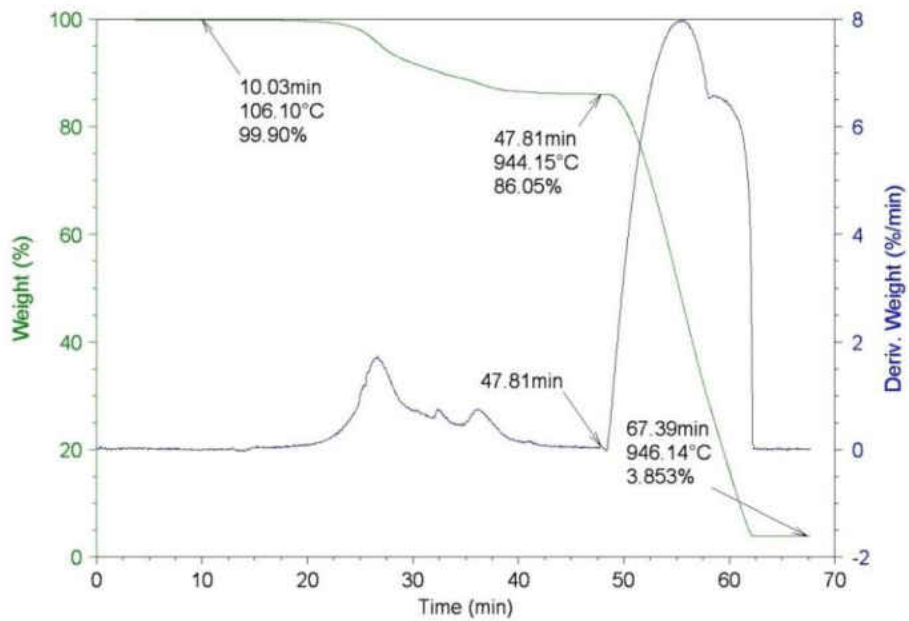


Figure D-20: Moisture Content/Volatile Matter/Fixed Carbon/Ash Content Evolution for 492 °C\_Vac (test 2) Coke Sample

APPENDIX E  
GC SimDist Liquid Analysis

Table E.1: Retention Times of Standard Components for Liquid Analysis (6-27-12)

Component	BP (°C)	RT (min)
Dichloromethane (solvent)	39.9	2.20800
n-Hexane	68.8	2.56400
n-Heptane	98.4	3.71600
n-Octane	125.6	6.15067
n-Nonane	150.7	7.84667
n-Decane	174.1	8.92133
n-Tridecane	233.9	10.92133
n-Hexadecane	280.9	12.46000
n-Nonadecane	329.8	13.81067
n-Tricosane	380.1	15.40400

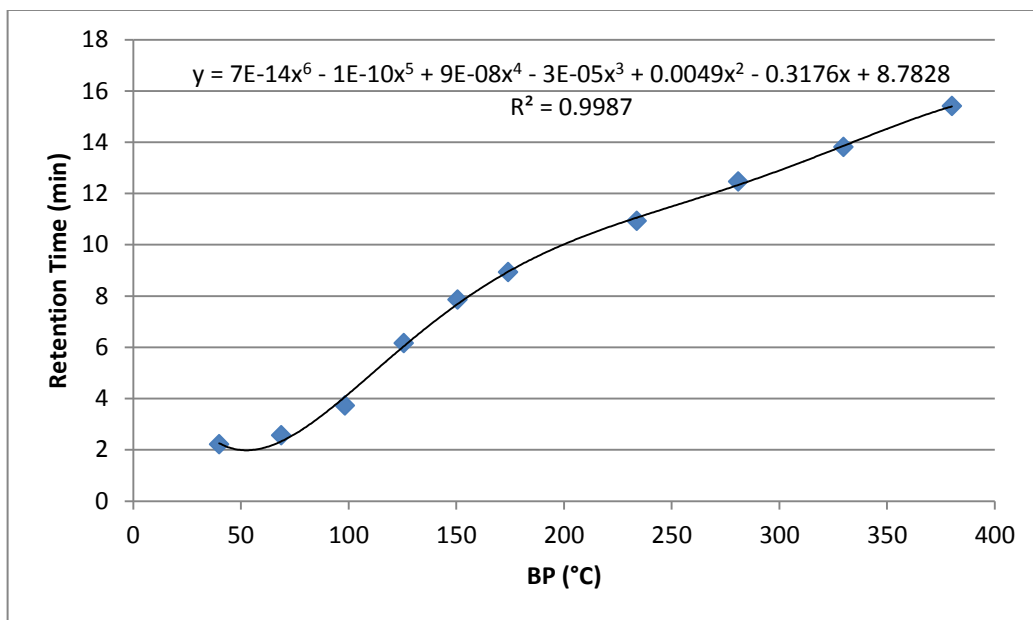


Figure E.1: Calibration Curve of Standard Components for Liquid Analysis (6-27-12)

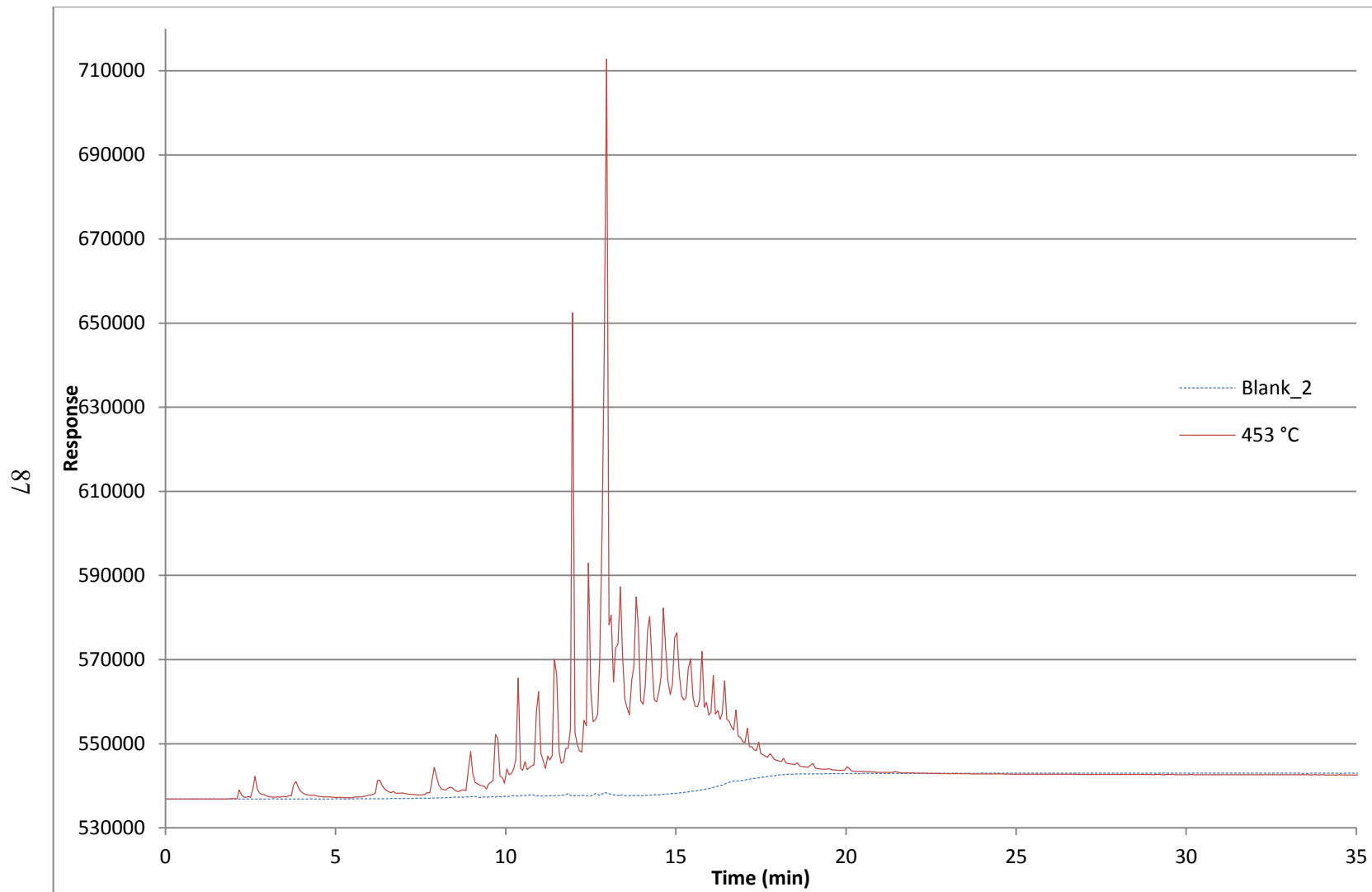


Figure E.2: Graph of 453 °C Atmospheric Pressure Coking Liquid Analysis

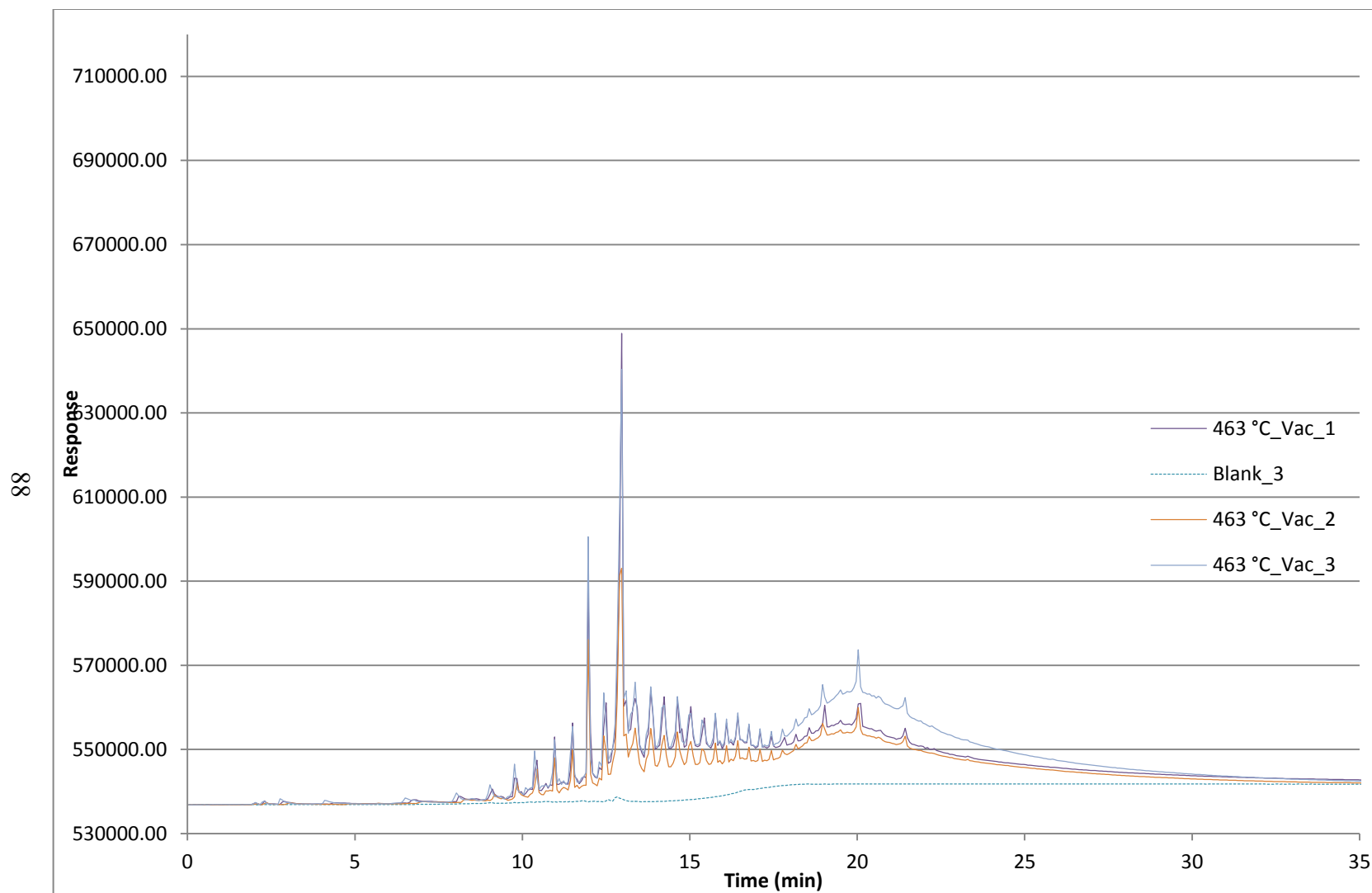


Figure E.3: Graph of 463 °C Vacuum Pressure Coking Liquid Analysis

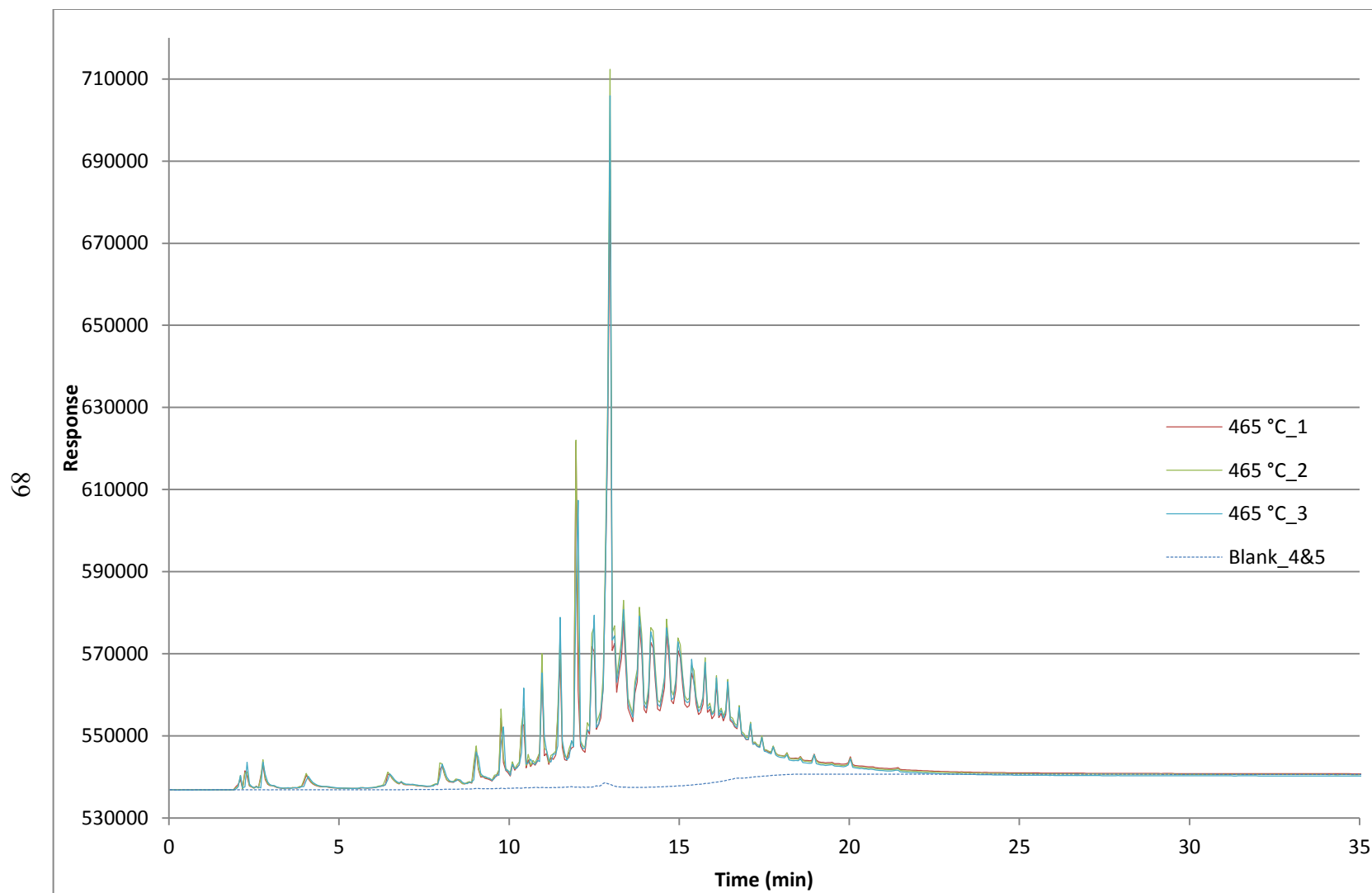


Figure E.4: Graph of 465 °C Atmospheric Pressure Coking Liquid Analysis

Table E.1 shows the retention times collected from analyzing the standard on 6-27-12. This data was then plotted in Figure E.1 to find an equation to relate boiling point to retention time. Figure E.2, E.3, and E.4 show the response for each sample and the blank that was subtracted from the samples for analysis.

Table E.2: Retention Times of Standard Components for Liquid Analysis (6-29-12)

Component	BP (°C)	RT (min)
Dichloromethane (solvent)	39.9	2.45867
n-Hexane	68.8	3.08933
n-Heptane	98.4	4.35200
n-Octane	125.6	6.56267
n-Nonane	150.7	8.18800
n-Decane	174.1	9.17733
n-Tridecane	233.9	11.05600
n-Hexadecane	280.9	12.52000
n-Nonadecane	329.8	13.82933
n-Tricosane	380.1	15.39867

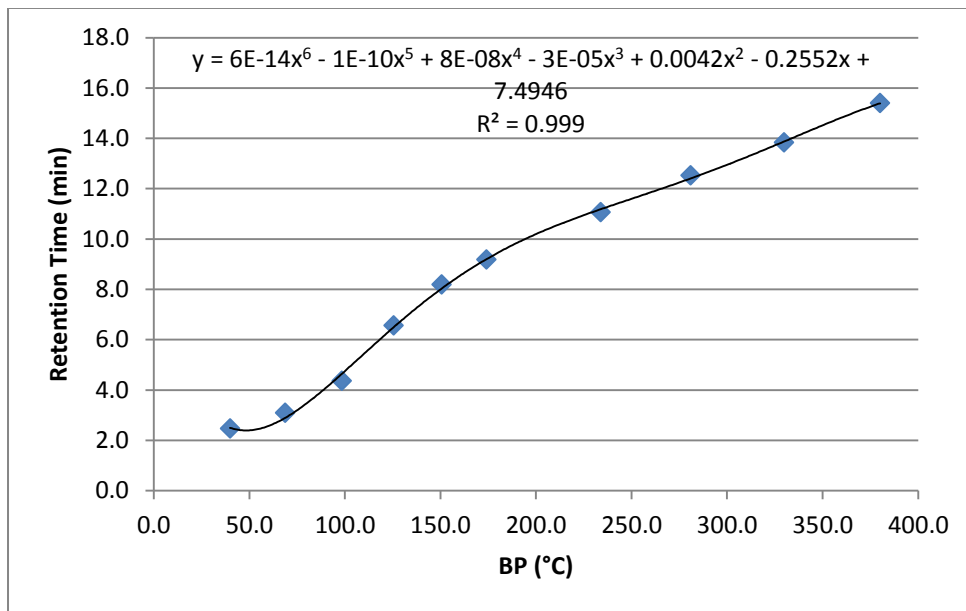


Figure E.5: Calibration Curve of Standard Components for Liquid Analysis (6-29-12)

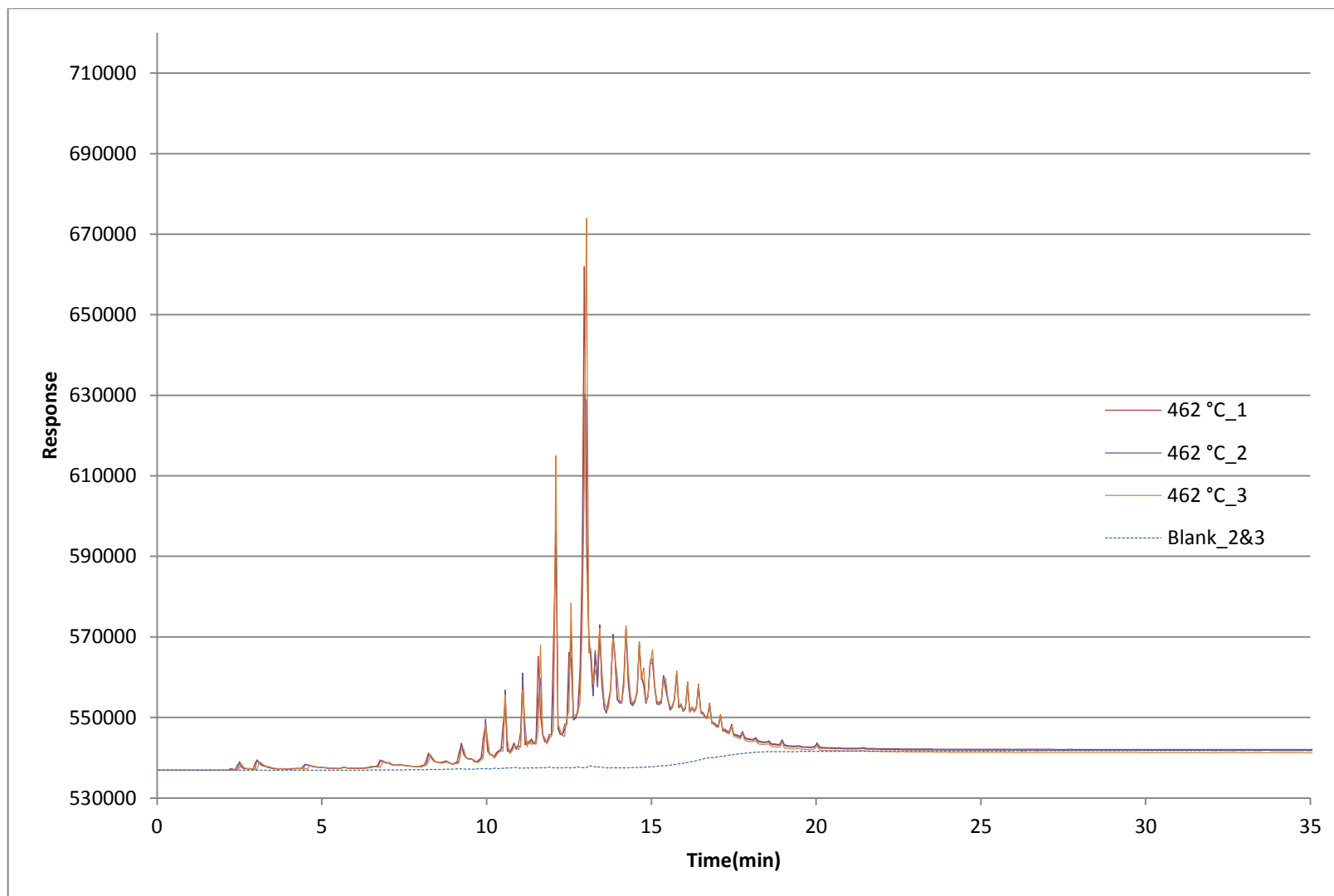


Figure E.6: Graph of 462 °C Atmospheric Pressure Coking Liquid Analysis



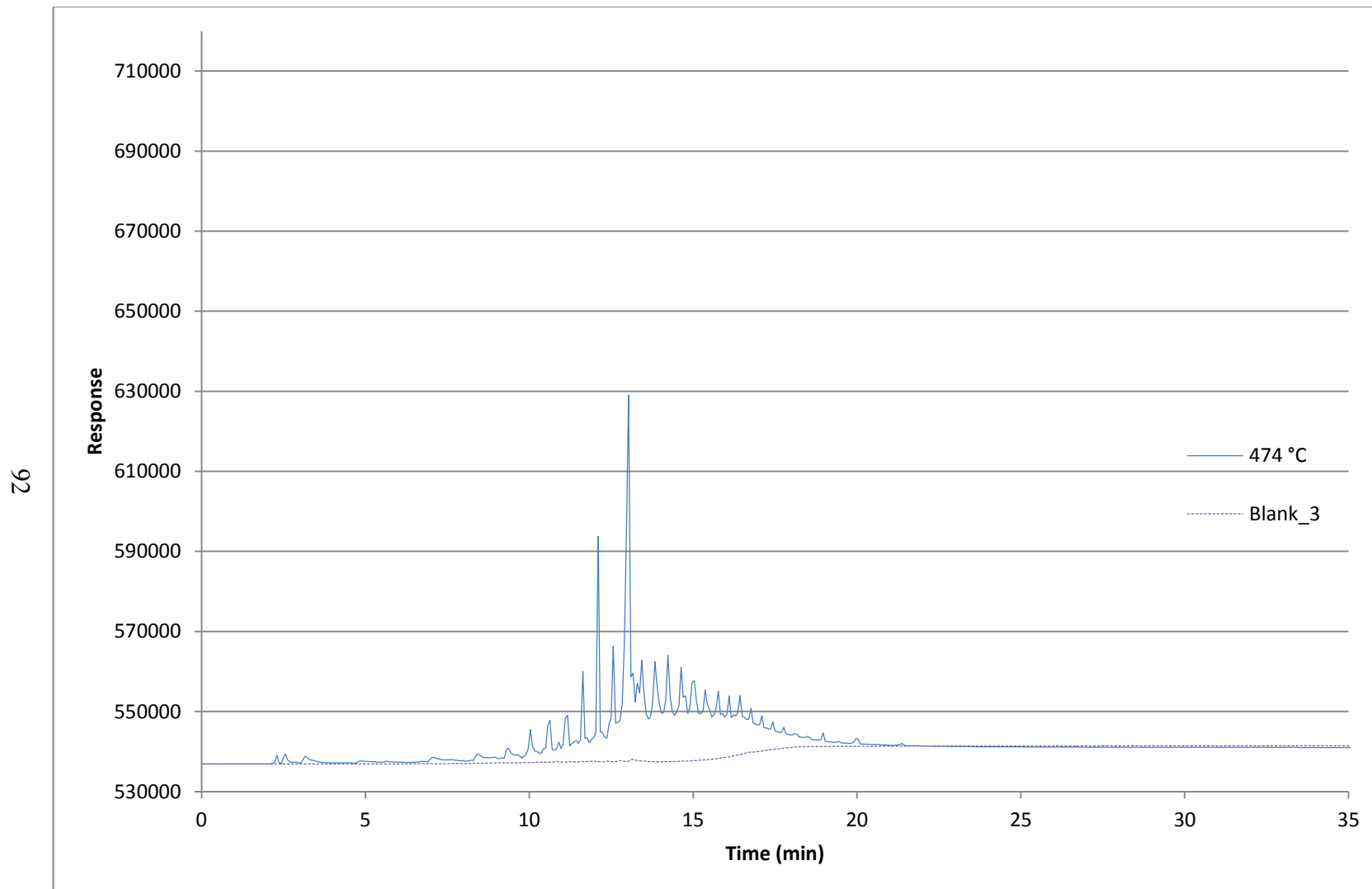


Figure E.7: Graph of 474 °C Atmospheric Pressure Coking Liquid Analysis

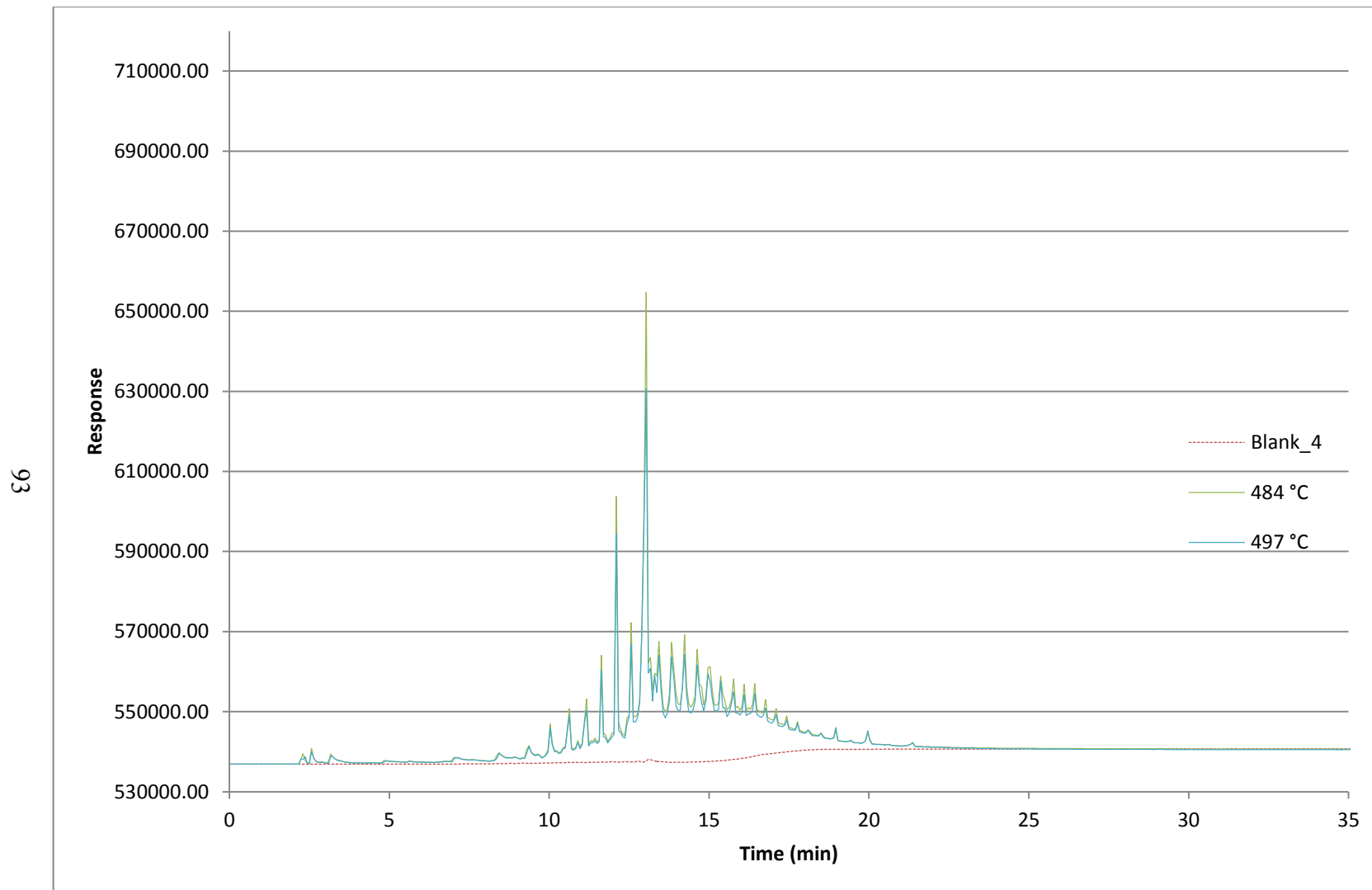


Figure E.8: Graph of 484 °C and 497 °C Atmospheric Pressure Coking Liquid Analysis

Table E.2 shows the retention times collected from analyzing the standard on 6-29-12. This data was then plotted in Figure E.2 to find an equation to relate boiling point to retention time. Figure E.6, E.7, and E.8 show the response for each sample and the blank that was subtracted from the samples for analysis.

Table E.3: Retention Times of Standard Components for Liquid Analysis (7-5-12)

Component	BP (°C)	RT (min)
Dichloromethane (solvent)	39.9	2.60133
n-Hexane	68.8	3.40000
n-Heptane	98.4	4.78667
n-Octane	125.6	6.80133
n-Nonane	150.7	8.36400
n-Decane	174.1	9.32533
n-Tridecane	233.9	11.17067
n-Hexadecane	280.9	12.60400
n-Nonadecane	329.8	13.86133
n-Tricosane	380.1	15.37200

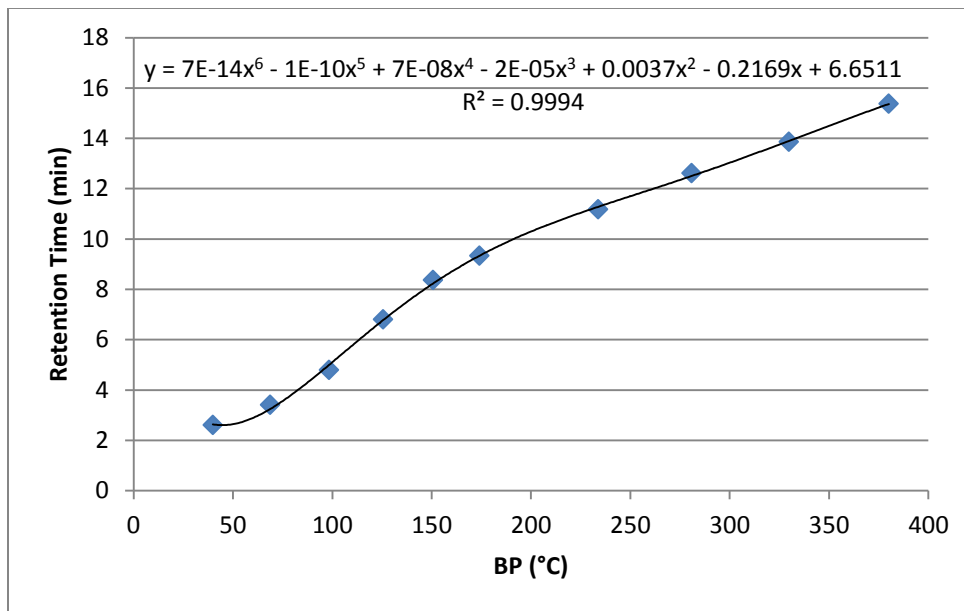


Figure E.9: Calibration Curve of Standard Components for Liquid Analysis (7-5-12)

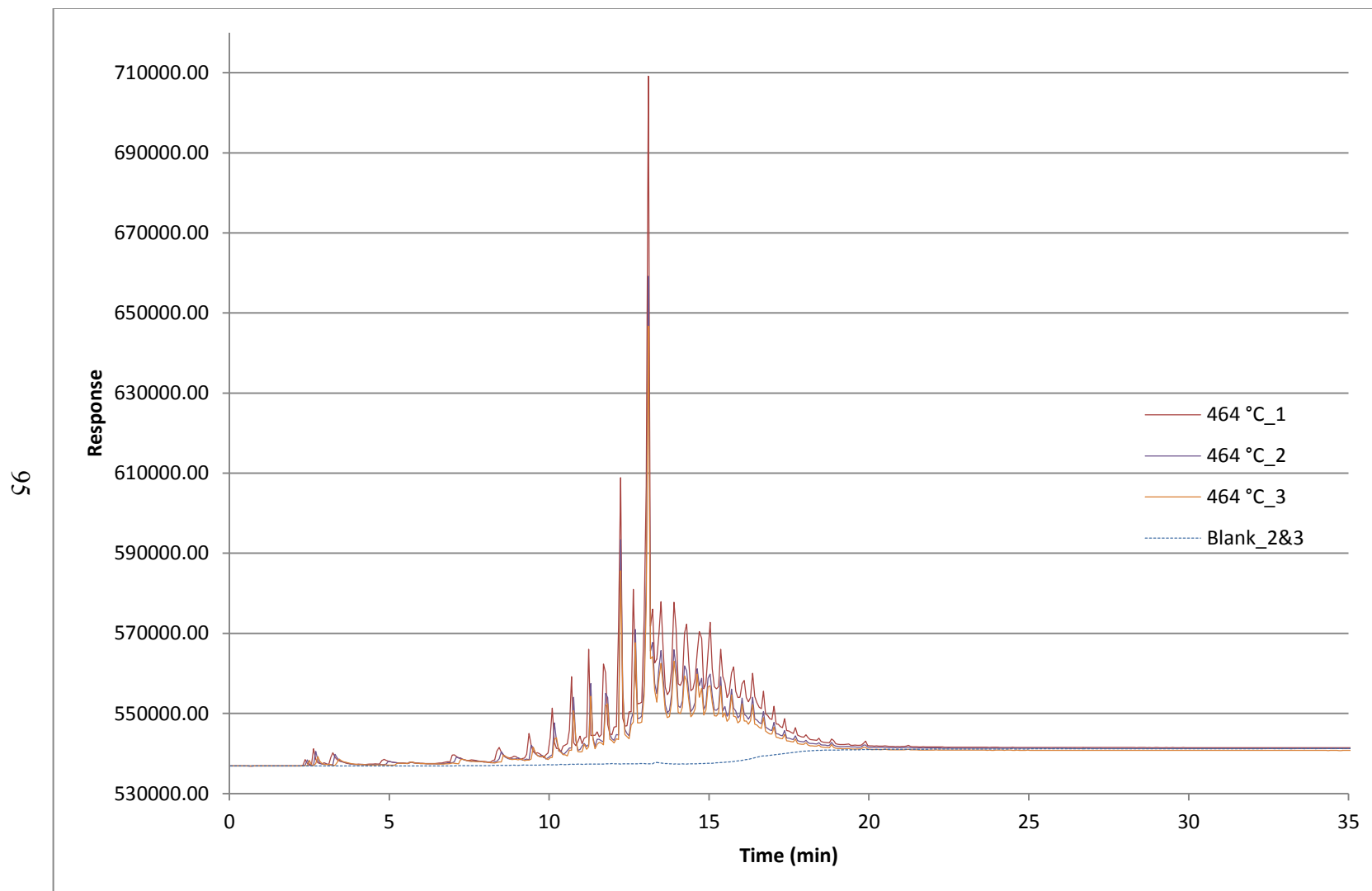


Figure E.10: Graph of 464 °C Atmospheric Pressure Coking Liquid Analysis

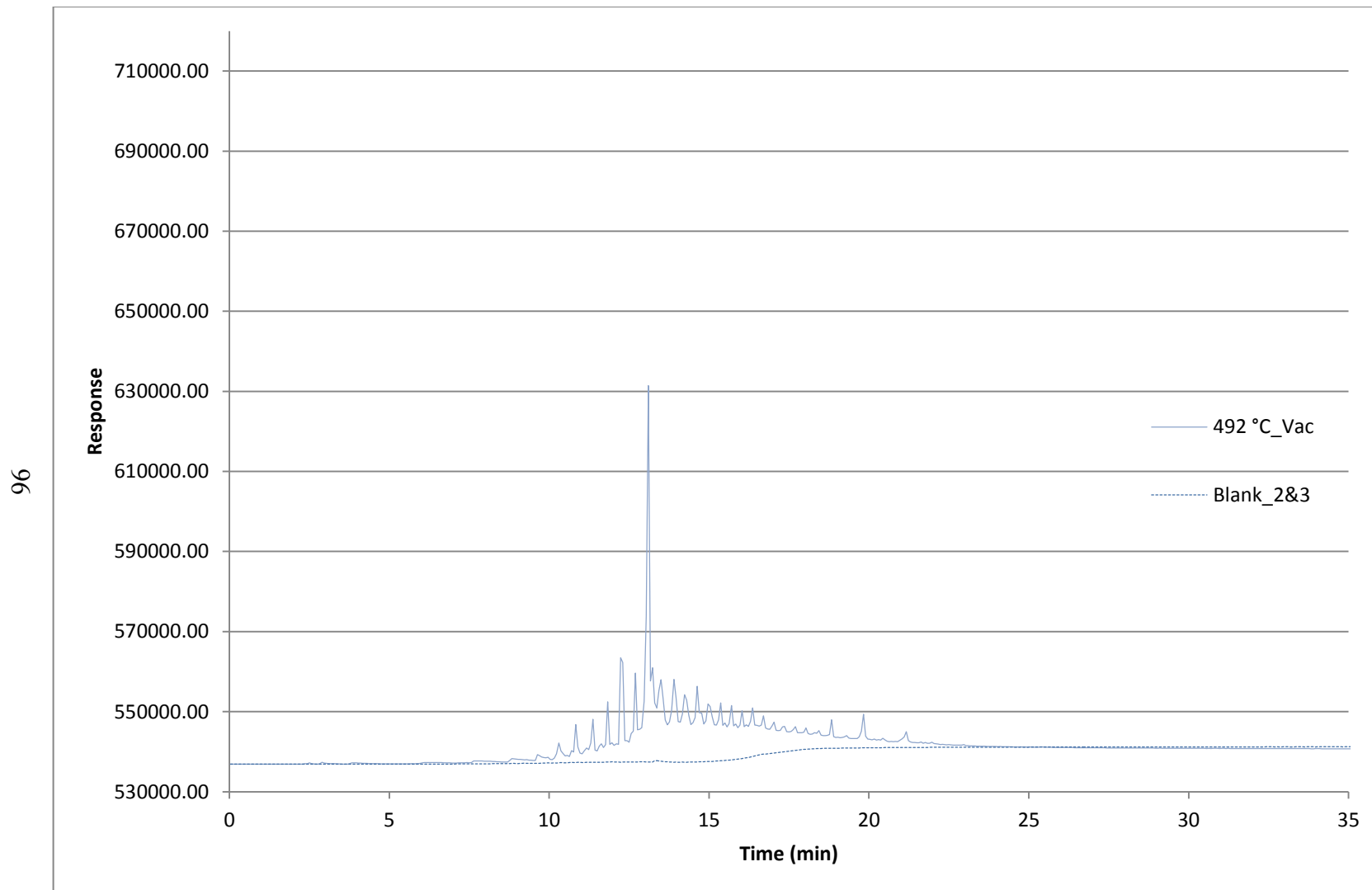


Figure E.11: Graph of 492 °C Vacuum Pressure Coking Liquid Analysis

Table E.3 shows the retention times collected from analyzing the standard on 7-5-12. This data was then plotted in Figure E.3 to find an equation to relate boiling point to retention time. Figure E.10 and E11 show the response for each sample and the blank that was subtracted from the samples for analysis.

APPENDIX F  
Acid Analysis Calibrations

Table F.1: Data from the Standard Mixture used for finding Density of the Mixture

Standard	Octanoic Acid (g)	Dodecane (g)	Amount of Acid (weight %)	Total Mass (g)	Density of Mixture (g/mL)
1	0.0000	0.0000	0.00%	0.0000	0.7490
2	0.0893	8.9287	0.99%	9.0180	0.7503
3	0.3570	7.1527	4.75%	7.5097	0.7554
4	1.0497	6.9982	13.04%	8.0479	0.7667
5	1.7503	5.2546	24.99%	7.0049	0.7836

Table F.2: Data from the Standard Mixture used for Calibration

Standard	Density of Mixture (g/mL)	Acid Concentration (mol/L)	Peak Height (abs units)
1	0.7490	0.00	-0.005
2	0.7503	1266	0.104
3	0.7554	6117	0.487
4	0.7667	17034	1.194
5	0.7836	33354	2.001

Table F.1 and F.2 show the data gathered and calculated for the standard mixture used for calibration. The mass of octanoic acid ( $\rho = 0.91$ , MW = 144.22) and dodecane ( $\rho = 0.749$ , MW = 170.34) were measured and mixed to make the standard mixture. The weight % of acid was calculated from these masses. The density of the mixture was calculated by first calculating the volume of each component in the mixture ( $m_i / \rho_i$ ). Then dividing the total mass by the total volume produces the density of the mixture. The concentration (mol/L) of acid was calculated by multiplying the weight % of acid by the molecular weight of acid and by the density of the mixture. A calibration curve was constructed by plotting the peak height with the concentration (mol/L) of acid. The acid

concentration was used for the calibration curve instead of the weight % of acid because the liquid samples contain an unknown, complex mixture of acids in with the hydrocarbons

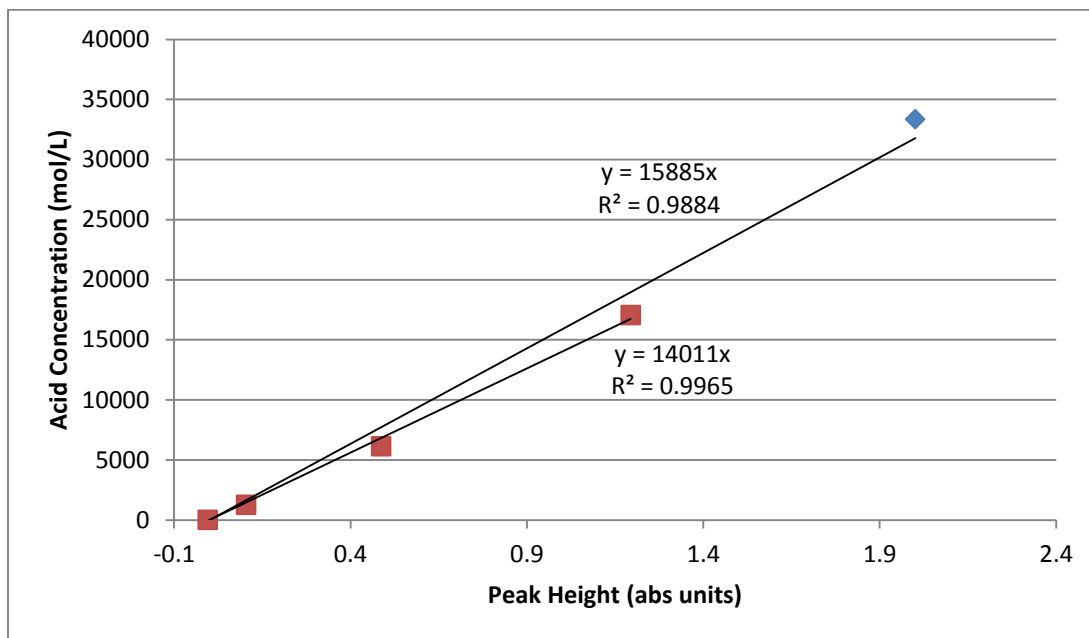


Figure F.1: Graph of the Acid Concentration vs. Peak Height for Acid Analysis Calibration

Figure F.1 shows the graph of the calibration curve for acid analysis. Trendlines were added to the graph for all of the calibration points and for only the first four calibration points. Using only the first four calibration points produced a better fit of the trendline for the data and is still inside the range of peak heights that were measured for the samples. Therefore this trendline will be used for finding the acid concentration.



Appendix G  
Gas Chromatography Calibrations & Additional Analysis

A calibration bag consisting of 10 % volume fraction hydrogen diluted in nitrogen was mixed and used for construction of a calibration curve.

Table G.1: Data for Hydrogen Calibration of Gas Chromatography

Injected Vol. ( $\mu\text{L}$ )	TCD Signal Response ( $\text{mV}\cdot\text{min}$ )		
	trial 1	trial 2	trial 3
100	227.1584	228.2564	233.3156
200	449.6630	443.1992	447.7020
400	854.7198	836.3654	860.7360
600	1266.6592	1232.1832	1261.3170
800	1635.8380	1640.3160	1637.9994
1000	2022.1700	2001.9256	2034.1544

Each injected volume was run in triplicate and the average TCD signal response was found and plotted versus the volume of hydrogen.

Table G.2: Averages for Hydrogen Calibration of Gas Chromatography

Injected Vol. ( $\mu\text{L}$ )	Average TCD Signal Response ( $\text{mV}\cdot\text{min}$ )	Volume $\text{H}_2$ ( $\mu\text{L}$ )
0	0	0
100	229.5768	10
200	446.8547333	20
400	850.6070667	40
600	1253.386467	60
800	1638.051133	80
1000	2019.416667	100

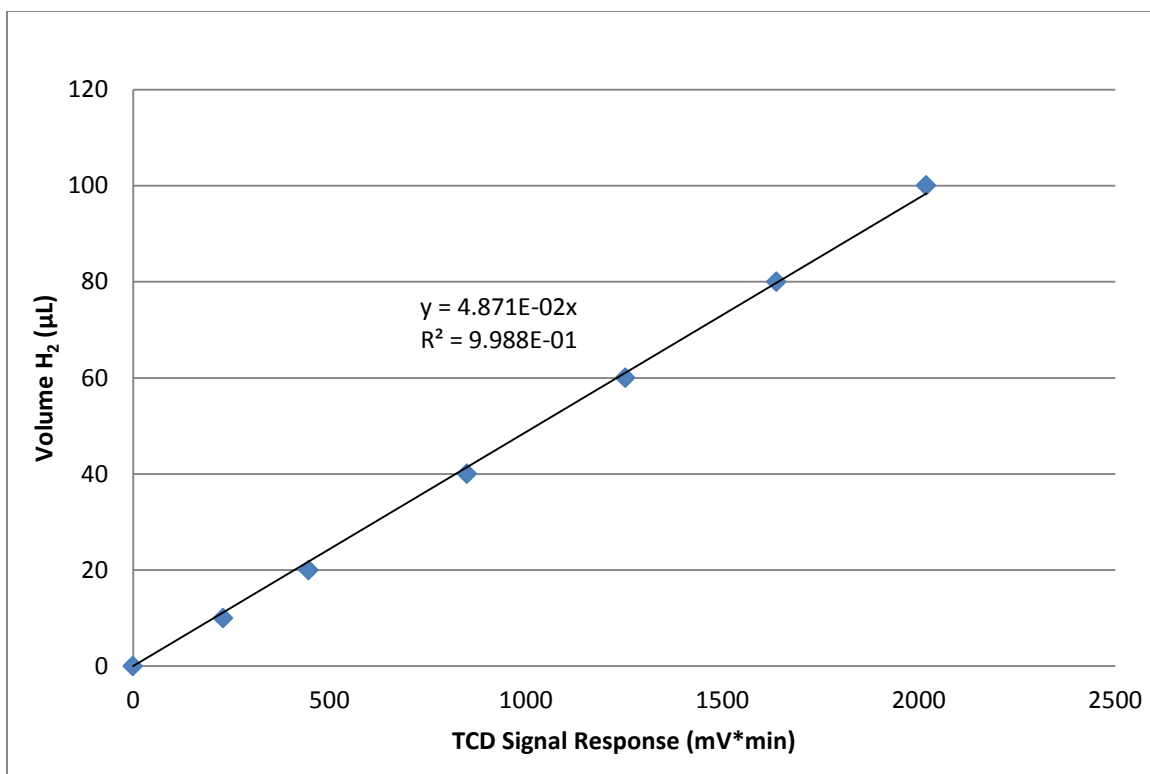


Figure G.1: Graph of Hydrogen Volume vs. TCD Signal Response used for Hydrogen Calibration

Figure G.1 shows the graph of the hydrogen calibration curve for gas chromatography. The equation of the trendline was used to find the volume of hydrogen in the unknown gas samples.

Another calibration bag consisting of carbon monoxide, carbon dioxide, and propane diluted into nitrogen was used. The volume fractions for carbon monoxide, carbon dioxide, and propane were 12 %, 20 %, and 8 %, respectively. This calibration bag was mainly used to construct a calibration curve for carbon used in analysis for gas chromatography. However, the calibration bag was also used each day analysis was performed in order to confirm proper conversion of carbon monoxide and carbon dioxide by means of the catalyst inside the methanizer. It was taken into account that the propane

gas used for calibration was not completely pure. Ethane and propene also existed with the propane, although the purity could be calculated from the analysis.

Table G.3: Data for Carbon Calibration of Gas Chromatography

Mole (Vol.) Percent C <sub>3</sub> H <sub>x</sub>		Gas Purity		FID Signal Response (mV*min)		
8.00%		93.3%		trial 1	trial 2	trial 3
CO+CO <sub>2</sub> +C <sub>3</sub> H <sub>x</sub> Volume (μL)	Volume C <sub>3</sub> H <sub>x</sub> (μL)	Carbon Number -	Volume of Carbon (uL equiv.)			
300	22.40	3	67.19	22730.4652	23324.3923	22952.6924
200	14.93	3	44.79	16340.4844	16599.1038	16671.5552
100	7.47	3	22.40	8352.6414	8317.7004	8430.0474

Each injected volume was run in triplicate and the average FID signal response was found. Since the injection volume was known, the volume of propane could be found by multiplying by percent of propane in the calibration bag and then by the purity of propane. Finally, the volume of carbon can be found.

Table G.4: Averages for Carbon Calibration of Gas Chromatography

CO+CO <sub>2</sub> +C <sub>3</sub> H <sub>x</sub> Volume (μL)	Volume C <sub>3</sub> H <sub>x</sub> (μL)	Carbon Number -	Volume of Carbon (uL equiv.)	FID Signal Response (mV*min)
300	22.40	3	67.19	23002.5166
200	14.93	3	44.79	16537.0478
100	7.47	3	22.40	8366.7964
0	0.00	3	0.00	0.0000

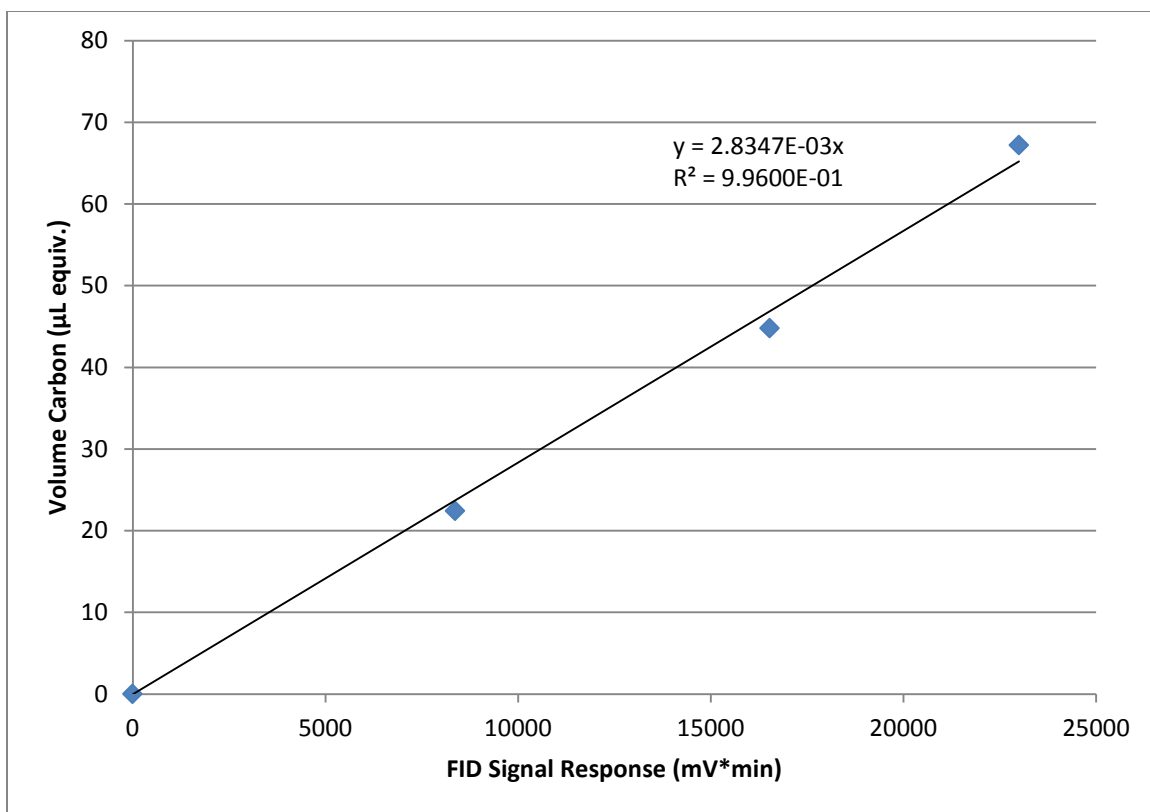


Figure G.2: Graph of Carbon Volume vs. FID Signal Response used for Carbon Calibration

Figure G.2 shows the graph of the carbon calibration curve for gas chromatography. The equation of the trendline was used to find the volume of carbon in the unknown gas samples.

## REFERENCES

- [1] C. Li and K. Suzuki, "Tar property, analysis, reforming mechanism and model for biomass gasification—An overview," *Renewable and Sustainable Energy Reviews*, vol. 13, no. 3, pp. 594-604, Apr. 2009.
- [2] Y. S. Kim, S. U. Jeong, W. L. Yoon, H. K. Yoon, and S. H. Kim, "Tar-formation kinetics and adsorption characteristics of pyrolyzed waste lubricating oil," *Journal of Analytical and Applied Pyrolysis*, vol. 70, no. 1, pp. 19-33, Oct. 2003.
- [3] I. C. B. A. International Carbon Black Association, "What is Carbon Black," 2006. [Online]. Available: <http://www.carbon-black.org/index.html>. [Accessed: 16-Jul-2012].
- [4] P. Paraskeva, D. Kalderis, and E. Diamadopoulos, "Production of activated carbon from agricultural by-products," *Journal of Chemical Technology and Biotechnology*, vol. 83, pp. 581-592, 2008.
- [5] M. Ahmedna, W. E. Marshall, and R. M. Rao, "Production of granular activated carbons from select agricultural by-products and evaluation of their physical , chemical and adsorption properties," *Bioresource technology*, vol. 71, pp. 113-123, 2000.
- [6] E. Mora, C. Blanco, V. Prada, R. Santamaria, M. Granda, and R. Menendez, "A study of pitch-based precursors for general purpose carbon fibres," *Carbon*, vol. 40, pp. 2719-2725, 2002.
- [7] M. Fan, W. Marshall, D. Daugaard, and R. C. Brown, "Steam activation of chars produced from oat hulls and corn stover.," *Bioresource technology*, vol. 93, no. 1, pp. 103-7, May 2004.
- [8] W. K. Lafi, "Production of activated carbon from acorns and olive seeds," *Biomass and Bioenergy*, vol. 20, pp. 57-62, 2001.
- [9] M. L. Martínez, M. M. Torres, C. a. Guzmán, and D. M. Maestri, "Preparation and characteristics of activated carbon from olive stones and walnut shells," *Industrial Crops and Products*, vol. 23, no. 1, pp. 23-28, Jan. 2006.

- [10] D. Savova et al., "Biomass conversion to carbon adsorbents and gas," *Biomass and Bioenergy*, vol. 21, pp. 133-142, 2001.
- [11] C. Srinivasakannan, "Production of activated carbon from rubber wood sawdust," *Biomass and Bioenergy*, vol. 27, no. 1, pp. 89-96, Jul. 2004.
- [12] M. Hamza, "Crude oil refining: Where does Delayed Coking fit in?," Duluth, MN, 2008.
- [13] S. Raseev, "Industrial Implementation of Thermal Processes," in *Thermal and Catalytic Processes in Petroleum Refining*, D. G. Suciu, Ed. New York, NY: Taylor & Francis Group, LLC, 2003.
- [14] The American Petroleum Institute Petroleum HPV Testing Group, "Petroleum Coke Category Analysis and Hazard Characterization," 2007.
- [15] G. C. Hughes, M. I. Wohlgenant, and B. J. Doerksen, "Handbook of Petroleum Refining Processes," Ponca City, Oklahoma, 2004.
- [16] R. J. Tosta and E. M. Inzunza, "Structural Evaluation Of Coke Of Petroleum And Coal Tar Pitch For The Elaboration Of Anodes In The Industry Of The Aluminum," *Light Metals*, pp. 887-892, 2008.
- [17] S. Birghila, I. C. Popovici, and A. Dumitru, "Study on physical-chemical properties of petroleum cokes," 2011.
- [18] E. Furimsky, "Characterization of cokes from fluid & flexi-coking of heavy feeds," *Fuel Processing Technology*, vol. 67, pp. 205-230, 2000.
- [19] D. Sullivan and J. Speight, "A new continuous coking process," 2011.
- [20] R. Naef, "Buss SMS Canzler Scrape Surface Heat Exchanger," Grand Forks, ND, 2011.
- [21] The American Petroleum Institute Petroleum HPV Testing Group, "Petroleum coke test plan," 2000.
- [22] Y. Sahin, "Environmental Impacts of Biofuels," *Energy Educ. Sct. Technol. Part A. Energy Sci. Res.*, vol. 26, no. 2, pp. 129-142, 2011.
- [23] H. Balat, "Prospects of biofuels for a sustainable energy future: A critical assessment," *Energy Education Science and Technology*, vol. 24, no. 2, pp. 85-111, 2010.

- [24] A. A. Apostolakou, I. K. Kookos, C. Marazioti, and K. C. Angelopoulos, "Techno-economic analysis of a biodiesel production process from vegetable oils," *Fuel Processing Technology*, vol. 90, no. 7–8, pp. 1023-1031, Jul. 2009.
- [25] A. Demirbas, "Biofuels sources, biofuel policy, biofuel economy and global biofuel projections," *Energy Conversion and Management*, vol. 49, no. 8, pp. 2106-2116, Aug. 2008.
- [26] L. J. Loppacher and W. A. Kerr, "Can biofuels become a global industry?: Government policies and trade constraints," *Energy Politics*, vol. 5, pp. 7-27, 2005.
- [27] A. S. Ramadhas, S. Jayaraj, and C. Muraleedharan, "Use of vegetable oils as I.C. engine fuels—A review," *Renewable Energy*, vol. 29, no. 5, pp. 727-742, Apr. 2004.
- [28] J. Yang, P. G. Stansberry, J. W. Zondlo, and A. H. Stiller, "Characteristics and carbonization behaviors of coal extracts," *Fuel Processing Technology*, vol. 79, no. 3, pp. 207-215, Dec. 2002.
- [29] T. Takatsuka, R. Kajiyama, and H. Hashimoto, "A practical model of thermal cracking of residual oil," *Journal of Chemical Engineering of Japan*, pp. 304-310, 1988.
- [30] "ASTM\_D3173-03(2008): Standard Test Method for Moisture in the Analysis Sample of Coal and Coke." pp. 426-428.
- [31] "ASTM\_D3175-07: Standard Test Method for Volatile Matter in the Analysis Sample of Coal and Coke." pp. 434-438.
- [32] "ASTM\_D3174-04: Standard Test Method for Ash in the Analysis Sample of Coal and Coke from Coal." pp. 429-433.
- [33] "ASTM\_D2887-02: Standard Test Method for Boiling Range Distribution of Petroleum Fractions by Gas Chromatography." pp. 1-13.
- [34] K. V. Padmaja, N. Atheya, a. K. Bhatnagar, and K. K. Singh, "Conversion of Calotropis procera biocrude to liquid fuels using thermal and catalytic cracking," *Fuel*, vol. 88, no. 5, pp. 780-785, May 2009.